ADVANCED MASTERS IN STRUCTURAL ANALYSIS
OF MONUMENTS AND HISTORICAL CONSTRUCTIONS

Master's Thesis

Jaime Gonzalez

Assesment of current standards for evaluation of shear FRP strengthening of concrete beams

This Masters Course has been funded with support from the European Commission. This publication reflects the views only of the author, and the Commission cannot be held responsible for any use which may be made of the information contained therein.

Italy | 2010

DECLARATION

Name: Jaime Hernán González Libreros

Email: jaimegonzalez78@yahoo.com

Title of the Msc Dissertation: Assessment of current standards for evaluation of FRP Strengthening of concrete beams

Supervisor(s): Prof. Carlo Pellegrino

Year: 2010

I hereby declare that all information in this document has been obtained and presented in accordance with academic rules and ethical conduct. I also declare that, as required by these rules and conduct, I have fully cited and referenced all material and results that are not original to this work.

I hereby declare that the MSc Consortium responsible for the Advanced Masters in Structural Analysis of Monuments and Historical Constructions is allowed to store and make available electronically the present MSc Dissertation.

University: University of Padova

Date: July 21st, 2010

Signature:

_____

ACKNOWLEDGEMENTS

I would like to acknowledge the financial support of the European Commission to carry on this Master. I also would like to express my gratitude to my thesis supervisor Professor Carlo Pellegrino for his help and advice during the execution of this document. I want to thank to the academic and administrative staff at the Czech University in Prague, the University of Minho and at the University of Padua.

I want to thank my classmates for all the great memories and for making this year so interesting. Finally, I have to highlight the importance of the support giving by my family during my stay abroad.

ABSTRACT

The strengthening of structures with FRP composites has become an important alternative for the retrofitting of structures. However, it has been shown that the equations proposed by current standards still need to be validated in order to obtain more reliable formulations for the design. In this paper, the improvement of an existing database of experimental data for beams strengthened with externally bonded FRP for shear is carried out in order to compare those results with the ones predicted by the recommendations given by the ACI 440, the *fib* BULLETIN 14 and the CNR-DT 200. The evaluation of these codes is made based on the correlation between the experimental and the theoretical data and the structural level of safety obtained by the use of the codes. In addition, the model proposed by Pellegrino and Modena (2008) is assessed, comparing its performance to the selected codes. The evaluation of the codes showed that their recommendations should be improved and updated, especially for beams including shear steel reinforcement. The Pellegrino and Modena model proved to usually have a better behavior than the codes for beams with and with shear steel reinforcement.

Keywords: FRP composites, shear strengthening, concrete beams, design codes, safety factor, correlation factor.

RIASSUNTO

“Analisi delle normative vigenti per la valutazione del rinforzo a taglio di travi in calcestruzzo mediante FRP”

Il rinforzo delle strutture con materiali compositi FRP è diventata una importante alternativa per l'adeguamento delle strutture. E’ stato, tuttavia, dimostrato che le equazioni proposte dalle normative vigenti devono ancora essere convalidate in modo da ottenere formulazioni più affidabili per la progettazione. In questa relazione viene effettuato il miglioramento di un database esistente contenente dati sperimentali riguardanti travi rinforzate a taglio mediante FRP applicati esternamente, al fine di confrontare tali risultati con quelli previsti dalle indicazioni fornite dall’ACI 440, dal *fib* BULLETIN n.14 e dalle istruzioni CNR-DT 200. La valutazione di queste normative è effettuata sulla base della correlazione tra i dati sperimentali e quelli teorici e del livello di sicurezza strutturale ottenuto con l'uso delle normative. Viene, inoltre, valutato il modello proposto da Pellegrino e Modena (2008), confrontando le sue prestazioni alle norme selezionate. La valutazione delle norme ha dimostrato che le loro indicazioni dovrebbero essere migliorate e aggiornate, soprattutto per le travi che contengono armatura a taglio in acciaio. Il modello di Pellegrino e Modena ha dimostrato di avere solitamente un comportamento migliore di quello delle normative per travi con o senza armatura a taglio in acciaio.

Parole chiave: materiali compositi FRP, rinforzo a taglio, travi di cemento, norme per la progettazione, fattore di sicurezza, fattore di correlazione.

RESUMEN

"Estudio de códigos utilizados para la evaluación del reforzamiento a cortante de vigas de concreto utilizando FRP"

El reforzamiento de estructuras con materiales compuestos tipo FRP se ha convertido en una alternativa importante para el mejoramiento de las estructuras. Sin embargo, se ha demostrado que las ecuaciones propuestas por los códigos actuales necesitan ser validadas para obtener formulaciones más confiables para el diseño. En este documento, el mejoramiento de una base de datos experimentales de vigas de concreto reforzadas a cortante con materiales FPR se llevo a cabo con el fin de comparar estos resultados con los que se obtienen con las recomendaciones de los códigos ACI 440, el *fib* BULLETIN 14 y el CNR-DT 200. La evaluación de estos códigos se hizo con base a la correlación entre los datos experimentales y teóricos además del nivel de seguridad alcanzado con su uso. Adicionalmente, el modelo propuesto por Pellegrino y Modena (2008) es evaluado y su desempeño es comparado con los códigos seleccionados. La evaluación de los códigos muestra que sus recomendaciones deberían ser actualizadas y mejoradas, especialmente para vigas que presentan refuerzo de acero a cortante. El modelo de Pellegrino y Modena, por su parte, mostro generalmente un mejor comportamiento que los códigos, tanto para vigas con refuerzo de acero a cortante como para aquellas sin refuerzo.

Palabras clave: Compuestos FRP, reforzamiento a cortante, vigas de concreto, códigos de diseño, factor de seguridad, factor de correlación.

Table of Contents

1. INTRODUCTION 1

1.1. Types of traditional shear strenghtening 1

1.2. Strengthening with FRP 3

1.3. Scope of the document 4

2. FIBER REINFORCED POLYMERS (FRP) 7

2.1. Matrices 8

2.1.1. Epoxy resins 9

2.1.2. Polyester resins 9

2.1.3. Vinyl ester 9

2.2. Fibers 10

2.2.1. Carbon fibers 11

2.2.2. Glass fibers 12

2.2.3. Aramid fibers 12

2.2.4. Other types of fibers 13

2.3. Fillers 13

2.4. Additives and modifiers 14

2.5. Adhesives 15

2.6. Properties of FRP strengthening systems 15

2.6.1. Thermal expansion coefficient 16

2.6.2. Mechanical properties 16

2.7. Techniques for FRP strengthening 17

2.7.1. Wet lay-up systems 18

2.7.2. Pre-cured elements 18

2.7.3. Prepreg systems 19

3. ACI 440 : GUIDE FOR THE DESIGN AND CONSTRUCTION OF EXTERNALLY BONDED FRP SYSTEMS FOR STRENGTHENING CONCRETE STRUCTURES 21

3.1. Khalifa et al model (1998) 22

3.2. V_f according to ACI 440 26

4. FIB BULLETIN 14: EXTERNALLY BONDED FRP REINFORCEMENT FOR RC STRUCTURES . 29

5. CNR-DT 200/2004: GUIDELINES FOR THE DESIGN AND CONSTRUCTION OF EXTERNALLY BONDED FRP SYSTEMS FOR STRENGTHENING EXISTING STRUCTURES 33

6. EVALUATION OF CODES 37

6.1. Comparison parameters 37

6.1.1. Correlation coefficient (R^2) 37

6.1.2. Global safety factor (SF) 38

6.1.3. Demerit points classification 39

6.2. Total Shear Strength 39

6.2.1. Variation of variable θ in the EC2 + fib BULLETIN 43

6.2.2. EC2 + CNR-DT 200 45

6.3. FRP Contribution 48

6.4. Influence of strengthening scheme 51

6.4.1. U-Jacket configuration 51

6.4.2. Side bonded configuration 54

6.5. Influence of steel shear reinforcement 58

6.5.1. U-Jackets configuration 58

6.5.2. Side bonded configuration 62

6.6. Overall comparison 65

7. PELLEGRINO AND MODENA MODEL (2008) 69

7.1. Total Shear Strength 71

7.2. FRP Contribution 72

8. CONCLUSIONS 75

9. REFERENCES 77

List of Figures

Figure No. 1. Traditional techniques to strengthen concrete beams for shear (Taljsten, 2002). 2

Figure No. 2. Common externally bonded FRP strengthening configurations (Lima et al, 2007). 3

Figure No. 3. Possible arrangements for externally bonded FRP strengthening (Lima et al, 2007). 4

Figure No. 4. Typical uniaxial tension stress-strain diagrams for different fibers and comparison with steel. 11

Figure No. 5. Stress-strain relationship for fibers, matrix and FRP. 17

Figure No. 6. Ratio of $\varepsilon_{fe}/\varepsilon_{fu}$ in terms of $\rho_f E_f$ according to Khalifa et al (1998). 23

Figure No. 7. Effective width of FRP for a) U-Jacket and b) Bonded only on two beam sides (Khalifa et al., 1998). 25

Figure No. 8. Comparison of experimental results to the results using the ACI 440 procedure. 27

Figure No. 9. Comparison of experimental results to the equations proposed by Triantafillou and Antonopoulos (2000). 30

Figure No. 10. Triantafillou (1998) and Triantafillou and Antonopoulos (2000) model comparisons (taken from Sas et al (2009)). 32

Figure No. 11. Triantafillou (1998) and Triantafillou and Antonopoulos (2000) model comparisons (taken from Sas et al (2009)). 33

Figure No. 12. Comparison of experimental and theoretical values for the evaluated codes. 40

Figure No. 13. Comparison of experimental and theoretical values for ACI318M-05 + ACI 440. 40

Figure No. 14. Comparison of experimental and theoretical values for EC2 + FIB Bulletin 14. 41

Figure No. 15. Comparison of experimental and theoretical values for IBC + CNR-DT 200. 41

Figure No. 16. Selection of optimal θ: Left: Inside range. Right: Outside range. 44

Figure No. 17. Comparison of experimental and theoretical values for EC2 + FIB Bulletin 14 (optimal θ). 44

Figure No. 18. Comparison of experimental and theoretical values for CNR-DT 200 + EC2 or + IBC. 46

Figure No. 19. Comparison of experimental and theoretical values for EC2 + CNR-DT 200. 46

Figure No. 20. Comparison of experimental and theoretical values for EC2 + CNR-DT 200 (optimal θ). 47

Figure No. 21. Comparison of experimental and theoretical FRP contribution. 48

Figure No. 22. Comparison of experimental and theoretical values for ACI 440. 49

Figure No. 23. Comparison of experimental and theoretical values for *fib* Bulletin 14. 50

Figure No. 24. Comparison of experimental and theoretical values for CNR-DT 200. 50

Figure No. 25. Comparison of experimental and theoretical FRP contribution for U-jacket configuration. 52

Figure No. 26. Comparison of experimental and theoretical values for ACI 440. 52

Figure No. 27. Comparison of experimental and theoretical values for *fib* BULLETIN 14. 53

Figure No. 28. Comparison of experimental and theoretical values for CNR-DT 200. 53

Figure No. 29. Comparison of experimental and theoretical FRP contribution for Side bonded configuration. 55

Figure No. 30. Comparison of experimental and theoretical values for ACI 440. 56

Figure No. 31. Comparison of experimental and theoretical values for *fib* BULLETIN 14. 56

Figure No. 32. Comparison of experimental and theoretical values for CNR-DT 200. 57

Figure No. 33. Comparison of experimental and theoretical values for ACI 440 without shear steel reinforcement. 58

Figure No. 34. Comparison of experimental and theoretical values for *fib* bulletin 14 without shear steel reinforcement. 59

Figure No. 35. Comparison of experimental and theoretical values for CNR-DT 200 without shear steel reinforcement. 59

Figure No. 36. Comparison of experimental and theoretical values for ACI 440 with and without shear steel reinforcement. 60

Figure No. 37. Comparison of experimental and theoretical values for *fib* bulletin 14 with and without shear steel reinforcement. 60

Figure No. 38. Comparison of experimental and theoretical values for CNR-DT 200 with and without shear steel reinforcement. 61

Figure No. 39. Comparison of experimental and theoretical values for ACI 440 without shear steel reinforcement..... 62

Figure No. 40. Comparison of experimental and theoretical values for *fib* bulletin 14 without shear steel reinforcement. 62

Figure No. 41. Comparison of experimental and theoretical values for CNR-DT 200 without shear steel reinforcement. 63

Figure No. 42. Comparison of experimental and theoretical values for ACI 440 with and without shear steel reinforcement. 64

Figure No. 43. Comparison of experimental and theoretical values for *fib* bulletin 14 with and without shear steel reinforcement. 64

Figure No. 44. Comparison of experimental and theoretical values for CNR-DT 200 with and without shear steel reinforcement. 65

Figure No. 45. Typical failure of: Left: U-jacketed and Right: side-bonded beams (Pellegrino and Modena, 2008). 69

Figure No. 46. Forces acting in the cross section of Left: U-jacketed and Right: side-bonded beams (Pellegrino and Modena, 2008). 69

Figure No. 47. Comparison of experimental and theoretical values for Pellegrino and Modena Model – Total Shear Strength. 71

Figure No. 48. Comparison of experimental and theoretical values for Pellegrino and Modena Model – V_{frp} contribution. 72

Figure No. 49. Comparison of experimental and theoretical values for Pellegrino and Modena Model for U-jacket scheme– V_{frp} contribution..... 73

Figure No. 50. Comparison of experimental and theoretical values for Pellegrino and Modena Model for Side bonded scheme– V_{frp} contribution. 73

List of Tables

Table No. 1. Properties of different types of Matrices. 10

Table No. 2. Typical properties of fibers. 11

Table No. 3. Reduction factors for FRP Shear reinforcement. 21

Table No. 4. Summary of tests used by Khalifa et al (1998). 22

Table No. 5. Summary of tests used by Triantafillou and Antonopoulos (2000). 29

Table No. 6. Partial safety factors proposed by the *fib* BULLETIN 14. 31

Table No. 7. Comparison of codes based on structural safety. 39

Table No. 8. Comparison of codes based on structural safety. 43

Table No. 9. Comparison of EC2 + *fib* BULLETIN with constant or varying θ. 45

Table No. 10. Comparison of CNR-DT 200 with IBC or EC2. 47

Table No. 11. Comparison of EC2 + CNR-DT 200 with constant or varying θ. 48

Table No. 12. Comparison of codes for FRP shear contribution based on structural safety. 51

Table No. 13. Comparison of codes for FRP shear contribution for U-jacket configuration. 54

Table No. 14. Comparison of codes for FRP shear contribution for Side bonded configuration. 57

Table No. 15. Comparison of codes for FRP shear contribution with and without shear steel reinforcement (U-jacket configuration). 61

Table No. 16. Comparison of codes for FRP shear contribution with and without shear steel reinforcement (Side bonded configuration). 65

Table No. 17. Overall comparison of the codes. 66

Table No. 18. Assessment of Pellegrino and Modena Model for Total Shear Strength. 71

Table No. 19. Assessment of Pellegrino and Modena Model for V_{frp} Contribution. 74

1. INTRODUCTION

The retrofit of existing reinforced and prestressed concrete structures has always been a crucial field where Civil engineering has to give solutions. Despite of the natural aging and damage of structures and materials, there are many other reasons that make necessary the structural intervention such as:

- To eliminate structural problems or distress which result from unusual loading or exposure conditions, inadequate design or poor construction practice.
- To be conform to current codes and standards.
- To allow the feasibility of changing the use of a structure to accommodate a different use from the present one.
- Environmental effects.
- Lack of preservation of the structure.
- Random loading or fire and impact effects.

This need for renovation and rehabilitation of structures has lead to seek of a new generation of materials which can make the intervention easier and more effective. Fiber reinforced polymers (FRP) belong to this new generation of materials. The ways of retrofitting with those materials can be divided into categories. The first is related to the externally bonded FRP (EBR) usually in the form of laminated or roving and second the near surface mounted (NSM), into superficial structural members' grooves, FRPs in the form of bars or laminates.

The use of externally bonded fiber reinforced polymer reinforcement to strengthen reinforced concrete structures is becoming an increasingly popular retrofit technique. The light weight and formability of FRP reinforcement makes the system easy to install. In addition, these materials are an excellent option for external reinforcement due to properties that make them noncorrosive, nonmagnetic and, generally, resistant to chemicals.

The strengthening with externally bonded FRP sheets has been applied to many types of reinforced concrete elements or structures such as columns, beams, slabs, walls, chimneys, tunnels and silos. The use of FRP reinforcement is generally divided as flexural strengthening, improving the confinement and ductility of compression members, and shear strengthening.

1.1. Types of traditional shear strenghtening

In general, as presented by Taljsten (2002), six different traditional methods to strengthen concrete beams for shear can be recognized as shown in Figure No. 1.

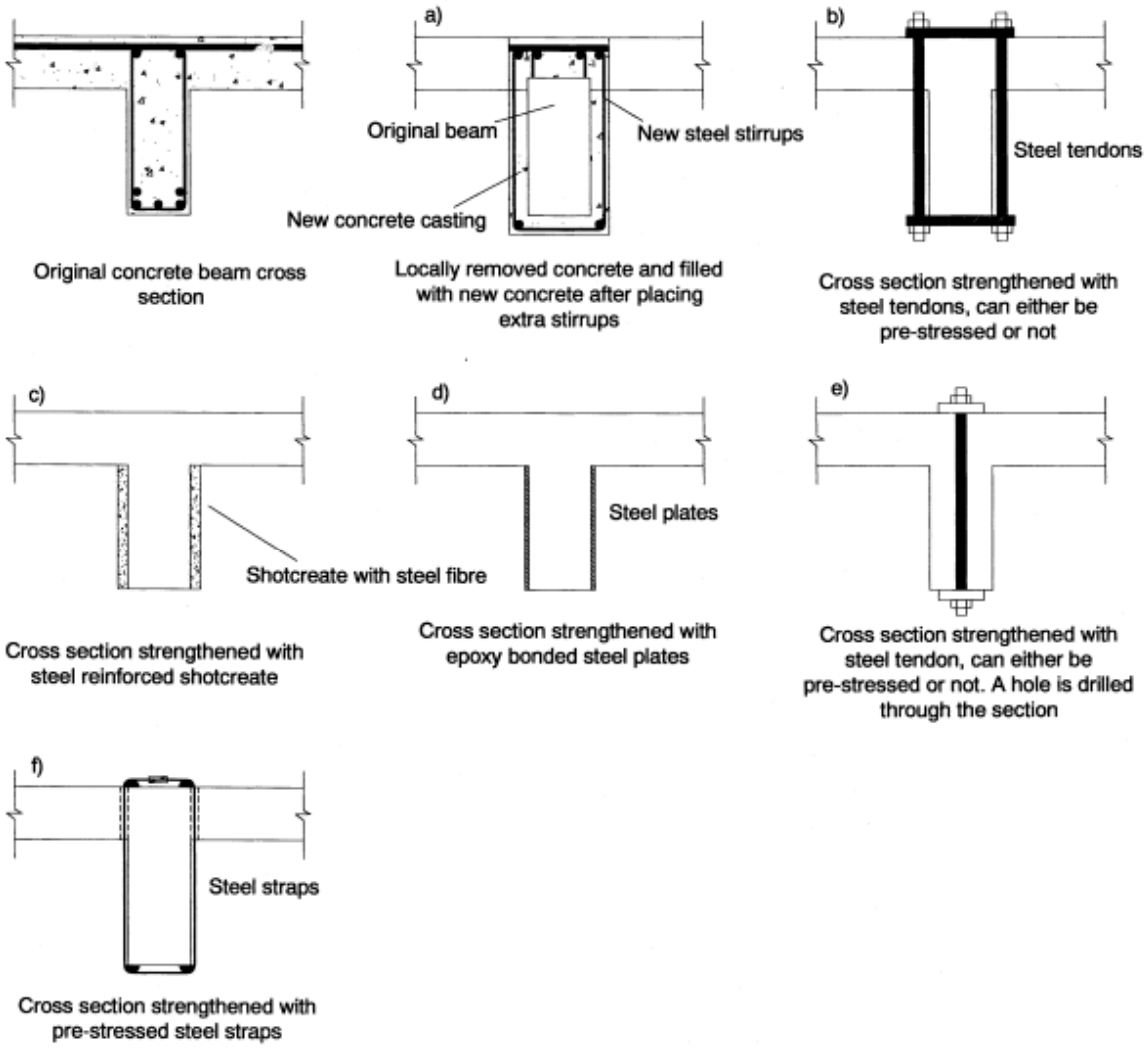

Figure No. 1. Traditional techniques to strengthen concrete beams for shear (Taljsten, 2002).

Method (a), most commonly used, consists in the creation of a new wider section with the steel reinforcement anchored in the compressive zone, which gives a higher shear capacity to the structure. This method consists in the placement of new stirrups, mounted around the original cross section and new concrete is cast or sprayed onto the structure. This method is time consuming and in many cases not cost effective.

Method (b) can be easier to carry out than method (a) but unfortunately the drilling of the holes through the slab can have the risk of cutting the bending reinforcement. In addition, the cast of new concrete above the bolts can be also required.

According to Taljsten (2002), method (c) can be used in cases where limited strengthening is required. Together with method (d), the main drawback corresponds to the fact that the strengthening material cannot be anchored in the compressive zone. In this part, however, it has to be said that steel plates are considered as the forerunners for CFRP plates or sheets. Method (e), which consists in a big hole

is drilled through the cross section and then a steel tendon, pre-stressed or not, is cast. The main drawbacks correspond to the ones exposed for method (b).

Method (f) consists in steel straps wrapped around the section. This method requires small damage in the cross section but the straps are sensitive to impact loads or vandalism.

1.2. Strengthening with FRP

Up to now, FRP has been used for strengthening of reinforced concrete structures in thousands of applications worldwide. If compared to the adoption of steel jackets or epoxy bonded steel plate, the FRP strengthening shows several advantages: the work with heavy steel parts is avoided, such as all the risks related to the corrosion. Compared to the adoption of the concrete jackets, the FRP systems avoid effects such as an undesirable increase of stiffness and weight.

For elements with shear resistance deficiencies, a higher load carrying capacity can be achieved by bonding the FRP reinforcement systems with the fibers as orthogonal as practically possible to the critical shear crack plane for an optimal configuration, or with the fibers perpendicular to the beam axis for a more practical setting. Common configurations of strengthening are shown in Figure No. 2 (Lima et al, 2007). They include full wrapping of the cross section (a, W) which corresponds to the most efficient scheme but it is most commonly used in columns where access to all four sides of the column is usually available. In beams applications, where an integral slab makes it impractical to completely wrap the member the shear strength can be improved by wrapping the FRP system around three sides of the member (U jacketing, U), b) or bonding to the two sides of the member (side bonding, S, c). Additional mechanical anchorage systems can be provided to enhance the behavior of U jacketing or side bonded configurations where the available bond length is short (d and e). Although all the three techniques have been shown to improve the shear strength of a member, completely wrapping the section is the most efficient followed by the U-jacketing (ACI 440). It is important to highlight that for U-jacketing of rectangular or T-section beam, delamination of the end portions of the FRP reinforcement can be avoided by using laminates/sheets and/or bars installed in the direction of the member longitudinal axis. In such case, the behavior or the U-wrap strengthening can be considered as equivalent to that of a completely wrapped member, provided that the effectiveness offer by these devices is proven (CNR-DT 200).

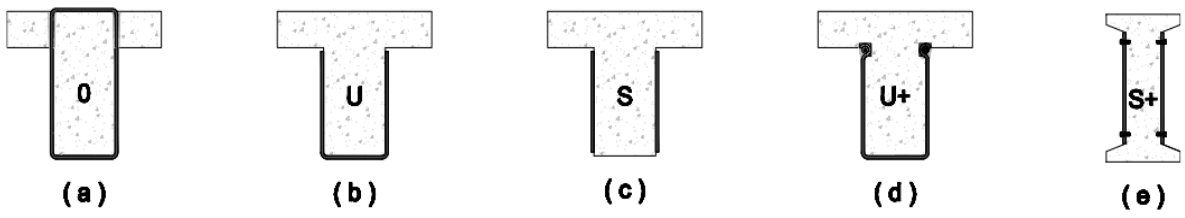

Figure No. 2. Common externally bonded FRP strengthening configurations (Lima et al, 2007).

Each of the aforementioned strengthening configurations may be set in several possible arrangements (see Figure No. 3). External FRP reinforcement can be applied in a discontinuous fashion, with gaps between following strips or continuously, with strips next to each other.

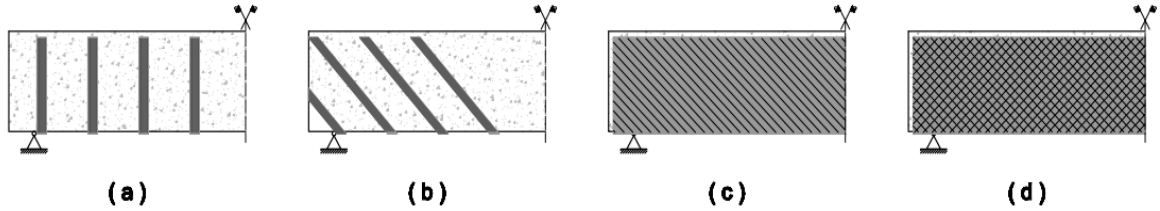

Figure No. 3. Possible arrangements for externally bonded FRP strengthening (Lima et al, 2007).

Composites are a strong candidate for strengthening of concrete structures. They can be used as flexible fabrics to wrap around corners and on convex surfaces or they can be used as prefabricated laminates in various sizes and shapes. In both cases, the preparation of the concrete surface is essential for good bond and strengthening effect. In most cases, sandblasting or grinding is used but also water blasting can be an alternative. The surface should be free from contaminants such as grease, oil, dust, etc., before the adhesive is applied.

1.3. Scope of the document

The document is intended to improve an existing database of experimental tests carried out on concrete beams strengthened with FRP. In order to do so, an extensive literature review on research papers performed in the topic was carried out. This allowed obtaining an important number of points that were used to verify the accuracy of the existing codes for the evaluation of the contribution of the FRP to the shear strength.

First, a description of the FRP materials itself is presented, in order to establish the main advantages and drawbacks of their use as well as having an overall view of their components, properties and available strengthening techniques.

Three codes were selected for the comparison: the ACI 440, the *fib* BULLETIN and the CNR-DT 200. A description of the basis of the codes and the proposed equations are presented in chapters 3, 4 and 5. With this information, a comparison between the codes was performed with the objective of study based in three main parameters: the correlation coefficient (R^2), the global safety factor (SF) and the demerit classification system. This was used in order to obtain the correlation between the experimental values found in the literature review and the theoretical results produced by the codes.

Finally, the model proposed by Pellegrino and Modena (2008) for the strengthening of concrete beams using U-jacket or side bonded configurations is compared with the codes that obtained the better performance in order to establish the accuracy and reliability of this model.

As final remark, it has to be said that the equations are presented in the units of the codes, unless otherwise specified. The name and symbols of the variables used correspond to the ones used in the codes or articles investigated but in the required cases, the correspondence with the variables of the other codes is introduced.

2. FIBER REINFORCED POLYMERS (FRP)

FRP is a composite material generally consisting of carbon (CFRP), aramid (AFRP) or glass (GFRP) fibers with a sufficient aspect ratio (length to thickness) to provide a reinforcing function in one or more directions when combined with a polymeric matrix (either thermosetting or thermoplastic). One of the main differences of FRP with traditional materials as steel or aluminum is its anisotropy, understood as uniform properties in the direction of the applied load. This means that FRP composite properties are directional, implying that the best performance of the fibers is achieved in the direction of the placement. Taking this is into account, composites can be assumed as similar to reinforced concrete where the rebar is embedded in an isotropic matrix called concrete (Megalooikonomou, 2007).

In this part, it is important to notice that the FRPs are made at least of two materials than can be easily distinguishable which present different physical and mechanical properties. As consequence, the FRP produced will exhibit different properties from those of its constituents (see 2.6). Besides the resins (matrices) and reinforcements (fibers), FRP can contain fillers and additives. Each of these constituent materials or ingredients plays an important role in the processing and final performance of the end product. The resin or polymer (matrix) is the glue that holds the composite together and influences the physical properties of the end product. The reinforcement provides the mechanical strength; the fillers and additives are used during the process as performance aids to impart special properties to the end product.

For the strengthening of civil structures, FRPs are available mainly in form of thin unidirectional strips made by pultrusion and flexible sheets or fabrics, made of fibers respectively in one or at least two directions.

The selection of the materials to use is a critical step in the FRP realization. Fibres and resins have to be studied so that they can work properly together. It has to be taken into account that a good resin for a kind of fiber will not be necessary good for another and even though the fiber and resin work well together, the bonding to the concrete is not automatically guarantied.

The main advantages that FRPs offer when they are compared to traditional strengthening techniques are summarized here:

- High tensile strength.
- Low weight and high strength-to-weight ratio.
- Directional strength.
- High impact strength.
- Low maintenance.
- Easy installation procedures.

- High durability (no corrosion) and tensile strength.
- Electromagnetic permeability
- Practically unlimited availability in terms of geometry and size.
- Easy application in confined space, due to the small thickness of the fibers.

However the composites also present disadvantages that can be neglected such as:

- Need of protection against fire and ultraviolet rays.
- Need of specialized technicians.
- Cannot be anchored.
- Linear elastic behavior (material without ductility).
- The cost of materials for retrofitting can be several times higher than that for traditional methods.
- Some FRP materials have incompatible thermal expansion coefficients with concrete and masonry.
- Reduction of tensile strength and Young modulus when they are under continuous drench or alkaline environment.
- Bonding problems which can lead to premature fragile collapse of the retrofitted member due to a mechanism known as debonding.

In addition to the limitations listed before, the thermal expansion coefficient represents an important factor that has to be taken into account. For standard FRP materials this value is very low and, although this characteristic can be positive when the polymers are used alone, it can become a problem when FRP and RC are incompatible and their exposure to high temperature, such a fire event, can result in a premature deterioration of the materials, detachments and possible collapse.

2.1. Matrices

As it was said before, for a structural composite material, the matrix is usually a polymer which can be either thermosetting type or thermoplastic type, with the first being the most common one (Caicedo, 2007). The main functions of the matrices consist in protecting the fibers against abrasion or environmental corrosion, to bind the fibers and to distribute the load. The matrix has an important influence in some mechanical properties of the composite such as the transverse modulus and strength, and the shear and compression properties. Physical and chemical characteristics of the matrix such as melting or curing temperatures, viscosity and reactivity with fibres influence the choice of the fabrication process. Hence, proper selection of the matrix material for a composite system requires that all these factors be taken into account.

The main advantages of thermosetting resins include low viscosity that allows for a relative easy fiber impregnation, good adhesive properties, room temperature, etc. the drawbacks, in the other hand, are a limited range of operating temperatures, with the upper bound limit given by the glass transition temperature, poor toughness with respect to fracture and sensitivity to moisture during field applications.

Epoxy resins, polyester and vinyl ester are the most common polymeric matrix materials used with high performance reinforcing fibers. A description of their main features is given below.

2.1.1. Epoxy resins

Epoxy resins have a well-established record in a wide range of composite parts, structures and concrete repair. A major benefit of epoxy resins over unsaturated polyester resins is their lower shrinkage but also have an outstanding durability but are in general more expensive. In order to achieve specific performance features, epoxy resins can be formulated with different materials or blended with other epoxy resins. Different hardeners, used to controlled the cure rates in order to match process requirements, give different properties to the finished composite.

Epoxies are used primarily for fabricating high performance composites with superior mechanical properties, resistance to corrosive liquids and environments, superior electrical properties, good performance at elevated temperatures, good adhesion to a substrate, or a combination of those benefits (Megalooikonomou, 2007). However, they don't have particularly good UV resistance. For operating temperatures higher than 60℃, the resin should be suitably selected by taking into account the variations of its mechanical properties. There are usually no significant restrictions for the minimum operating temperature.

2.1.2. Polyester resins

Polyester resins have a lower viscosity compared to epoxy resins, are very versatile, and highly re-active. Their mechanical strength and adhesive properties are typically lower than those of epoxy resins.

The family of polyester resins for composite materials is typically composed of isophthalic, orhophthalic and bisphenolic resins. For both high temperatures and chemically aggressive aggressive environment applications, vinylester resins are often used; they represent a compromise between the performance of traditional polyester resins and that of epoxy resins.

2.1.3. Vinyl ester

Vinyl esters were developed to combine the advantages of epoxy resins with the better handling/faster cure, which are typical for unsaturated polyester resins. These resins are produced by reacting epoxy resin with acrylic or methacrylic acid. Vynil esters offer mechanical toughness and excellent corrosion resistance. These enhanced properties are obtained without complex processing, handling or special shop fabricating practices that are typical epoxy resins.

Table No. 1 presents a summary of the mechanical properties of the epoxy , polyester and vinyl ester matrices.

Table No. 1. Properties of different types of Matrices.

Matrices	Density (Kg/m^3)	Tensile Strenght (Mpa)	Young's Modulus (Gpa)	Failure Strain (%)
Epoxy	1200-1300	55-130	2.8-4.1	3.0-10.0
Polyester	1100-1460	35-104	2.1-4.1	<5.0
Vinyl ester	1120-1320	73-81	3.0-5.5	3.5-5.5

As final remark, it has to be said that recently, polymer-modified cement-based mortars have also become available in some applications. It is expected that these mortars will be used more and more in the near future, due to the benefits in application that come from their inorganic nature.

2.2. Fibers

The primary function of fibers or reinforcements is to carry load along the length of the fibers to provide strength and stiffness in one direction. Reinforcements can be oriented to provide tailored properties in the direction of the loads imparted on the end product. Reinforcements can be both natural and man-made. Many materials are capable of reinforcing polymers. Some materials, such as the cellulose in wood, are naturally occurring products. Most commercial reinforcements, however, are man-made such as glass, carbon or aramid fibers. The fibers volume fraction is equal to about 50-70% for the strips and about 25-35% for the sheets (Peloso, 2003)

Most reinforcements for either thermosetting or thermoplastic resins receive some form of surface treatments, either during fiber manufacture or as a subsequent treatment. Other materials applied to fibers as they are produced include resinous binders to hold fibers together in bundles and lubricants to protect fibers from degradation caused by process abrasion.

As it is possible to note from Figure No. 4, the fibers used for strengthening exhibit higher strength than steel and a linear elastic behavior up to failure without the yield plateau characteristic of the steel. It is important to notice that for each material, a range is presented which depends on the high or low elastic modulus available for the different fibers.

Differently from the steel, the fibers have a high degree of anisotropy, due to the particular, highly oriented, microstructure involving different behavior changing with the direction of the actions. Table No. 2 summarizes the principal characteristics, relative to the longitudinal direction for the most commonly used fibers. It is important to highlight that these values are only indicative of static strength of unexposed fibers. The design values must account both for the presence of resin in the mixtures and for the reduction due to long-term loading or environmental exposure.

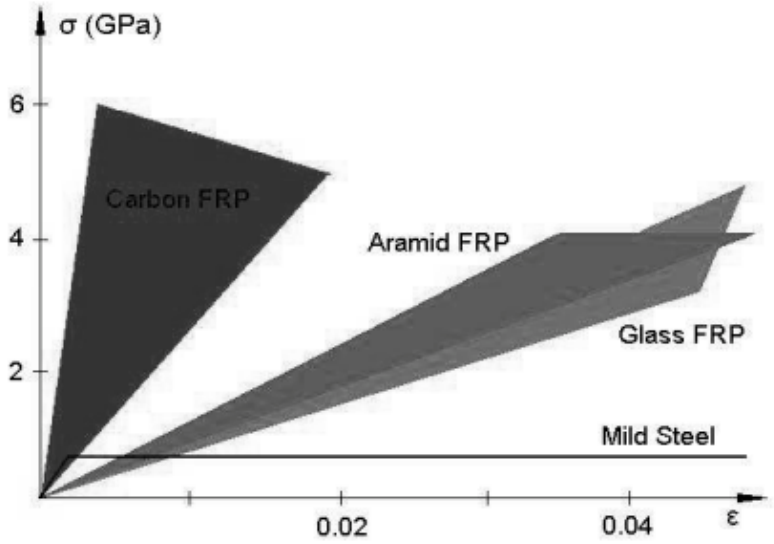

Figure No. 4. Typical uniaxial tension stress-strain diagrams for different fibers and comparison with steel.

Table No. 2. Typical properties of fibers.

Material	Elastic Modulus (kN/mm2)	Tensile strength (N/mm2)	Ultimate tensile strain (%)
Carbon			
High strength	215-235	3500-4800	1.4-2.0
Ultra high strength	215-235	3500-6000	1.5-2.3
High modulus	350-500	2500-3100	0.5-0.9
Ultra high modulus	500-700	2100-2400	0.2-0.4
Glass			
E	70-75	1900-3000	3.0-4.5
AR	70-75	1900-3000	3.0-4.5
S	85-90	3500-4800	4.5-5.5
Aramid			
Low modulus	70-80	3500-4100	4.3-5.5
High modulus	115-130	3500-4000	2.5-3.5

From the previous graphic and table, it is possible to see that the elastic Young modulus varies with the raw material, particularly it has to be noted that for glass and aramid fibers, the modulus is lower than for steel. This can involve problems in reinforcing of structures, leading to high value of deformation.

2.2.1. Carbon fibers

They are used mainly for their high performance and are characterized by high Young Modulus as well as high strength. In general, the tensile strength is equal to glass while its modulus is about three to four times higher. However, they have a high degree of variation with the raw material. It is possible to

distinguish among several types of carbon fibers classified with respect to the elastic modulus referred to as high and ultrahigh elastic modulus or to the tensile strength.

They are more expensive than glass fibers but offer an excellent combination of strength, low weight and high modulus. They are less sensitive to creep rupture and fatigue and show a slight reduction of the long-term tensile strength. Among other characteristics, it is important to point out their low thermal dilatation coefficients (both transversal and longitudinal), good resistance to the fatigue and excellent behavior against chemical agents and moisture.

Carbon fiber composites have more brittle behavior than glass or aramid fibers but their failure strengths are larger. Other deficiencies are that they can cause galvanic corrosion when used next to metals and their low strength against impacts.

Carbon fibers are supplied in a number of different forms, from continuous filament tows to chopped fibers and mats. The highest strength and modulus are obtained by using unidirectional continuous reinforcement. Twist-free tows of continous filament carbon contain 1000 to 75000 individual filaments which can be woven or knitted into woven roving and hybrid fabrics with glass fibers and aramid fibers.

2.2.2. Glass fibers

They are the cheapest and the most widely used for their good performance to cost ratio. They are obtained by extrusion of silicon material through holes with decreasing diameter with a final value that ranges from 20 to 3 μm. They are considered the predominant reinforcement for polymer matrix composites due to their high electrical insulating properties, low susceptibility to moisture and high mechanical properties. Other commercial compositions include “S” glass, with higher strength, heat resistance and modulus, as well as some specialized glass reinforcements with improved chemical resistance, such as AR glass (alkali resistant).

Glass is generally a good impact resistant fiber but weighs more than carbon or aramid. Glass fibers have excellent characteristics, equal to or better than steel in certain forms.. Composites made from this material exhibit very good electrical and thermal insulation properties.

The lower modulus requires special design treatment where stiffness is critical. Besides this problem, corrosion, low resistance to abrasion, moisture and to long term or cyclic loads are the greatest shortcomings.

2.2.3. Aramid fibers

These fibers are in production since 1972: first, the American society Du Pont, using as raw material a polymer, the aromatic polyamide or aramid, produced and commercialized them as Kevlar^{tm}.

Aramid fibers offer good mechanical properties at a low density with the added advantage of toughness and damage/impact resistance, i.e. damage tolerance, fatigue and thermal actions.. They are characterized as having reasonably high tensile strength, a medium modulus and a very low

density as compared to glass and carbon. The tensile strength of aramid fibers is higher than glass fibers and the modulus is about 50% higher than glass. These fibers increase the impact resistance of composites and provide products with higher tensile strengths. Aramid fibers are insulators of both electricity and heat. They are resistant to organic solvents, fuels and lubricants.

Limitations of use are involved by the exposure to moisture and ultraviolet rays: the humidity increases the shrinkage due to the interaction between the water and the fiber molecular structure, while the sun light reduces the strength of the aramid to half in 200 days but, fortunately, this problem can be overcame using a specific protective resins that has to be applied to the FRP just after placing.

Regardless of the material, reinforcements are available in forms to serve a wide range of processes and end-product requirements. Materials supplied as reinforcement include roving, milled fiber, chopped strands, continuous, chopped or thermo formable mat but also bars. Reinforcement materials can be designed with unique fiber architectures and be performed (shaped) depending on the product requirements and manufacturing process.

2.2.4. Other types of fibers

Fibers can be obtained from the polyethylene, showing good strength, low electric conductibility, high resistance to water, chemical products, abrasion and impact loads. The problem is that these fibers do not work well with heat and suffer slow deformation, due to the shrinkage and relaxation, more than this the resin impregnates them with some difficulty.

Another possibility is to use ceramic material, although this type of fibers exhibit very interesting characteristics (tensile strength between 0.5 and 2. GPa, even with temperatures of about 1200℃), they are not used for the high cost and because their characteristics would not be in any case used.

2.3. Fillers

Use of inorganic fillers in composites is increasing. The inorganic filler materials that can be used with composites include calcium carbonate, kaolin, alumina trihydrate and calcium sulfate. Fillers not only reduce the cost of composites, but also frequently impart performance improvements that might not otherwise be achieved by the reinforcement and resin ingredients alone. Fillers can improve mechanical properties including fire and smoke performance by reducing organic content in composite laminates. Also, filled resins shrink lees than unfilled ones, thereby improving the dimensional control of molded parts. Important properties, including water resistance, weathering, surface smoothness, stiffness, dimensional stability and temperature resistance, can all be improved through the proper user of fillers.

The thermosetting resin segment of the composite industry has taken advantage of the properties of fillers for many years. More recently, the thermoplastic industry has begun to make widespread use of inorganic fillers. Breakthroughs in chemical treatment of fillers that can provide higher filler loadings and improved laminate performance are accelerating this trend.

When used in composite laminates, inorganic fillers can account for 40 to 65% by weight. They perform a function similar to silica fume in concrete. In comparison to resins and reinforcements, fillers are the least expensive of the major ingredients. These materials are nevertheless very important in establishing the performance of the composite laminate for the following reasons:

- Reduce the shrinkage of the composite part.
- Influence the fire resistance of laminates.
- Lower compound cost.
- Serve to transfer stresses between the primary structural components of the laminate.
- Help maintaining fiber-loading uniformity by carrying reinforcing fibers along with the flow as resin is moved on the mold during compression molding.
- Improve crack resistance, particularly in sharp corners.

Some fillers are chemically modified by treating the surface area of the particles with a coupling agent. These coupling agents help to improve the chemical bond between the resin and filler and can reduce the resin demand.

2.4. Additives and modifiers

A wide variety of additives are used in composites to modify materials properties and tailor the laminates's performance. Although these materials are generally used in relatively low quantity by weight compared to resins, reinforcements or fillers, they perform critical functions.

Additives used in thermosetting and thermoplastic composites include the following:

- Low shrink/ low profile
- Fire resistance
- Air release
- Emission control
- Viscosity control
- Electrical conductivity
- Toughness
- Antioxidants
- Antistatic agents
- Foaming agents
- Plasticizers

- Slip and blocking agents
- Heat stabilizers
- Ultraviolet stabilizers

2.5. Adhesives

Adhesives are used to attach composites to themselves as well as to other surfaces. Adhesive bonding is the method of choice for bonding thermosetting composites and is sometimes used for thermoplastic composites. There are several considerations involved in applying adhesives effectively. The joint or interface connection must be engineered to select the proper adhesive and application method to ensure bond strength. Careful surface preparation and cure are critical to bond performance.

Adhesives should be used in joint design where the maximum load is transferred into the component using the loading characteristics of the adhesive and the composite material. The most common adhesives are acrylics, epoxies and urethanes. A high-strength bond with high-temperature resistance would indicate the use of an epoxy, whereas a moderate temperature resistance with good strength and rapid cure might use an acrylic. For applications where toughness is needed, urethane might me selected.

2.6. Properties of FRP strengthening systems

The first general consideration about the physical characteristic of the FRP is that they are different in longitudinal and transversal directions, referring to the fiber disposition, due to the heterogeneity and the anisotropy involved from the particular structure of the material. Heterogeneity derives from the fact that FRP is an ensamble of different materials with different characteristics. Anisotropy is due both to micro- and macrostructure; the fibers themselves exhibit anisotropy due to the particular molecular structure.

The mechanical properties and composition of FRP composites can be tailored for their intended use. The type and quantity of materials selected in addition to the manufacturing process to fabricate the product, will affect the mechanical properties and performance. Important considerations for the design of composite products include:

- Geometry: shape and dimensions
- Fiber orientation: the orientation with respect to the symmetry axes of the material; when random, the composite characteristics are similar to an isotropic material. In all other cases, the composite can be considered as an anisotropic material.
- Fiber concentration: volume fraction, distribution (dispersion).
- Type of fiber reinforcement
- Percentage of fiber or fiber volume
- Type of resin

- Volume of production (to help determine the best manufacturing method)
- Manufacturing process
- Service conditions.

2.6.1. Thermal expansion coefficient

Due to the anisotropy, two different coefficients are needed in order to characterize the FRP (longitudinal and transversal). Thermal behavior is very important when the FRP is used together with concrete or steel, because the different expansion of these materials can lead to high stresses at the interface between them increasing the risk of debonding.

The two expansion coefficients can be evaluated starting from the ones relative to the constituent materials, their elastic modulus and their volume fraction in the compound:

$$\alpha_L = \frac{1}{E_L}(\alpha_f v_f E_f + \alpha_m v_m E_m) \tag{1}$$

$$\alpha_T = (1+v_f)\alpha_f v_f + (1+v_m)\alpha_m v_m - \alpha_L \upsilon_{LT} \tag{2}$$

Where α is the thermal expansion coefficient, υ is the poisson modulus, *E* is the Young modulus and *v* is the volume fractions. The subscripts *L* and *T* stand for longitudinal and transversal direction with respect to the fibers direction respectively. *LT* is the maximum between the two directions, finally the subscripts *m* and *f* indicate the material which the parameter refers to: matrix or fibers.

2.6.2. Mechanical properties

As it was said before, in FRP materials, fibers provide both loading carrying capacity and stiffness to the composite while the matrix is necessary to guarantee the sharing of the load among fibers and to protect them from the environment. Most FRP materials are made of fibers with high strength and stiffness, while their strain at failure is lower than that of the matrix.

Although FRP is a non homogenous material, when working with its mechanical properties is better to consider it like such referring in this way to the classical continuum mechanic schematization. Unfortunately, the anisotropy cannot be neglected, leading to a higher number of strictly necessary parameters to characterize the behavior (transversal and longitudinal values of normal and shear elastic modulus, Poisson modulus and bulk modulus).

All the required coefficients are often evaluated starting from the characteristics of the FRP components and their volume fraction, instead of testing the FRP itself, obviously the problem becomes to determinate the characteristics of the fibers and matrix. All the formulations in literature involve critics but also clear advantages: for instance, it is possible to reduce the testing time when some materials are used to produce different FRP compounds varying the percentage of fibers and

resin involved in the manufacturing. This may be accomplished by applying the so call “rule of mixtures” simplification as follows:

$$E = E_f v_f + E_m v_m \tag{3}$$

$$\sigma = \sigma_f v_f + \sigma_m v_m \tag{4}$$

It remains clear that with the equations above, just an approximation of the desired value can be obtained. A more detailed prediction should be achieved through tensile testing which allows taking into account all the fibers and matrix characteristics as well as micro-structural aspects such as fiber diameter, distribution and parallelism of fibers, volume fractions and the fiber-matrix interfacial properties.

Due to the fact that the stiffness and strength of the fibers are much larger than the respectively values of the matrix, the properties of the FRP are highly governed by the properties and the cross sectional area of the bare fibers. Figure No. 5 shows the stress-strain relationship for fiber, matrix and the resulting FRP material. The resulting FRP material has lower stiffness than fibers and fails at the same strain of the fibers themselves. In fact, beyond such ultimate strain, load sharing from fibers to the matrix is prevented.

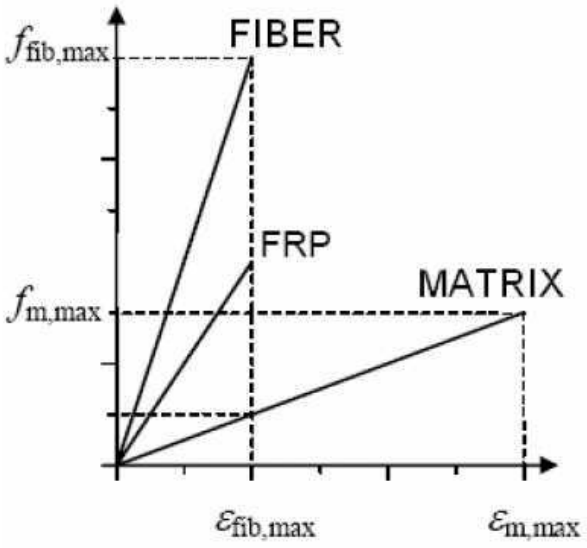

Figure No. 5. Stress-strain relationship for fibers, matrix and FRP.

2.7. Techniques for FRP strengthening

Different varieties of externally bonded FRP reinforcement systems exist, which are related to the constituent materials, the form and the technique of the FRP strengthening. Generally, these can be subdivided into two main categories:

- Wet lay up (or cured in-situ) systems
- Prefab (or pre-cured) systems.
- Prepreg systems.

The suitability of each system depends on the type of structure that shall be strengthened. For example, prefabricated strips are generally best suited for plane and straight surfaces, whereas sheets or fabrics are more flexible and can be used to plane as well as to convex surfaces.

These techniques involve the application of the FRP external reinforcement to the concrete element surface with the fibers as parallel as possible to the direction of the principal tensile stress. Several layers of fibers are superposed until the desired thickness is reached; when dry fibers are used the resin has to be applied both to the structure that need the reinforcement and to the fibers after their positioning.

All the required operation can be done automatically using a special machine, particularly helpful when the fibers must be applied on great areas. This automated technique involves the wrapping with continuous wet fibers placed with a slight angle around the element calling for retrofit. Although this technique involves good quality control and velocity of installation, it needs elements with circular cross section to be applied.

When hand lay up is used, to achieve a better final product some options are available, unfortunately implying higher costs. To provide a better elimination of the eventual entrapped air, a roller can be passed on the fibers, after the application of the epoxy resin. Otherwise, as well as for the moulding, the vacuum bat can be used for the improvement of the longitudinal reinforcement. To obtain in-situ fast curing or good bonding in those regions where the temperature is too low to allow cold curing, a hearing device can be used.

2.7.1. Wet lay-up systems

Installation on the substrate requires saturating resin usually after a primer has been applied. Two different process can be used to apply the fabric. In the first one, the fabric can be applied directly into the resin which has been applied uniformly onto the substrate. In the second process, the fabric can be impregnated with the resin in a saturator machine and then applied wet to the sealed substrate.

For this case, the final thickness of the FRP laminate cannot be estimated in a deterministic fashion. Therefore, it is recommended to refer to both mechanical and geometrical properties of dry fabric according to the technical data sheets provided by the FRP manufacturer in order to establish the properties of the composite.

2.7.2. Pre-cured elements

Manufactured in various shapes, by pultrusion or lamination, pre-cured systems are directly bonded to the structural member to be strengthened. Pre-cured composites are characterized by a unidirectional

disposition of fibers. For this case, manufactures typically provide mechanical characteristics referred to the laminate cross-section having a well specified size.

2.7.3. Prepreg systems

Manufactured with unidirectional or multidirectional fiber sheets or fabrics preimpregnated at the manufacturing plant with partially polymerized resin and delivered in rolls. They may be bonded to the member to be strengthened with (or without) the use of additional resins. The resins may receive pre-polymerization treatments.

3. ACI 440 : GUIDE FOR THE DESIGN AND CONSTRUCTION OF EXTERNALLY BONDED FRP SYSTEMS FOR STRENGTHENING CONCRETE STRUCTURES

The nominal shear strength of a concrete member strengthened with an FRP system should exceed the required strength as shown in the equation No. 5:

$$\phi V_n \geq V_u \tag{5}$$

According to the ACI 440, the nominal shear strength (Equation No. 6) can be computed by adding the contribution of the FRP reinforcing (V_f) to the contributions of the concrete (V_c) and the shear steel reinforcement (stirrups, ties or spirals, V_s). It also states that the value of V_f should be modified by the reduction factor ψ_f that depends on the type of wrapping scheme as shown in Table No. 3:

$$\phi V_n = \phi(V_c + V_s + \psi_f V_f) \tag{6}$$

Table No. 3. Reduction factors for FRP Shear reinforcement.

ψ_f =0.95	Completely wrapped members
ψ_f =0.85	Three-sided U-wraps or bonded face plies

The formulation proposed by the ACI 440 in order to obtain the contribution of the FRP reinforcement to the total shear capacity of concrete beams (V_f) is based mainly in the work carried out by Khalifa et at (1998).

He considers a design approach where the fracture of the FRP sheet is quite similar to the approach used to compute the contribution of steel shear reinforcement, taking into account the rupture point of the FRP sheets instead of the yield point of steel for the ultimate condition. However, based on the work done by Triantafillou (1998), it was considered that the rupture of the FRP sheets rupture happens at values lower than their ultimate strength due to stress concentration. Khalifa proposes that the contribution of the externally bonded FRP sheets to the shear capacity of an RC beam may be computed as:

$$V_f = \frac{A_{fv} f_{fe} (\sin\alpha + \cos\alpha) d_f}{s_f} \tag{7}$$

Where A_f is the area of shear reinforcement, f_{fe} is the effective tensile stress in FRP sheet in direction of principal fibers, α is the angle between the orientation of the fibers in the sheet and the longitudinal axis of the beam. In order to compute the tensile stress in the FRP shear reinforcement at ultimate

(f_{fe}), which corresponds to the only unkown in the previous equation, the level of strain that can be developed in the FRP shear reinforcement at ultimate has to be computed:

$$f_{fe} = \varepsilon_{fe} E_f \tag{8}$$

The value of ε_{fe} depends on the failure modes of the FRP and of the strengthened reinforced concrete member. As guidance, the ACI 440 provides about the determination of the effective strain for different configurations of FRP laminates and failure modes, based on the work of Khalife, as it was said before, specially for U-jacket or two-sided bonded beams. Taking this into account a brief description of the design approach by Khalifa is presented before introducing the equations and recommendations found within the ACI 440 Standard.

3.1. Khalifa et al model (1998)

For Khaliya, f_{fe} can be computed as:

$$f_{fe} = R f_u \tag{9}$$

Where R is the ratio between the effective strain (ε_{fe}) and the ultimate strain (ε_{fu}). In his work, Khalifa proposed two equations for R in order to represent two possible failure modes: FRP rupture and delamination of the FRP from the concrete surface.

For rupture, Khalifa used the results of 48 beams tested with different kinds of FRP and schemes of reinforcement, which main features are summarized in the Table No. 4. The approach used consisted in compute the values of ε_{fe} for the different beams using equation No. 7 and the values of V_f experimentally founded. The values computed in this fashion were then plotted against the respective axial rigidities ($\rho_f E_f$) of the FRP sheets. Equation No. 10 was then computed by regression of the experimental data (Figure No. 6). It has to be noticed that the researchers also proposed an upper limit of R equal to 0.5 when found by 10 in order to maintain the shear integrity of the concrete because for higher levels of strains, the width of the shear cracks would imply lost of aggregate interlock with the subsequent reduction of the concrete shear capacity.

$$R = 0.5622(\rho_f E_f)^2 - 1.2188(\rho_f E_f) + 0.778 \leq 0.50 \tag{10}$$

Table No. 4. Summary of tests used by Khalifa et al (1998).

REFERENCE	SHEAR STRENGTHENING MATERIAL			Number of samples
	Fibers	Configuration	β°	
Sato et al (1996)	Carbon	Sheet bonded to beam sides	90	2
	Carbon	Sheet in form of U-jacket	90	2
Sato et al (1997)	Carbon	Sheet in form of U-jacket	90	1

REFERENCE	SHEAR STRENGTHENING MATERIAL			Number of samples
	Fibers	Configuration	β°	
Uji (1992)	Carbon	Sheet bonded to beam sides	90	3
	Carbon	Sheet wrapped around the beam	90	1
Funakawa et al (1997)	Carbon	Sheet wrapped around the beam	90	3
Umezu et al (1997)	Carbon	Sheet wrapped around the beam	90	3
Araki et al (1997)	Carbon	Sheet wrapped around the beam	90	5
	Aramid	Sheet wrapped around the beam	90	3
Chajes et al (1997)	Aramid	Sheet in form of U-jacket	0/90	1
	Carbon	Sheet in form of U-jacket	0/90	1
	Carbon	Sheet in form of U-jacket	45/135	1
Ohuchi et al (1994)	Carbon	Sheet wrapped around the beam	90	13
Triantafillou (1997)	Carbon	Sheet bonded to beam sides	90	9
			Total	48

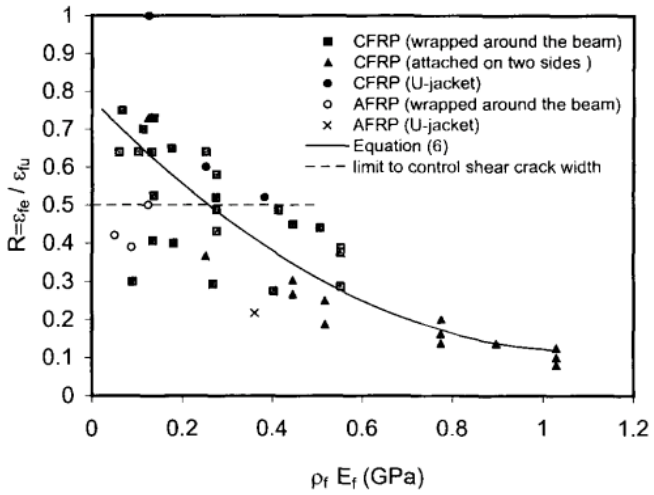

Figure No. 6. Ratio of $\varepsilon_{fe}/\varepsilon_{fu}$ in terms of $\rho_f E_f$ according to Khalifa et al (1998).

However, Khalifa clarifies that even though the equation proposed seems to be accurate enough for different types of FRP, reinforcement schemes and values of β, further investigation is required in order to obtain specific equations that take into account these kinds of parameters, including data obtained from future research in this field. In addition it has to be said that the information provided in the paper of Khalifa is not enough to reproduce this equation, because the information of the tests made by Ohuchi et al does not include values for V_{fexp} and f_{fu} of the shear strengthening material.

For beams that are not wrapped around the beam entirely, FRP delamination becomes a more likely failure mode. This can be explained by the transference of tensile stresses from the FRP sheets to the concrete surface at either side of a crack by interfacial bond stresses. Khalifa presents a design approach that considers the strength of the concrete and the bonded surface configuration.

The ultimate load capacity of a FRP sheet in a bonded area limited by the effective bond length and the width of the bonded sheet is function of the bond stress at failure (τ_{bu}) which is linear function of the stiffness according to the experimental data considered by Khalifa (see equation No. 11):

$$P_{\max} = L_e w_f \tau_{bu} = L_e w_f k \left(\frac{f_c'}{42} \right)^{2/3} E_f t_f \tag{11}$$

In the previous equation *k* corresponds to a experimental constant equal to 110.2x10^{-6} 1/mm and the effective bond length (L_e), understood as the length of FRP that includes the active bonded area, can be computed according to equation No. 12, based on the work carried out by Maeda et al in 1997 and used by Khalifa:

$$L_e = e^{6.134 - 0.58 \ln(t_f E_f)} = \frac{461.3}{(t_f E_f)^{0.58}} \tag{12}$$

Taking into account that the force P_{max} is developed in both sides, the effective stress can be computed as follows:

$$2P_{\max} = A_f f_{fe} \tag{13}$$

Replacing equations 12 and 13 in 12 and considering the elastic behavior of the FRP sheets, the expression for R for a failure mode caused by deboding and that shouldn't be used for fully wrapped beams is:

$$R = \frac{0.0042 (f_c')^{2/3}}{(E_f t_f)^{0.58} \varepsilon_{fu}} \tag{14}$$

However, in order to use the values found through equation No. 14, the concept effective width should be introduced. The effective width (w_{fe}) is defined as the width of the portion of the FRP that extends past the crack by effective bonded length. The value of w_{fe} depends on the shear crack angle (assumed to be 45°) and the bonded surface shown in Figure No. 7 and can be computed according to equations No. 15 and No. 16:

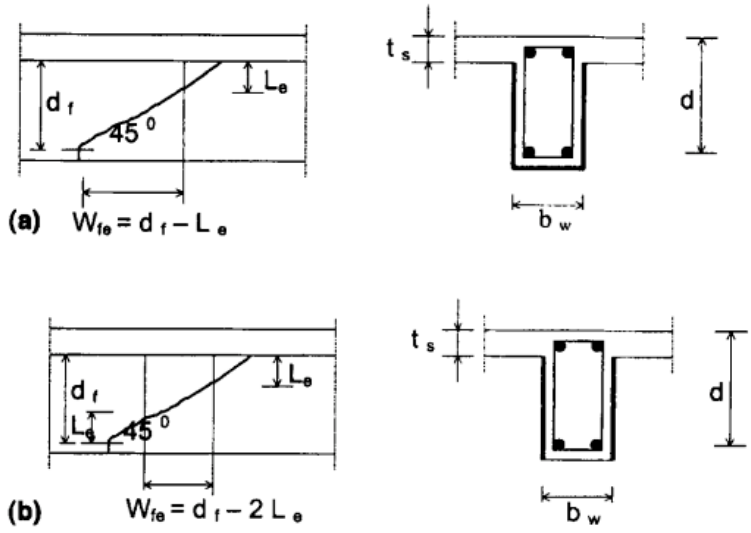

Figure No. 7. Effective width of FRP for a) U-Jacket and b) Bonded only on two beam sides (Khalifa et al., 1998).

$$w_{fe} = d_f - L_e \rightarrow for\, U - jacket \tag{15}$$

$$w_{fe} = d_f - 2L_e \rightarrow for\, two - sided\, bonded\, sheets \tag{16}$$

The final expression for R for this type of failure mode is obtained by multiplying equation No. 14 by the ratio of w_{fe}/d_f:

$$R = \frac{0.0042(f_c^{'})^{2/3} w_{fe}}{(E_f t_f)^{0.58} \varepsilon_{fu} d_f} \tag{17}$$

As pointed out by Sas et al (2009), the main limitation of this model corresponds to the limited data available at the moment of the model's derivation. This derivation is based mainly on test made using CFRP and β=90° but the authors recommend its use for any kind of sheets and orientation of the sheets which, again, implies that the model should be revised in order to obtain more specific equations.

It also has to be considered that even though it is stated that fully wrapped beams are more likely to have a failure mode governed by FRP delamination, the data of the test for these kind of beams, which actually corresponds to an important part of the database, were considered in order to obtain equation No. 10.

As long as the formulation for fully wrapped beams, the paper presented by Khalifa doesn't give much information about the database used in order to find the equations proposed. However, it is clear that

these equations were also based in a limited database and the same drawbacks explained before, apply here as well.

3.2. V_f according to ACI 440

For completely wrapped members, the rupture failure must be expected and it is described by the ACI 400 as loss of aggregate interlock of the concrete at fiber strains less than ultimate fiber strain. The formulation proposed, based on experience and the testing carried out by Priestley et al (1996), is:

$$\varepsilon_{fe} = 0.004 \leq 0.75\varepsilon_{fu} \tag{18}$$

It has to be said that even though equations 10 and No. 17 are based in testing, their use will imply obtaining considerable different results. Another important remark is related to the fact that the formulation of the ACI 440 neglects the influence of the axial rigidity that has shown to have an important influence as noticed by different authors (Khalifa et al 1998, Triantafillou 1998). However, this point will be retaken when the comparison of the theoretical values obtained by the codes and the experimental ones is performed.

For bonded U-wraps or bonded face plies, the ACI-440 agrees with the fact that the elements strengthened in this fashion are more likely to present a failure mode based on a mechanism of delamination of the FRP from the concrete before the loss of aggregate interlock of the section. Taking this into account, the bond stress becomes relevant in order to compute the ultimate level strain. The equation proposed by the ACI 440 is as follows:

$$\varepsilon_{fe} = k_v \varepsilon_{fu} \leq 0.004 \tag{19}$$

Where k is the bond-reduction factor that depends on the concrete strength, the type of wrapping scheme and the stiffness of the lamínate. The equations presented on ACI-440 that are based on the investigation carried out by Khalifa (1998) are as follows:

$$\kappa_v = \frac{k_1 k_2 L_e}{11900\varepsilon_{fu}} \leq 0.75 \tag{20}$$

$$L_e = \frac{416}{\left(nt_f E_f\right)^{0.58}} \tag{21}$$

The factors k_1 and k_2 take into account the concrete strength and the type of wrapping respectively.

$$k_1 = \left(\frac{f_c'}{27}\right)^{2/3} \tag{22}$$

$$k_2 = \frac{d_f - L_e}{d_f} \rightarrow for\, U\ wraps \tag{23}$$

$$k_2 = \frac{d_f - 2L_e}{d_f} \rightarrow for\, two-sided\ bonded \tag{24}$$

It is important to notice that in the ACI-440 it is stated that the equation for k_v has been validated for regions with low moments and high shear but it is expected to be conservative for cases where high moments are presented simultaneously with high shears.

The ACI 440 presents a graph where it is possible to compare the theoretical values of V_f found by the use of the equations above and the results reported by Khalifa et al (1998). In this graph it is possible to observe that the methodology proposed seems to be highly conservative for fully wrapped elements. In addition, based on the data presented in this graph, the data seems to be scarce, mainly for not fully wrapped specimens.

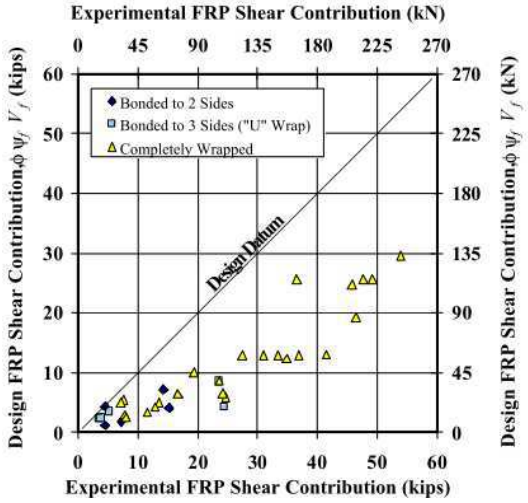

Figure No. 8. Comparison of experimental results to the results using the ACI 440 procedure.

However, in this point it has to be noticed that even though, the ACI 440 the work presents as main reference the work by Khalifa in 1998, the equations of that paper and the ones of the standard, are not the same. The main differences are found in the experimental coefficients for the bond length and the factor k_1. These differences imply a variation of more or less the 10% of the value of V_f (the factor

of 0.0042 proposed by Khalifa in the equation No. 17 changes to 0.0038 when computed according to ACI 440 recommendations). These differences could be explained by the incorporation of new tests to the database used by Khalifa, but this point is not clarified in the Standard. Furthermore, more recent investigation carried out by Khalifa (Khalifa et al (2000), Khalifa et al (2002)) has changed the form of the equation for delamination of the FRP sheets which hasn't been included in the formulation of the ACI 440.

4. FIB BULLETIN 14: EXTERNALLY BONDED FRP REINFORCEMENT FOR RC STRUCTURES

The Fib bulletin is based on the work carried out by Täljsten (1998), Triantafillou (1998) and Triantafillou and Antonopoulos (2000). In their reports they proposed the use of the effective strain as the strain level in which the FRP sheet is stressed when the concrete element reaches its shear capacity. The concept of this effective strain has been used by many researchers, including Khalifa et al (1998), as shown before.

In his model, Triantafillou (1998) used the classical truss analogy, treating the external FRP reinforcement as internal steel shear reinforcement, considering that the material develops the effective strain in the ultimate limit state in shear. The FRP contribution to the shear capacity can then be computed as:

$$V_{fd} = 0.9\varepsilon_{fd,e} E_{fu} \rho_f b_w d(\cot\theta + \cot\alpha)\sin\alpha \qquad (25)$$

In the previous equation the angle θ is the angle of diagonal crack . This equation is equivalent to equation No. 7, when the angle θ is considered to be equal to 45°, which is actuall y a usual assumption.

In order to compute the value of the effective strain, Triantafillou and Antonopoulos (2000), used the same methodology followed by Khalifa et al (1998), considering the results provided by different investigation in the field (see Table No. 5), but including a larger database due to the new results obtained in the years between the publications.

Table No. 5. Summary of tests used by Triantafillou and Antonopoulos (2000).

REFERENCE	SHEAR STRENGTHENING MATERIAL			Number of samples
	Fibers	Configuration	β°	
Berset (1992)	Glass	Sheet bonded to beam sides	45	2
Uji (1992)	Carbon	Sheet bonded to beam sides	90	3
	Carbon	Sheet wrapped around the beam	90	1
Al-Sulaimani et al (1994)	Glass	Sheet bonded to beam sides	90	2
Ohuchi et al (1994)	Carbon	Sheet wrapped around the beam	90	13
Chajes et al (1997)	Aramid	Sheet in form of U-jacket	90	1
	Carbon	Sheet in form of U-jacket	90	1
	Carbon	Sheet in form of U-jacket	45	1
	Glass	Sheet in form of U-jacket	90	1
Sato et al (1996)	Carbon	Sheet bonded to beam sides	90	2
	Carbon	Sheet in form of U-jacket	90	2
Antonopoulos (1996)	Carbon	Sheet bonded to beam sides	90	3
	Carbon	Sheet bonded to beam sides	45	1
Myyauchi et al (1997)	Carbon	Sheet wrapped around the beam	90	3

REFERENCE	SHEAR STRENGTHENING MATERIAL			Number of samples
	Fibers	Configuration	β°	
Taerwe et al (1997)	Carbon	Sheet in form of U-jacket	90	3
	Carbon	Sheet wrapped around the beam	90	1
Funakawa et al (1997)	Carbon	Sheet wrapped around the beam	90	3
Umezu et al (1997)	Carbon	Sheet wrapped around the beam	90	3
	Aramid	Sheet wrapped around the beam	90	12
Araki et al (1997)	Carbon	Sheet wrapped around the beam	90	5
	Aramid	Sheet wrapped around the beam	90	3
Sato et al (1997)	Carbon	Sheet in form of U-jacket	90	2
Ono et al (1997)	Carbon	Sheet wrapped around the beam	90	5
Taljsten (1997)	Carbon	Sheet bonded to beam sides	45	3
			Total	76

In order to obtain the equations for the effective strain, the researchers took into account that it depends on the effective bond length which is influenced by the bond conditions, the axial rigidity and the tensile strength of the concrete. With these considerations in mind, they developed a set of equations in order to compute the effective strain (see equations No. 26, No. 27 and No. 28). Figure No. 9 presents the normalized FRP strains in terms of the axial rigidity and the concrete strength for the database used and it also includes the equations proposed.

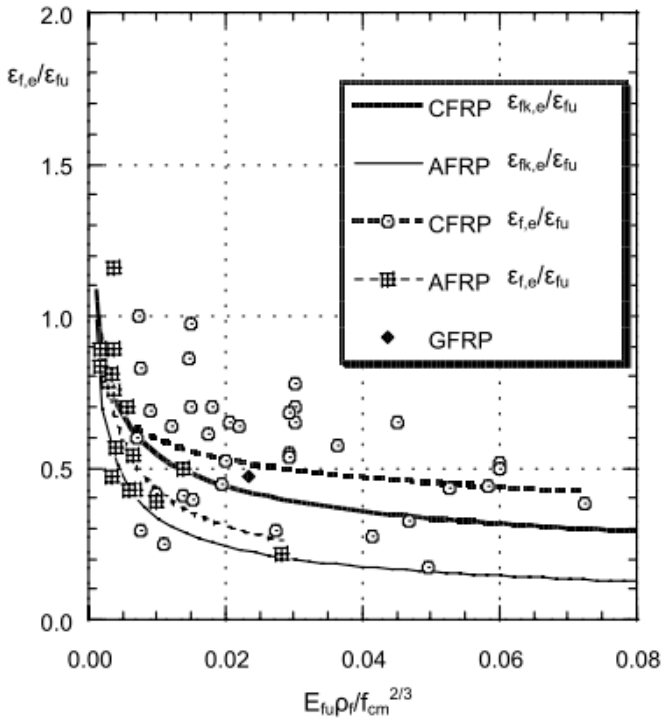

Figure No. 9. Comparison of experimental results to the equations proposed by Triantafillou and Antonopoulos (2000).

- For Fully wrapped (or properly anchored) CFRP-FRP fracture controls:

$$\varepsilon_{f,e} = 0.17\left(\frac{f_{cm}^{2/3}}{E_{fu}\rho_f}\right)^{0.30}\varepsilon_{fu} \tag{26}$$

- For side or U-shaped CFRP jackets:

$$\varepsilon_{f,e} = \min\left[0.65\left(\frac{f_{cm}^{2/3}}{E_{fu}\rho_f}\right)^{0.56} x10^{-3}, 0.17\left(\frac{f_{cm}^{2/3}}{E_{fu}\rho_f}\right)^{0.30}\varepsilon_{fu}\right] \tag{27}$$

- Fully wrapped AFRP (FRP fracture controls):

$$\varepsilon_{f,e} = 0.048\left(\frac{f_{cm}^{2/3}}{E_{fu}\rho_f}\right)^{0.47}\varepsilon_{fu} \tag{28}$$

The value used of effective strain used in the design, $\varepsilon_{fd,e}$, should be computed from the characteristic value, $\varepsilon_{fk,e}$, divided by the partial safety factor. The characteristic value, according to the recommendations of the fib bulletin should be taken as the 80% of the effective strain computed by the set of equations presented above. As long as the partial safety factor, the fib bulletin considers different values, regarding the type of failure mechanism expected:

Table No. 6. Partial safety factors proposed by the *fib* BULLETIN 14.

FAILURE MECHANISM	FRP TYPE	APPLICATION TYPE	
		A	B
FRACTURE	CFRP	1.2	1.35
	AFRP	1.25	1.45
	GFRP	1.3	1.5
DEBONDING	ALL	1.3	

In Table No. 6, application type A corresponds to the application of prefab FRB EBR systems where all the provisions are taken in order to obtain a high degree of quality control. Application type B, in the other hand, is related to the application of any system under difficult on-site working conditions.

As long as the limit for the effective strain, the *fib* BULLETIN proposes a value of 0.006 in order to maintain the integrity of concrete and secure the activation of the aggregate interlock. When this value if affected by the partial safety factor and multiplied by the 80% corresponding to the characteristic

value, a limitation approximately equal to 0.004 is achieved, which agrees with the one proposed by the ACI 440.

The main drawback of this approach pointed out in the Fib bulletin but also by Sas et al (2009), is that the model does not take into account the FRP bonded length explicitly. However, in the *fib* it is stated that this can be justified by:

- The effective bond length is typically a small fraction of the RC member's depth and, therefore, the partially ineffective FRP turns to be contained in to a small fraction of the total depth.
- The effect of short FRP bonded length might have been taken into account through the data fitting and experimental procedure.

Another drawback of the model is related to the limited data available when it was calibrated which leads to a inaccuracy in the prediction of the contribution of the FRP reinforcement to the shear capacity as can be seen in Figure No. 9 and Figure No. 10. However, Sas et al (2009) considered that the similar distribution around the bisector in Figure No. 10 can point out regression as being an acceptable method for deriving a viable model.

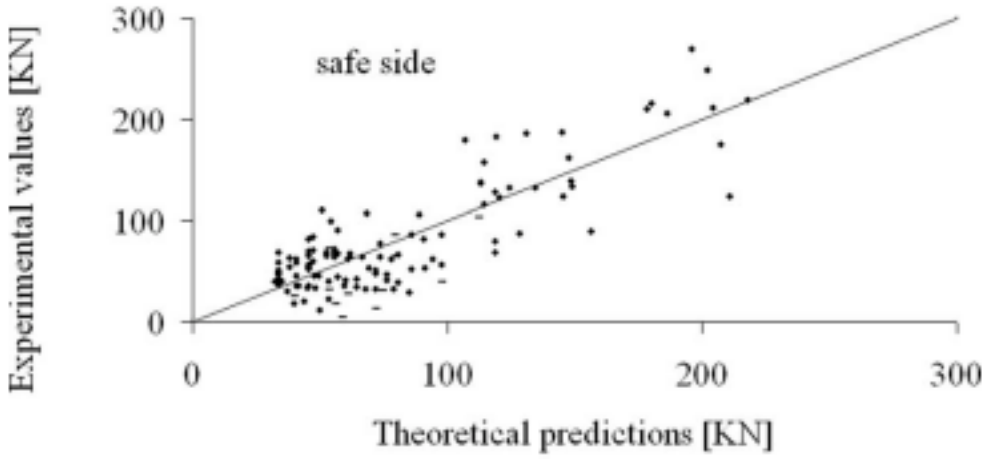

Figure No. 10. Triantafillou (1998) and Triantafillou and Antonopoulos (2000) model comparisons (taken from Sas et al (2009)).

5. CNR-DT 200/2004: GUIDELINES FOR THE DESIGN AND CONSTRUCTION OF EXTERNALLY BONDED FRP SYSTEMS FOR STRENGTHENING EXISTING STRUCTURES

According to the Italian guidelines, the shear capacity of FRP strengthened member should be evaluated as:

$$V_{Rd} = \min\left\{V_{Rd,ct} + V_{Rd,s} + V_{Rd,f}, V_{Rd,\max}\right\} \tag{29}$$

With $VR_{d,ct}$ and $V_{Rd,s}$ are the concrete and steel contribution strength computed according to the current building code. $VR_{d,f}$, in the other hand, corresponds to the FRP contribution. However, the code sets a maximum value of the total shear capacity ($V_{Rd,max}$) that should be evaluated as the ultimate strength of the concrete strut according, again, to the current building code.

For rectangular concrete members strengthened with a FRP side bonding configuration, the CNR-DT 200 proposes that the shear contribution should be calculated as:

$$V_{f,d} = \frac{1}{\gamma_{Rd}} \min\left\{0.9d, h_w\right\} f_{fed}\, 2t_f \frac{\sin\beta}{\sin\theta} \frac{w_f}{s_f} \tag{30}$$

In the previous equation, the partial factor (γ_{rd}) shall be assumed equal to 1.20, d is the member effective depth, h_w is the stem depth, t_f is the thickness of the adopted FRP system, β is the fibers angle with respect to the member longitudinal axis, t represents the angle of shear cracks (to be assumed equal to 45° unless a more detailed calcula tion is made) and w_f and p_f are FRP width and spacing respectively, measured orthogonally to the fiber direction (see Figure No. 11). For FRP strips installed one next to each other the ratio wf/pf shall be set equal to 1.0. The effective FRP design strength (f_{fed}) for this case should be computed following the next equations:

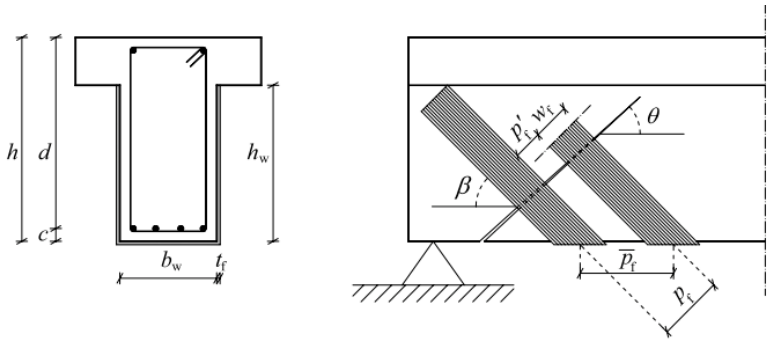

Figure No. 11. Triantafillou (1998) and Triantafillou and Antonopoulos (2000) model comparisons (taken from Sas et al (2009)).

$$f_{fed} = f_{fdd}\frac{z_{red,eq}}{\min\{0.9d, h_w\}}\left(1-0.6\sqrt{\frac{L_{eq}}{z_{red,eq}}}\right)^2 \quad (31)$$

$$z_{red,eq} = z_{red} + L_{eq} \quad (32)$$

$$z_{red} = \min\{0.9d, h_w\} - l_e \sin\beta \quad (33)$$

$$L_{eq} = \frac{s_f}{f_{fdd}/E_f}\sin\beta \quad (34)$$

$$l_e = \sqrt{\frac{E_f t_f}{2 f_{ctm}}} \quad (35)$$

Where le is the effective bond length and sf is the ultimate debonding slip assumed to be equal to 0.2 mm and Ef is the FRP young modulus of elasticity. The variable f_{fdd} represents the ultimate design strength, to be evaluated according to the next equations:

$$f_{fdd} = \frac{0.80}{\gamma_{fd}}\sqrt{\frac{2E_f G_{fk}}{t_f}} \quad (36)$$

$$G_{fk} = 0.03 k_b \sqrt{f_{ck} f_{ctm}} \quad (37)$$

For U-jacket, the expressions recommended are:

$$V_{f,d} = \frac{1}{\gamma_{Rd}} 0.9 d f_{fed} 2 t_f \left(\cot\theta + \cot\beta\right)\frac{w_f}{s_f} \quad (38)$$

$$f_{fed} = f_{fdd}\left(1 - \frac{1}{3}\frac{L_e \sin\beta}{\min\{0.9d, h_w\}}\right) \quad (39)$$

For the wrapped configuration, the equation proposed for Vf,d for U-jacket configuration should be used but f_{fed} is given by:

$$f_{fed} = f_{fdd}\left[1-\frac{1}{6}\frac{L_e \sin\beta}{\min\{0.9d, h_w\}}\right]+\frac{1}{2}\left(\phi_R f_d - f_{fdd}\right)\left[1-\frac{L_e \sin\beta}{\min\{0.9d, h_w\}}\right] \quad (40)$$

$$\phi_R = 0.2+1.6\frac{r_c}{b_w}; \qquad 0 \le \frac{r_c}{b_w} \le 0.5 \quad (41)$$

Where r_c is the corner radius of the section to be wrapped and b_w is the width of the member. The second term in the equation for f_{fed} should be considered only when it is greater than zero.

6. EVALUATION OF CODES

In this chapter, the comparison between the experimental values of different test carried out on concrete beams strengthened by FRP and the values predicted by the equations of the studied codes is presented. Before doing this, a brief description of the comparison parameters used is done, including the range considered as representative of a good performance (see 6.1).

The evaluation of the codes is made using the total database improved during the execution of this document. The total value of the theoretical shear strength (concrete, steel and FRP contribution) is compared without distinguishing the type of strengthened scheme used in the tests. In addition, the same comparison is carried out for the FRP contribution only.

However, a second type of comparison is performed dividing the database in groups depending on the type of strengthened scheme. After this, a new comparison is made considering whether or not the samples include shear reinforcement. For these two parts, only the FRP contribution is analyzed due to the results found in 6.2 and the reasons explained in 6.3.

6.1. Comparison parameters

In order to compare the different codes here studied, three different parameters are used. The codes will be assessed based on two main factors. The first one is related to the correlation between the theoretical and experimental values. However, in order to establish the real accuracy of the codes and how reliable they are, the safety achieved by each one will also be evaluated.

6.1.1. Correlation coefficient (R^2)

The first comparison parameter is based on the Pearson correlation coefficient (R). This coefficient is used in order to measure the correlation (linear dependence) between two variables, giving values between +1.0 and -1.0 inclusive. A value of 1.0 implies that a linear equation describes the relationship between the two variables, with all the data points on a line in which one variable increases as the other one does. A value of -1.0, on the other hand, implies that all the data points lie on a line in which if one variable increases, the other one decreases. A value of 0.0 implies that there is no linear correlation between the variables. The expression used to compute the Pearson coefficient for variables “x” and “y” is given below:

$$r = \frac{\sum (x-\bar{x})(y-\bar{y})}{\sqrt{\sum (x-\bar{x})^2 (y-\bar{y})^2}} \tag{42}$$

In the previous equation “$\bar{x}$” and “$\bar{y}$” corresponds to the points of the sample data. However, as a matter of routine, it is the squared of the Pearson coefficient (r^2 or R^2) the one that is used to compare the variables. This is because the correlation coefficient is misleading in suggesting the existence of more co-variation than exists, and this problem gets worse as the correlation approaches to zero. The

value of R^2 can be understood as the percent of the data that is the closest to the line of best fit. For example, if r=0.894, then R^2=0.800, which means that the 80% of the total variation of variable "y" can be explained by the linear relationship between "x" and "y" (as described by a linear regression equation). The other 20% of the total variation of "y" remains unexplained.

Considering the multiple variables involved and the experimental nature of most of the equations used by the codes, values of R^2 higher than 70% can be related to a good performance of the equations proposed by the guidelines. It is also important to highlight that higher values of R^2 just tell information about the good correlation between the theoretical and experimental values but they don't give information about the structural performance that could be achieved using a given code. In order to have a more clear understanding, it is recommended to see Figure No. 17 in which a value of R^2 close to the one considered as appropriate is obtained. However, in the same graph, it is possible to observe that all the most of the points fell in the side considered as unsafe, which implies that even though a reasonable correlation is achieved, the results would lead to a non-conservative design.

6.1.2. Global safety factor (SF)

The second parameter used corresponds to the global safety factor (SF) that is achieved by using a given code. This value is computed as the inverse of the coefficient of a trend line obtained by assuming a linear dependence between the theoretical and experimental values. In the figures that will be presented in this chapter, two straight lines are included. The first one, inclined 45°, represents the trend line that would be obtained if the theoretical values are equal to the experimental ones. This line also helps dividing the pairs of point into unsafe or safe. The dashed line, in the other hand, corresponds to the actual linear regression obtained for the set of data.

It has to be said that the SF factor is computed as the inverse of the linear coefficient because the graphs are made in a way that implies that the theoretical values are a function of the experimental ones. This was done considering that most of the equations are based in regressions obtained from the experimental data found by several researchers. In order to clarify this point, the following equation is presented:

$$V_{n,theo} = mV_{n,\exp} \rightarrow \frac{1}{m} = SF \tag{43}$$

It is important to notice that the regression line was computed considering a border condition which takes into consideration that a value of 0.0 in the experimental data ($V_{n,exp}$=0.0) should be related to a prediction of 0.0 by the theoretical equations ($V_{n,theo}$=0.0).

As limit of appropriate safety a value of 1.0 is selected taking into account that the theoretical values were computed with using the load and material safety factors included by the code. It is needed to point out that even if a value of SF higher than 1.0 is obtained, it doesn't imply that the code is completely safe because an important number of points could fell in the unsafe side of the graphs. An

example of this situation can be seen in Figure No. 15 in which a SF of 1.03 is obtained. Nevertheless, for that particular case, it is clear that a percentage of points close to the 50% are located in the unsafe side of the graph. Taking this into account, it is also important to know which percentage of the predicted values corresponds to unsafe predictions. In order to do so, a third parameter based on a demerit points classification is also used (see 6.1.3). However, the global safety factor represents a fast way to compare the different codes and in general. Values higher than 1.00 might be considered as adequate but a more detailed study of these factors should be made based on the results obtained using the demerit points classification system.

6.1.3. Demerit points classification

The third comparison parameter was made using the individual safety factors found for each pair of points. In order to do so, the "Demerit Points Classification" proposed by Lima et al (2007) was used but a modification in the classification of the safety factors was made in order to considerer the fact that the theoretical values here computed correspond to real and not characteristic values. This methodology consists in a weighed penalty evaluation taking into account the security factors. Table No. 7 presents a description of the classification for the safety factors and the penalty system used:

Table No. 7. Comparison of codes based on structural safety.

SAFETY FACTOR	CLASIFICATION	PEN
<0.60	Extremely Dangerous	10
0.60-0.80	Dangerous	5
0.80-1.00	Reduced Safety	2
1.00-1.40	Appropriate Safety	0
1.40-2.40	Conservative	1
>2.40	Extremely Conservative	2
		Summation

The procedure followed consists in multiply the percentage of values that fell inside a category times the respective penalty. At the end, a summation is made in order to obtain a global value for comparison. It has to be said that due to the fact that the percentage of points that are inside a category was used instead of the total number of points used by Lima et al, a comparison between the total database and the reduced ones can be performed easily, allowing a better assessment of the evaluated codes.

6.2. Total Shear Strength

Figure No. 12 presents the comparison of the experimental values (horizontal axis) and the theoretical values (vertical axis) of the total shear strength (concrete, steel and FRP strengthening contribution) of concrete beams computed following the directions described by the ACI-440, the FIB Bulletin 14 and the CNR-DT 200 for the total database obtained during the development of this document. In order to compute the contribution of the concrete and the steel reinforcement, the ACI 318M-05, the Eurocode 2 (EC2) and the IBC – 1996 (Italian building Code) were used and added to the results found by the ACI 440, FIB bulltin 14 and the CNR-DT 200 respectively. In addition, the Italian Guide for externally

bonded FRP systems was also used in conjunction with the Eurocode 2. The first conclusion that can be drawn from Figure No. 12 has to do with the fact that even though there is a considerable scatter within the three different series, it is possible to see a different tendency in each one of them. However, a best interpretation of the data can be performed using Figure No. 13, Figure No. 14 and Figure No. 15 in which the individual data for each code is presented.

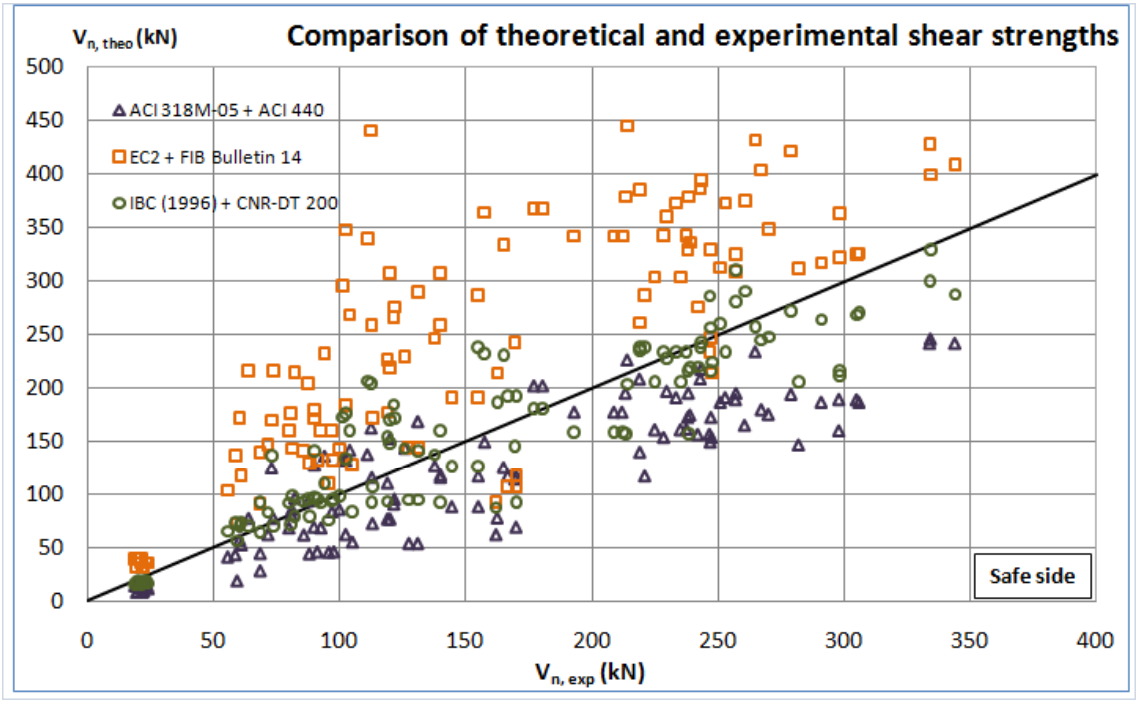

Figure No. 12. Comparison of experimental and theoretical values for the evaluated codes.

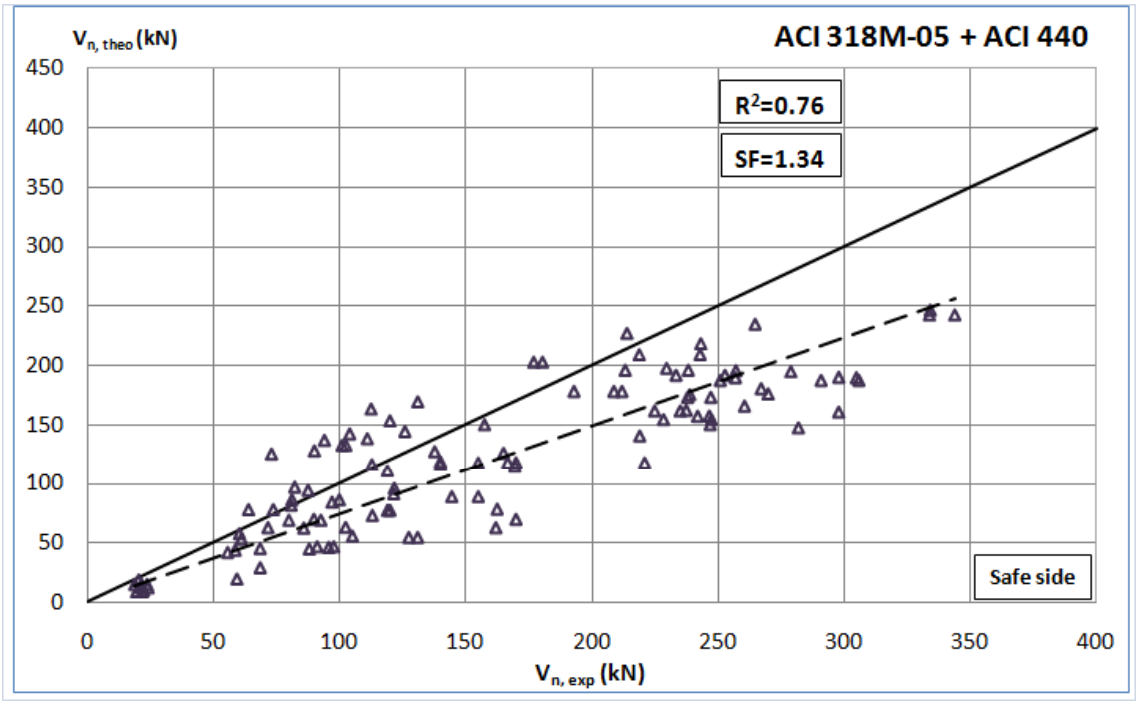

Figure No. 13. Comparison of experimental and theoretical values for ACI318M-05 + ACI 440.

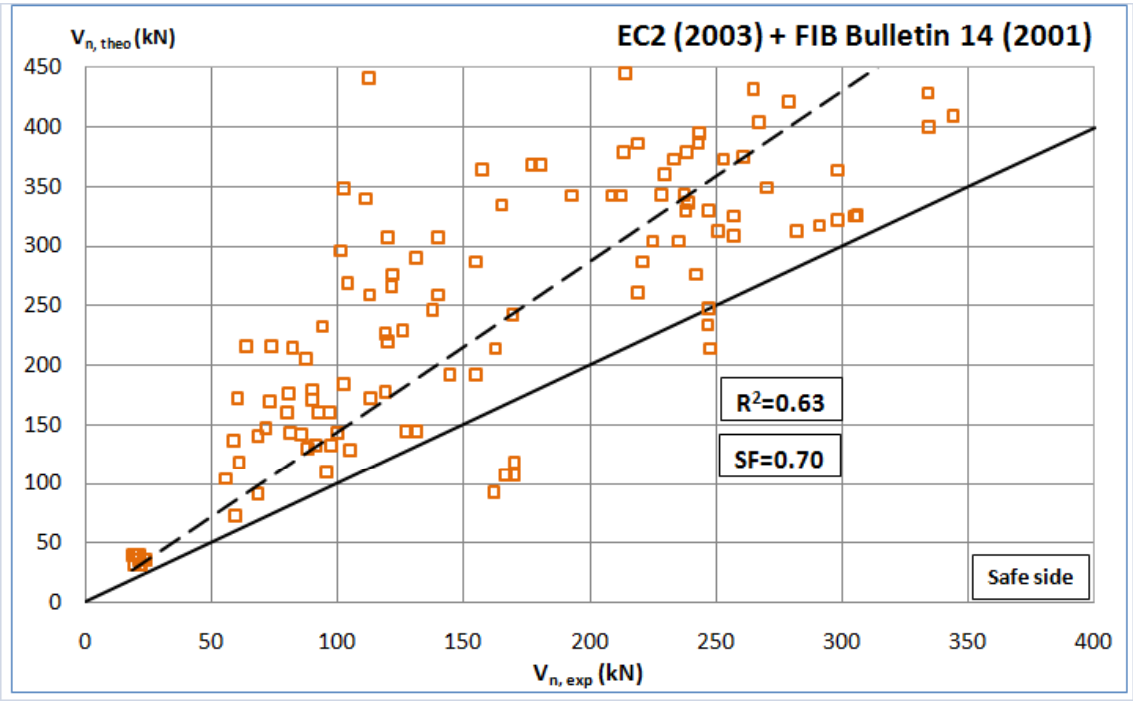

Figure No. 14. Comparison of experimental and theoretical values for EC2 + FIB Bulletin 14.

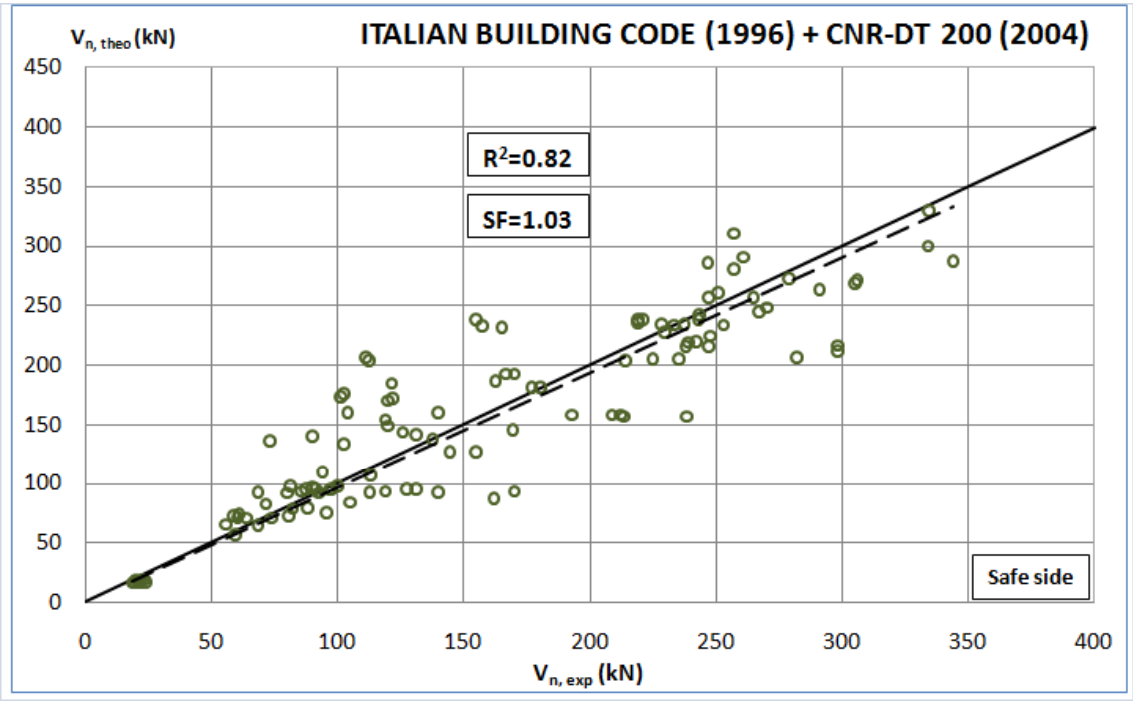

Figure No. 15. Comparison of experimental and theoretical values for IBC + CNR-DT 200.

Figure No. 13 presents the individual values for the ACI 318 + ACI 440. In that figure it is possible to observe that the use of these codes produce values that are mostly safe which leads to a SF=1.34, with a reduced number of points that fell in the unsafe side of the graph. Figure No. 14 corresponds to the comparison for the EC2 + FIB Bulletin 14. For this case, the observed trend differs from the one

obtained for the ACI 440 mainly in the fact that this combination predicts values that are mostly unsafe which leads to a safety factor lower than one (SF = 0.70). Finally, Figure No. 15 shows the behavior obtained for the IBC + CNR-DT 200. It is seen that for this case there is almost the same probability of obtaining safe or unsafe results, which agrees with the fact that the safety factor found is almost equal to 1.0 (SF=1.03).

Taking into account this information, it is possible to conclude that the ACI 318 + ACI 440 is by far the combination that predicts the safer results. The IBC + CNR-DT 200, even though has a SF higher than one, shows that there will be the same probability of obtaining safe or unsafe results and, therefore, are not able to generate an adequate level of safety. The EC2 + FIB Bulletin 14 has the worst performance of the three codes studied as long as the safety factor is concerned. As a matter of fact, just a small percentage of the data is located in the safe side of graph which leads to conclude that these codes are unable to produce not dangerous values and the combination of the equations could be inappropriate to be used in the design of externally bonded FRP systems for the shear strengthening of concrete beams.

As long as the dispersion of data is concerned, the value of R^2 obtained by the IBC + CNR-DT 200 (R^2= 0.82) is the higher one, but it has to be said that it is just 8% higher than the one computed for the ACI 318 + ACI 440 (R^2=0.76). Both of these values are above the limit considered as appropriate which implicates that the equations of these codes produce results that are correlated enough with the data of the experimental tests. The EC2 + FIB Bulletin 14, in the other hand, has a R^2=0.63 which is below the limit proposed in this document.

When these results are evaluated in conjunction with the ones obtained for the SF, it is possible to conclude that the equations of the EC2 + FIB Bulletin 14 fail in predicting safe results that have a low dispersion with the available experimental data. This behavior is completely opposite to the one found for the ACI 318 + ACI 440 which shows a good performance as long as these two parameters are concerned. The IBC + CNR-DT 200, even though have a high value of R^2, is not able to predict values that are mostly safe, which implies that a examination of their equations and hypothesis should be carried out in order to improve its performance.

After the previous discussion, it is clear that a more detailed evaluation is needed, just as it was stated in 6.1.2. In order to do so, the results of the “Demerit Points Classification” are presented in Table No. 8. As explained in 6.1.3, this table shows the penalty for each one of the categories included and the percentage of points that fell in a given category. The summations of these multiplications produce a number that will be used in order to compare the different codes. However, the table is also useful to identify which code has the largest percentage of unsafe results, which turns out to be an important parameter to be evaluated.

Table No. 8. Comparison of codes based on structural safety.

SAFETY FACTOR	CLASIFICATION	PEN	ACI 440	FIB Bulletin 14	CNR-DT 200
<0.60	Extr. Dangerous	10	0.009	0.425	0.044
0.60-0.80	Dangerous	5	0.071	0.354	0.097
0.80-1.00	Reduced Safety	2	0.106	0.168	0.292
1.00-1.40	Appropriate Safety	0	0.381	0.018	0.513
1.40-2.40	Conservative	1	0.407	0.035	0.054
>2.40	Extr. Conservative	2	0.027	0.000	0.000
		Summation	1.115	6.389	1.566

In Table No. 8 It is possible to observe that the combination of the EC2 with *fib* Bulletin presents the poorest performance among the analyzed codes, with a total summation that is almost 6 times the one obtained for the ACI 440. This result was highly anticipated by the trend and the safety factor found in Figure No. 14. Looking in detail Table No. 8, it is seen that just the 5.3% of the results predicted by this code are on the limit assumed for appropriate safety, with most of them found in the range considered as extremely dangerous. For the ACI 318M-05 + ACI 440 the lower value of summation is computed. As a matter of fact, less than the 8% of the results is in the range considers as dangerous or extremely dangerous. The IBC (1996) + CNR-DT 200 presents a better behavior than the *fib* Bulletin but fells far behind from the ACI 440. However, it is found that most of the values are still under the level accepted as safe and it is the code that has the highest percentage located in the appropriate safety range (51.3%).

6.2.1. Variation of variable θ in the EC2 + fib BULLETIN

An evaluation was made varying the values of the variable θ, for the equations of the EC2 and the *fib* BULLETIN. This variable is supposed to range between 21.8° and 45° but usually a value of 45° is used. However, it is possible to obtain an optimal value of θ which, in theory, would produce more accurate results. In order to do so, the summation of the contributions of the concrete, the steel and the FRP is made equal to the maximum of the shear strength permitted by the code (V_{RD}), as shown in the next equation:

$$(1)\ V_{Rd,s} + V_{Rd,f} = V_{Rd,\max}$$

If a value of θ that satisfies this equation inside the range is found, this value is used to compute the shear strength of the element. However, if the value found is not located inside the given range, θ is taken as the one of the values in the extremes of the range (21.8° or 45°), depending on the side in which the condition of equality for the previous equation is achieved. Figure No. 16 is presented in order to clarify the procedure.

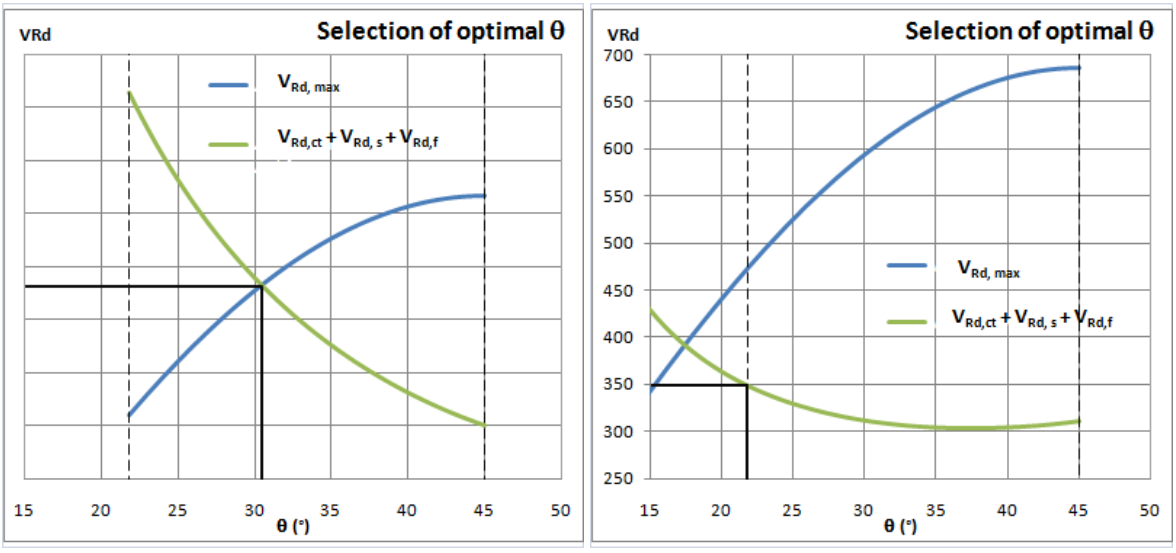

Figure No. 16. Selection of optimal θ: Left: Inside range. Right: Outside range.

When the results of R^2 and SF presented in Figure No. 17 are compared with the ones found in Figure No. 14, it is seen that there is just a slight improvement in both parameters. This result implies that performing this type of analysis that is supposed to be more accurate but time consuming, doesn't lead to an important the enhancement of the performance of the codes.

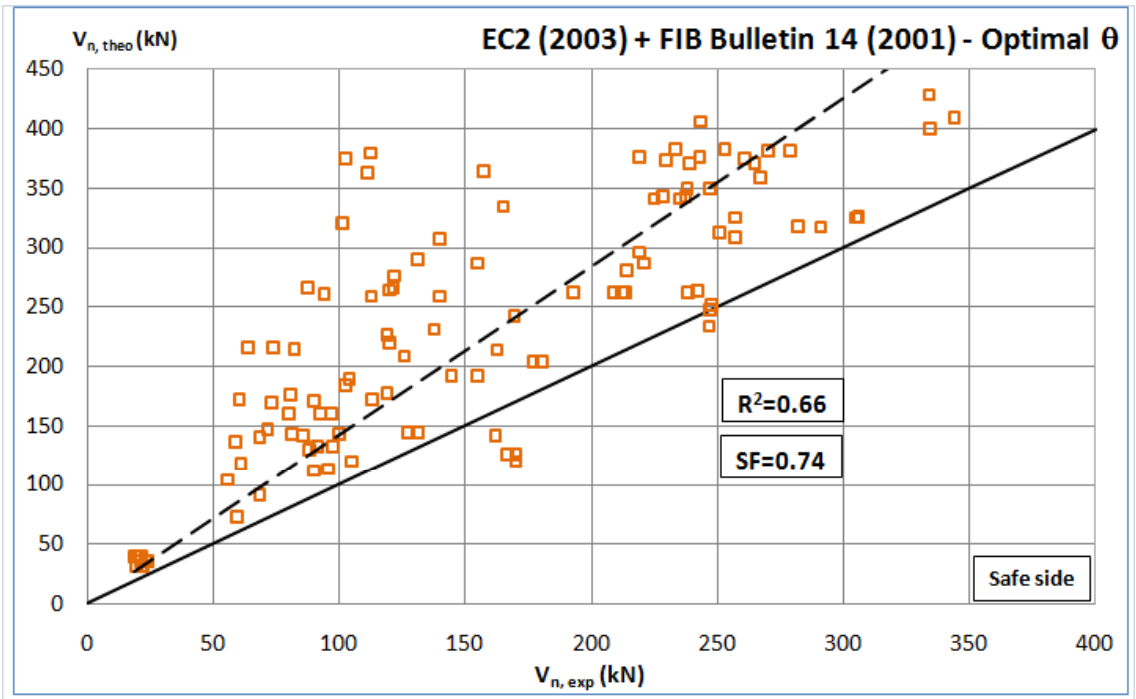

Figure No. 17. Comparison of experimental and theoretical values for EC2 + FIB Bulletin 14 (optimal θ).

As long as the demerit classification system, according to the results shown in Table No. 9, there is not an important improvement of the total summation. When the percentages of points below the safety factor of 0.8 are compared, it is seen that even though the values in the extremely dangerous zone are lower when θ varies, the total percentage in the dangerous or extremely dangerous zone remains practically equal.

Table No. 9. Comparison of EC2 + *fib* BULLETIN with constant or varying θ.

SAFETY FACTOR	CLASIFICATION	PEN	θ=45°	Varying θ
<0.60	Extr. Dangerous	10	0.425	0.389
0.60-0.80	Dangerous	5	0.354	0.363
0.80-1.00	Reduced Safety	2	0.168	0.204
1.00-1.40	Appropriate Safety	0	0.018	0.035
1.40-2.40	Conservative	1	0.035	0.000
>2.40	Extr. Conservative	2	0.000	0.000
		Summation	6.389	6.115

6.2.2. EC2 + CNR-DT 200

Even though the original Italian Guide for externally bonded FRP systems was made to use together with the Italian Building Code, it also establishes that it should be used with the current code. In Italy, the Italian Building Code is still used but it is also possible to perform the design following the recommendations of the Eurocode. For this reason, the evaluation of the CNR-DT 200 was carried out adding the contribution of the steel and the concrete to the total shear strength computed according to the EC2. This new evaluation was also made with the purpose of verify if the performance obtained using the IBC could be improved.

Figure No. 18 shows the comparison between the data found for the IBC or the EC2. Figure No. 19, on the other hand, shows the values of R^2 and SF found for the combination that includes EC2. It is seen that there is an important reduction in the value of R^2 that changes from 0.82 (see Figure No. 15) to 0.73 which implies a reduction of the 11% approximately. The new R^2, however, is still above the limit value which implies that the new combination has an appropriate correlation with the experimental data.

As long as the SF is concerned, an increase of the 9% is found, which allows concluding that the use of the EC2 will lead to safer results and seems to be more appropriate than the IBC.

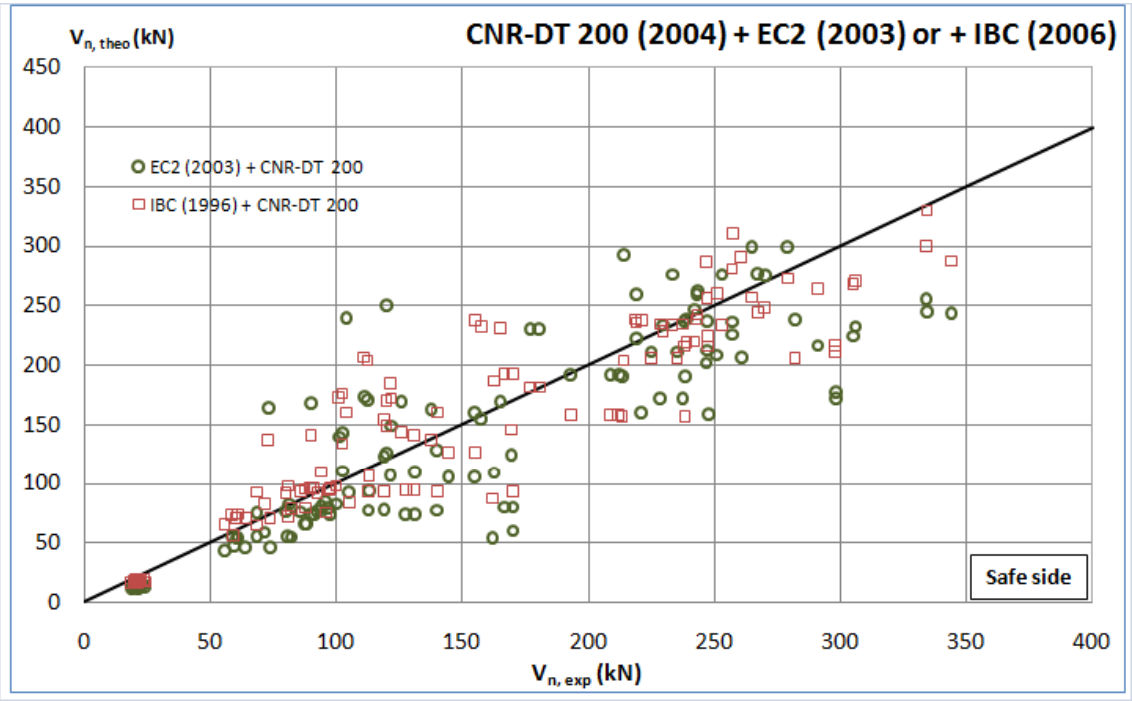

Figure No. 18. Comparison of experimental and theoretical values for CNR-DT 200 + EC2 or + IBC.

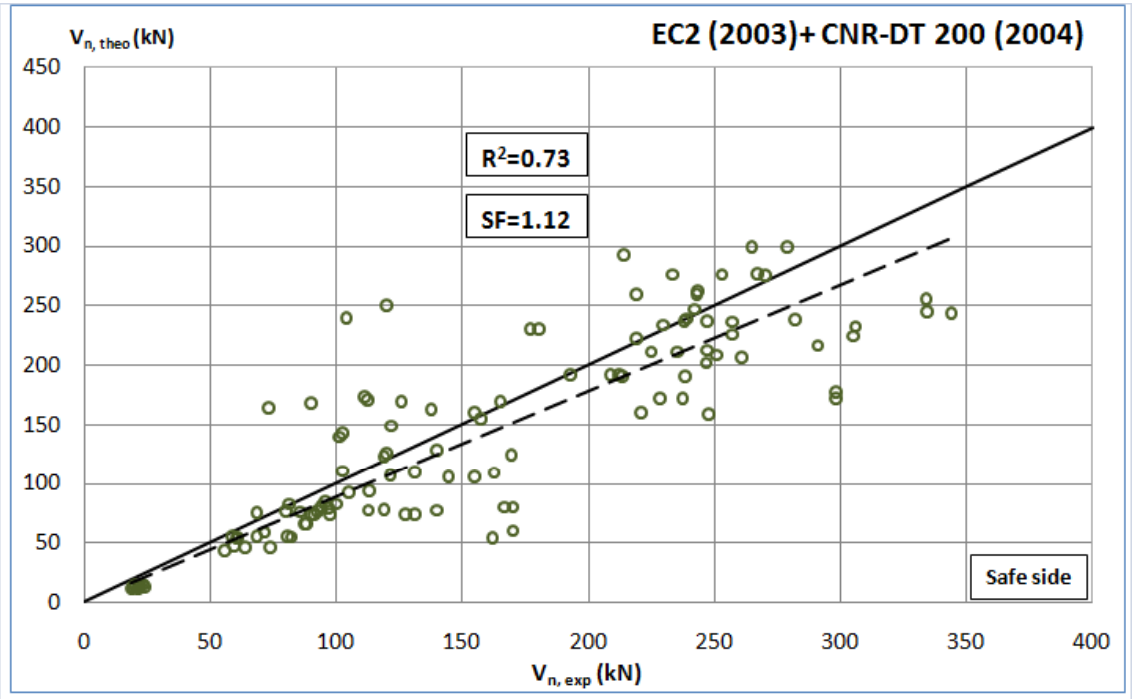

Figure No. 19. Comparison of experimental and theoretical values for EC2 + CNR-DT 200.

In Table No. 10 is possible to observe the comparison of the results found for the IBC and the EC2 in combination with the CNR-DT 200 for the demerit classification points procedure. It is seen that the total value of the summation found when the EC2 is used is lower than the one found for the IBC.

However, this value is still significantly higher than the one computed for the ACI 318 + ACI 440 combination (see Table No. 8).

The use of the EC2 has as consequence an important reduction of the data in the range considered as dangerous or extremely dangerous. When the IBC the percentage in this ranges is 43% but with the EC2 decreases to the 30%. In addition, with the EC2 most of the values are in the zone considered as appropriate safety while when the IBC was used, they were located in the reduced safety area.

Table No. 10. Comparison of CNR-DT 200 with IBC or EC2.

SAFETY FACTOR	CLASIFICATION	PEN	IBC	EC2
<0.75	Extr. Dangerous	10	0.044	0.035
0.75-1.00	Dangerous	5	0.097	0.071
1.00-1.25	Reduced Safety	2	0.292	0.195
1.25-1.75	Appropriate Safety	0	0.513	0.469
1.75-3.00	Conservative	1	0.053	0.212
>3.00	Extr. Conservative	2	0.000	0.018
		Summation	1.566	1.345

As it was done for the EC2 + *fib* BULLETIN (see 6.2.1), the influence of the angle θ was studied for the combination of EC2 + CNR-DT 200. Figure No. 20 presents the values of SF and R^2 found.

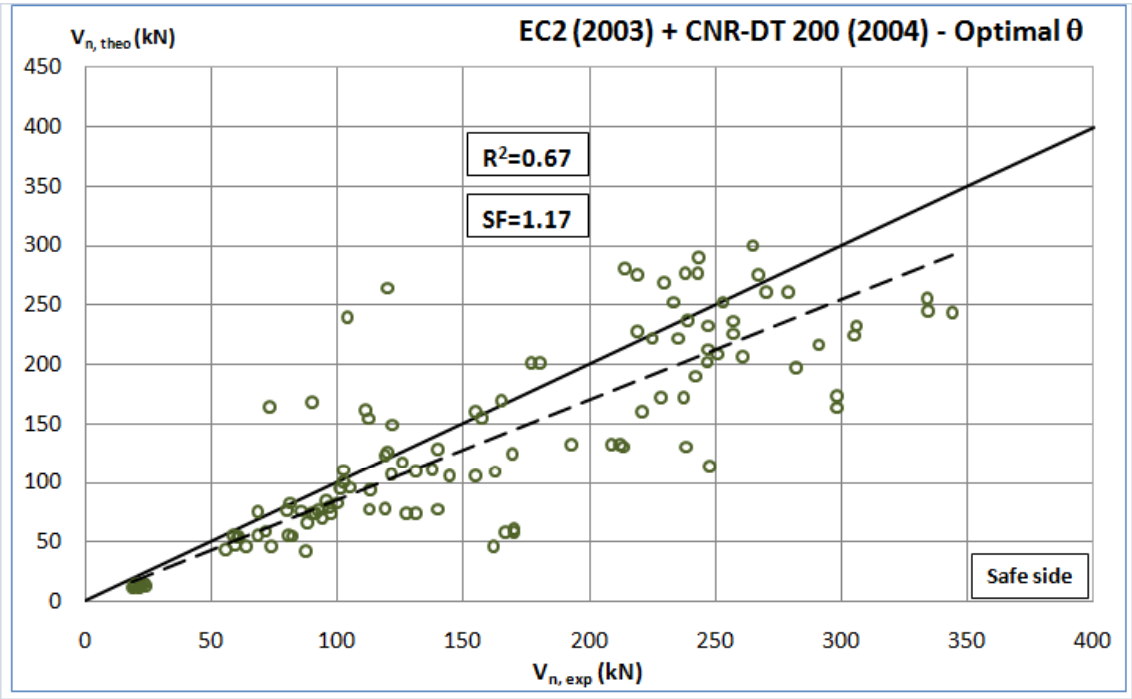

Figure No. 20. Comparison of experimental and theoretical values for EC2 + CNR-DT 200 (optimal θ).

It is seen that for this case just a slight improvement in the safety factor is achieved, when compared with Figure No. 19 as far as the SF is concerned. The correlation factor, on the other hand, presents a small reduction but again, not significant. As it was concluded for the EC2 + *fib* BULLETIN, the use of the optimal θ doesn't imply the achievement of a much better level of safety. This can also be concluded with the data of Table No. 11.

Table No. 11. Comparison of EC2 + CNR-DT 200 with constant or varying θ.

SAFETY FACTOR	CLASIFICATION	PEN	θ=45°	Varying θ
<0.60	Extr. Dangerous	10	0.035	0.035
0.60-0.80	Dangerous	5	0.071	0.035
0.80-1.00	Reduced Safety	2	0.195	0.159
1.00-1.40	Appropriate Safety	0	0.469	0.478
1.40-2.40	Conservative	1	0.212	0.257
>2.40	Extr. Conservative	2	0.018	0.035
		Summation	1.345	1.177

6.3. FRP Contribution

As it was seen before, there are great differences in the behavior when the guidelines are evaluated using the total contribution of the concrete, steel and FRP systems. Taking that into account, for this part, just the contribution of the FRP strengthening is studied (see Figure No. 21).

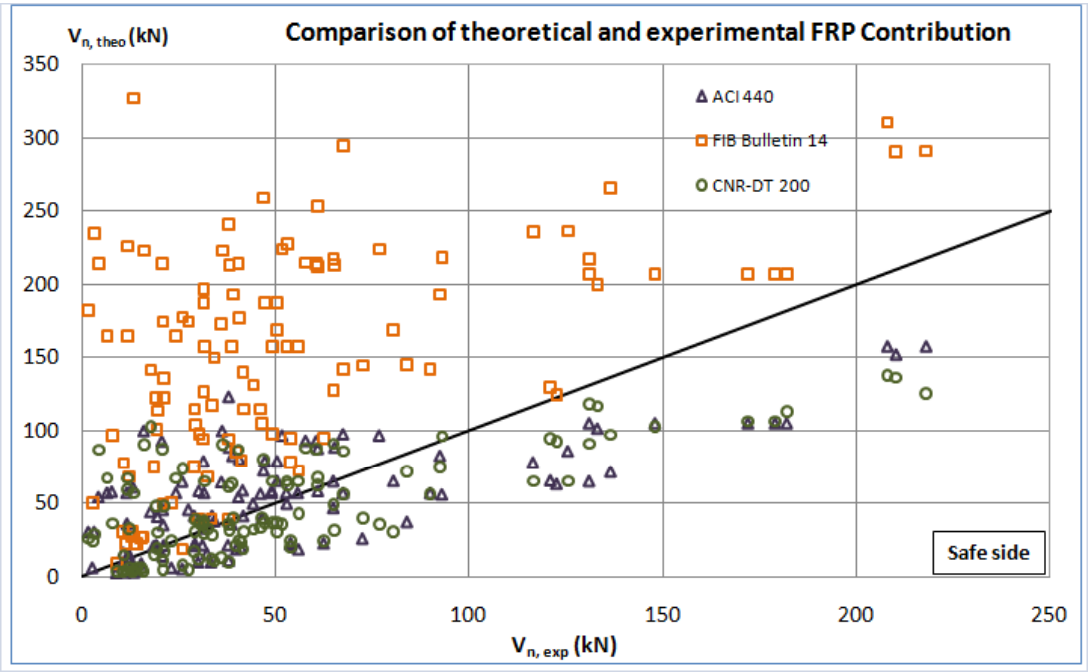

Figure No. 21. Comparison of experimental and theoretical FRP contribution.

In addition to the previous reason, it has to be said that the equations for concrete and steel contribution have been validated for a wider set of experimental data through the years while the

equations for the FRP systems, as it was pointed out in former chapters, are still in a process of development. In order to clarify the differences between the particular equations of the codes, the same procedure made in 6.2 was carried out, including only the results obtained from the ACI 440, the *fib Bulletin* and the CNR-DT 200. Figure No. 21 presents the comparison of the theoretical and experimental values obtained using the codes for the FRP contribution to the shear strength. Figure No. 22, Figure No. 23 and Figure No. 24 present in an individual fashion the trends for the different codes. It is seen that the *fib* bulletin has still the poorest performance as far as the SF is concerned when contribution of the FRP is studied; the safety factor is approximately 40% lower than the one presented in Figure No. 14. The ACI 440 presents a reduction in the SF, but it is still in the range of appropriate safety considered in this document. As far as the Italian guidelines are concerned, a major improvement in the safety is achieved, varying from a SF of 1.03, shown in Figure No. 15 (or 1.12, when the EC2 is used) to 1.33. This implies that when only the FRP contribution on the strengthening is studied, the CNR-DT 200 presents the better performance, as long as the SF is regarded. However, the ACI 440 is still able to predict values that can be considered as mostly safe. However, even though there is an improvement in the SF for the Italian Guideline, it also can be seen an important reduction in the correlation factor R^2. This behavior is also observed for the other two codes. As a matter of fact, when the FRP contribution is studied alone, neither of the codes reaches the target value selected as appropriate (R^2=0.70). The ACI 440 and the CNR-DT 200 have similar values of this factor (0.49 and 0.51, respectively) but the *fib* BULLETIN fells, again, far behind with an R^2=0.26, which could be anticipated just observing the high dispersion of the data presented in Figure No. 23.

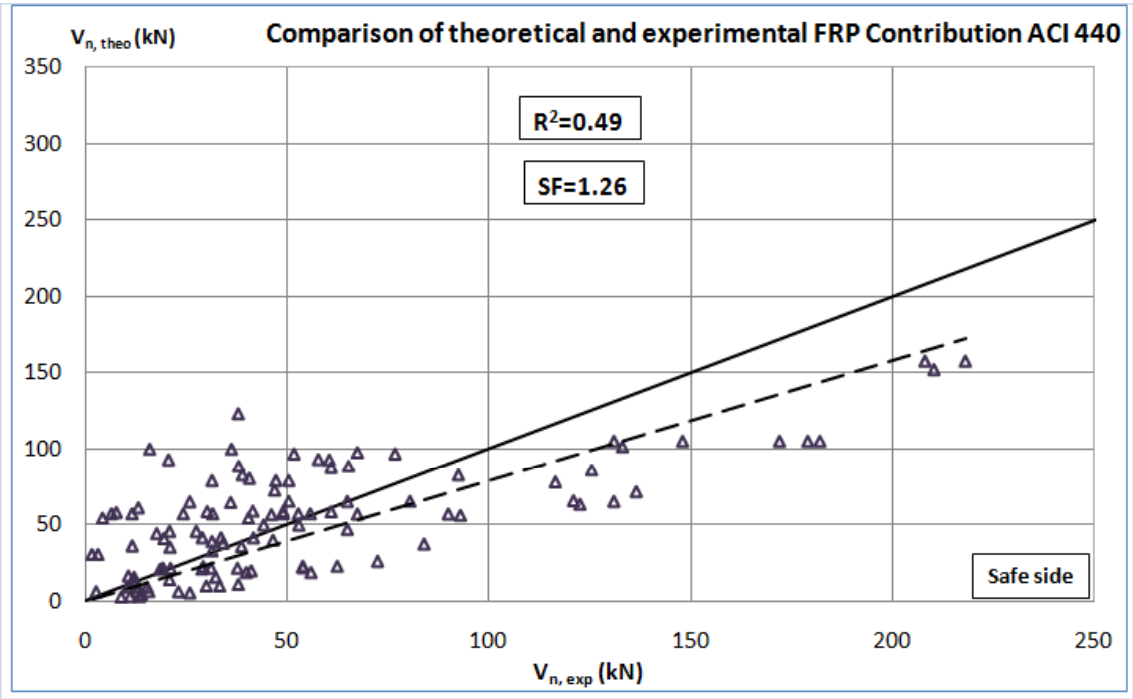

Figure No. 22. Comparison of experimental and theoretical values for ACI 440.

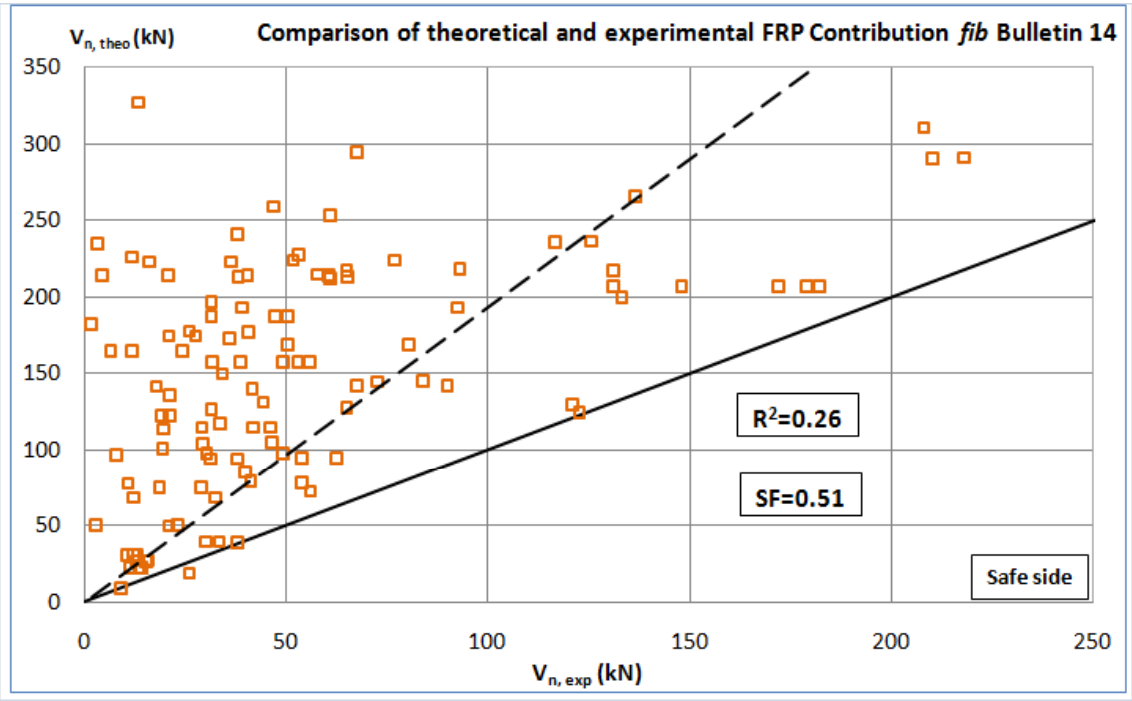

Figure No. 23. Comparison of experimental and theoretical values for *fib* Bulletin 14.

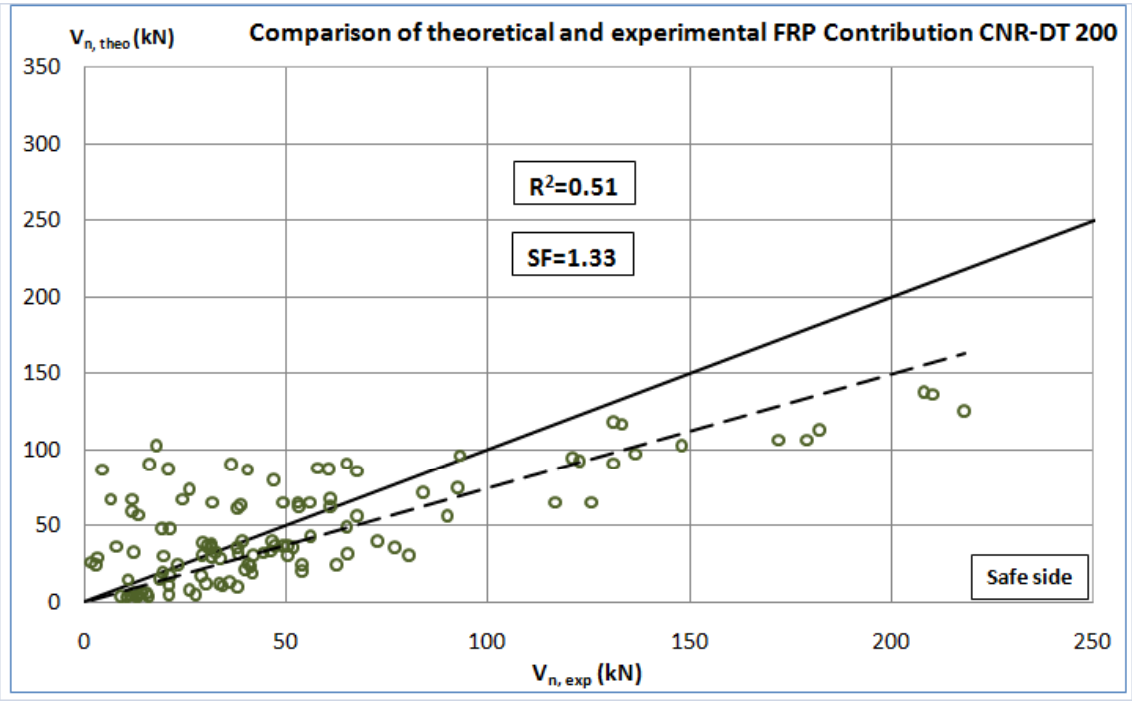

Figure No. 24. Comparison of experimental and theoretical values for CNR-DT 200.

Table No. 12 presents the results found for the Demerit Points Classification. It is seen that the Fib bulletin has, again, the poorest performance. It is also observed that for this code almost all the values

are in the range considered as dangerous, with most to the values being extremely dangerous. For this case, the performance is worst than when it is used in conjunction with the EC2.

For the case of the ACI 440, it is seen that when it works alone, the performance is a little bit worst and it gets closer to the one of the CNR-DT 200. As a matter of fact, for this case, the Italian recommendations are the ones with the lower value of the total penalties summation. It is also seen that for these two codes, the values of extremely conservative predictions increase with respect to the total contribution. It has to be said that for the ACI 440 security factors as high as 17.4 were found, which implies a high inaccuracy between the predicted and the theoretical values, even though the global performance of the model can be assumed as appropriate.

Table No. 12. Comparison of codes for FRP shear contribution based on structural safety.

SAFETY FACTOR	CLASIFICATION	PEN	ACI 440	FIB Bulletin 14	CNR-DT 200
<0.60	Extr. Dangerous	10	0.248	0.805	0.186
0.60-0.80	Dangerous	5	0.142	0.115	0.088
0.80-1.00	Reduced Safety	2	0.088	0.071	0.133
1.00-1.40	Appropriate Safety	0	0.186	0.009	0.195
1.40-2.40	Conservative	1	0.204	0.000	0.239
>2.40	Extr. Conservative	2	0.133	0.000	0.159
		Summation	3.832	8.770	3.124

6.4. Influence of strengthening scheme

The database was divided in order to study the accuracy of the codes for the different strengthening schemes considered. However, it has to be said that there are not enough test for the wrapped configuration and for that reason that scheme is not studied in this section. However, the lack of data about completely wrapped beams is understandable when it is considered that in real applications, strengthen a concrete beam in this fashion is not practical. It also has to be said that for this analysis, only the FRP contribution is considered. This is done taking into account the fact that the influence of the steel and shear contributions estimated by the respective codes don't allow having a clear understanding of the predictions given for the individual FRP contribution. In addition, as it was stated before, the scope of this document is to study the equations for FRP systems due to their more recent development and need of validation.

6.4.1. U-Jacket configuration

Figure No. 25 presents the general comparison between the theoretical and experimental values for the three considered codes when only the U-jacket tests are taken into account. The trend, as it could be expected, is similar to the one presented in Figure No. 21.

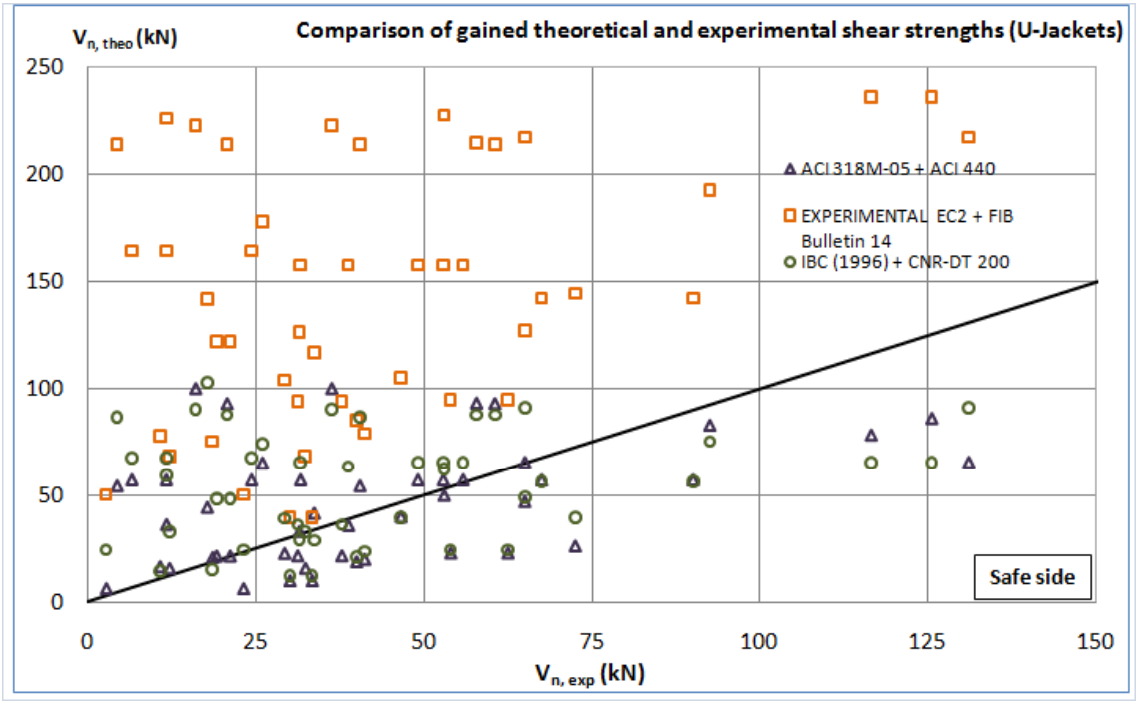

Figure No. 25. Comparison of experimental and theoretical FRP contribution for U-jacket configuration.

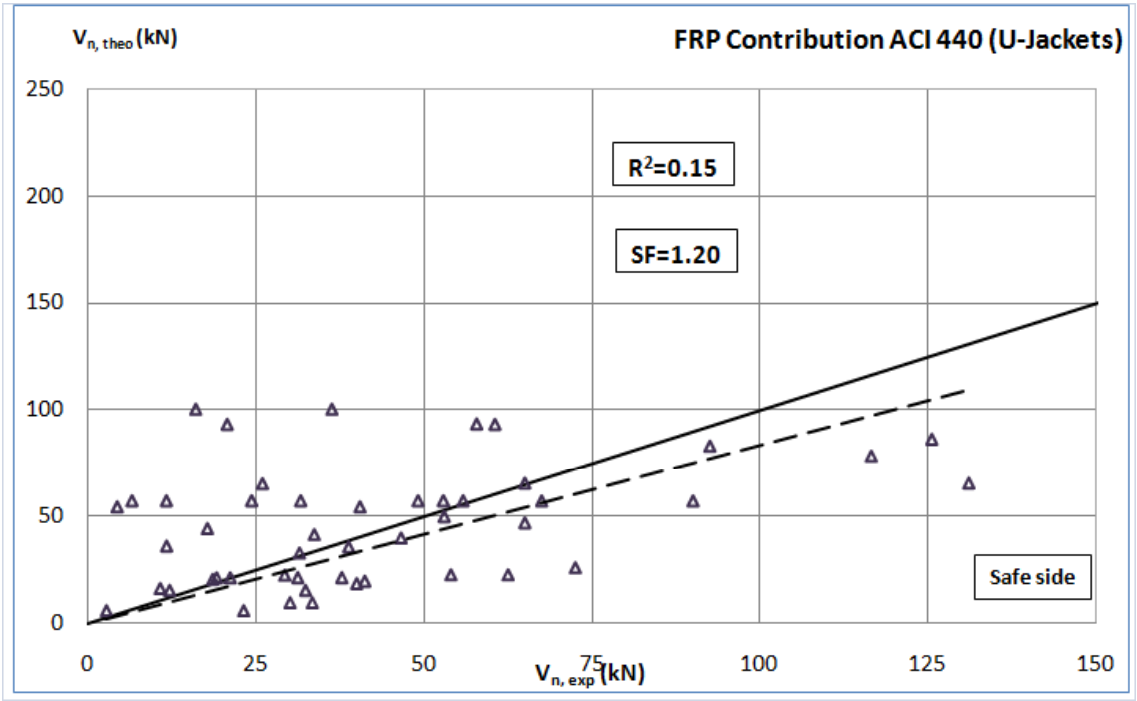

Figure No. 26. Comparison of experimental and theoretical values for ACI 440.

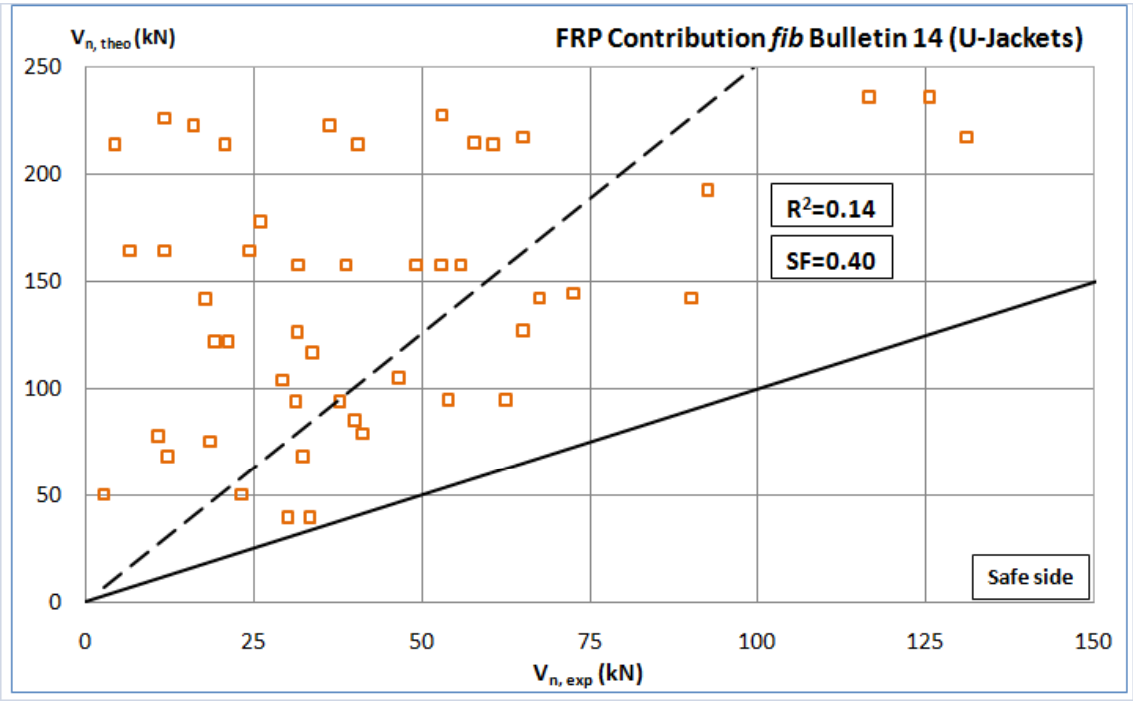

Figure No. 27. Comparison of experimental and theoretical values for *fib* BULLETIN 14.

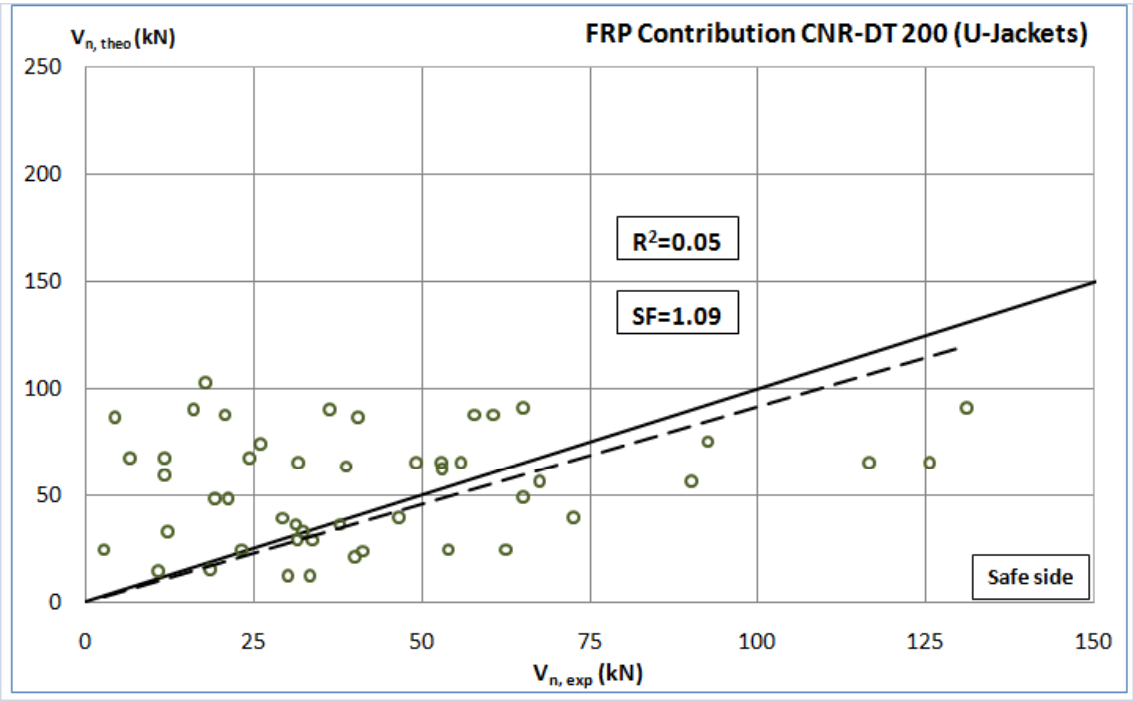

Figure No. 28. Comparison of experimental and theoretical values for CNR-DT 200.

Figure No. 26 presents the results according to the ACI 440. For this case, the safety factor found (1.20) is lower than the one found when all kind of tests were included. The reduction is not important and the achieved safety level is still on the appropriate safety range. However, there are an important

number of tests that produce unsafe results. Figure No. 27, which corresponds to the fib Bulletin, shows the lower safety factor achieved (SF=0.40) which can be considered as highly dangerous. As a matter of fact, the result presented in this figure is 25% lower than the one shown in Figure No. 23. This implies that the equations proposed by the fib bulletin for U-jacket configuration are inaccurate and will produce results highly dangerous. The data for the CNR-DT 200 is presented in Figure No. 28. For this case, a value of SF of 1.09 is found. This value is approximately 33% lower than the one found in Figure No. 24, which implies, again, that the probability of obtaining unsafe results increases for the case of U-jacket configurations. For the correlation factors, it is found a large reduction of the values. All the codes present values or R^2 lower than the appropriate target, ranging from 0.15 to 0.05. For this case, the CNR-DT presents the poorest performance.

As it was done before, Table No. 13 presents the results found for the Demerit Points Classification. It is seen that the ACI 440 presents the better performance which had already seen in Figure No. 27. However, it has to be noticed, that more than the 30% of the samples, for the three codes, are located under the reduced safety range. This implies that, even though for the ACI 440 and CNR-DT 200 average safety factors higher than one were found, the probability of obtaining unsafe results is bigger than the 30%. This implies that, in general, the equations propose by the three codes for U-jacket configuration should be improved in order to obtain appropriate values for design. Furthermore, the correlation factors found are highly disappointing and allow concluding that the equations are not able to replicate the behavior of concrete beams strengthened in this fashion.

Table No. 13. Comparison of codes for FRP shear contribution for U-jacket configuration.

SAFETY FACTOR	CLASIFICATION	PEN	ACI 440	FIB Bulletin 14	CNR-DT 200
<0.60	Extr. Dangerous	10	0.229	0.896	0.333
0.60-0.80	Dangerous	5	0.125	0.083	0.146
0.80-1.00	Reduced Safety	2	0.104	0.021	0.125
1.00-1.40	Appropriate Safety	0	0.229	0.000	0.167
1.40-2.40	Conservative	1	0.125	0.000	0.167
>2.40	Extr. Conservative	2	0.188	0.000	0.063
		Summation	3.625	9.417	4.604

6.4.2. Side bonded configuration

Figure No. 29 presents the general comparison between the theoretical and experimental values for the three considered codes when only the side bonded tests are taken into account. The trend, as it could be expected, is similar to the one presented in Figure No. 21 but a lower dispersion of the data for the ACI 440 and the CNR-DT 200 is observed.

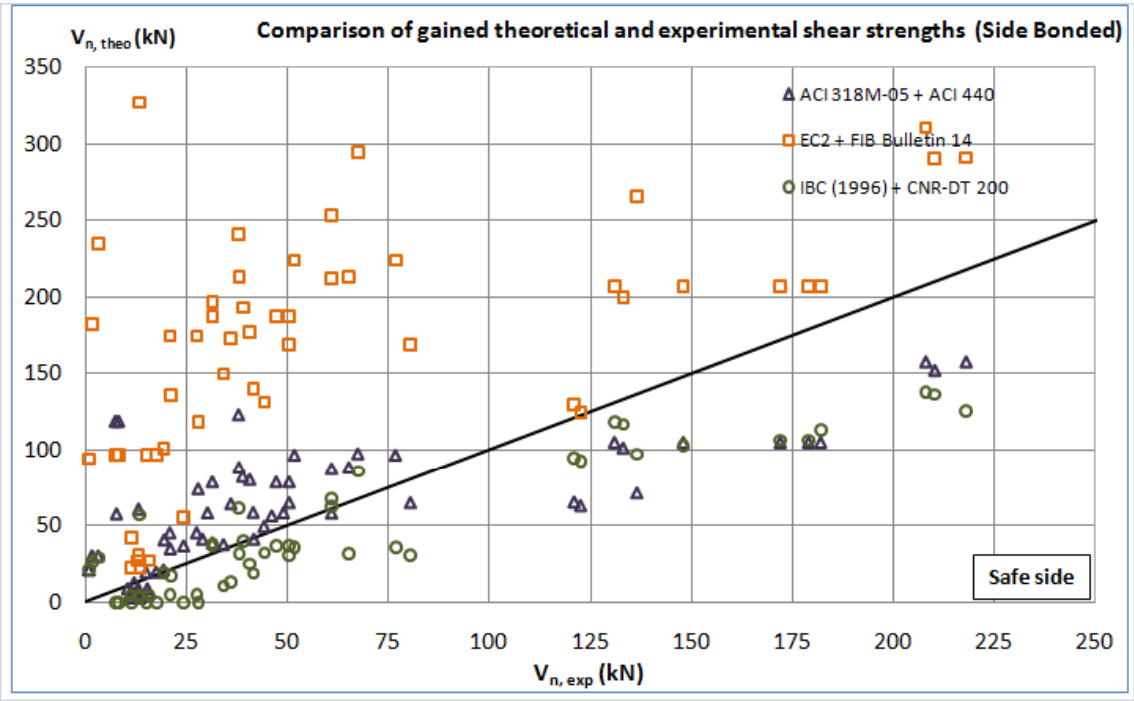

Figure No. 29. Comparison of experimental and theoretical FRP contribution for Side bonded configuration.

The data for the ACI 440 is presented in Figure No. 30. In this graph, it is possible to see that the safety factor found is approximately 6% higher than the one found for the U-jacket configuration (see Figure No. 26). The *fib* Bulletin, presents again a low safety factor, as can be seen in Figure No. 31. However, it is 35% higher than the one found for the U-jacket configuration. Unfortunately, the value found for the side bonded configuration is still in the extremely dangerous range proposed in this document. This implies that the use of this code should be avoided in order to obtain safe results. When the data for the CNR-DT is observed (see Figure No. 32), it can be seen that this presents the highest value of the safety factor found (SF=1.47). As a matter of fact, this value is the highest found for the side bonded or U-jacket configuration. When this result is compared with the one presented in Figure No. 28, it is easily seen that that the equations presented in the code for side bonded configuration are safer than the ones presented for the U-jacket configuration. The CNR-DT 200 also exhibits the higher value of the correlation coefficient (R^2=0.87) that is a sign of the accurate results that can be achieved by the use of this code for the strengthening of concrete beams using a side bonded configuration. The ACI 440 and the *fib* BULLETIN show, again, a poor performance as long as correlation is concerned. As a matter of fact, the values of R^2 obtained for these two codes are noteworthy, especially in the case of the European guideline.

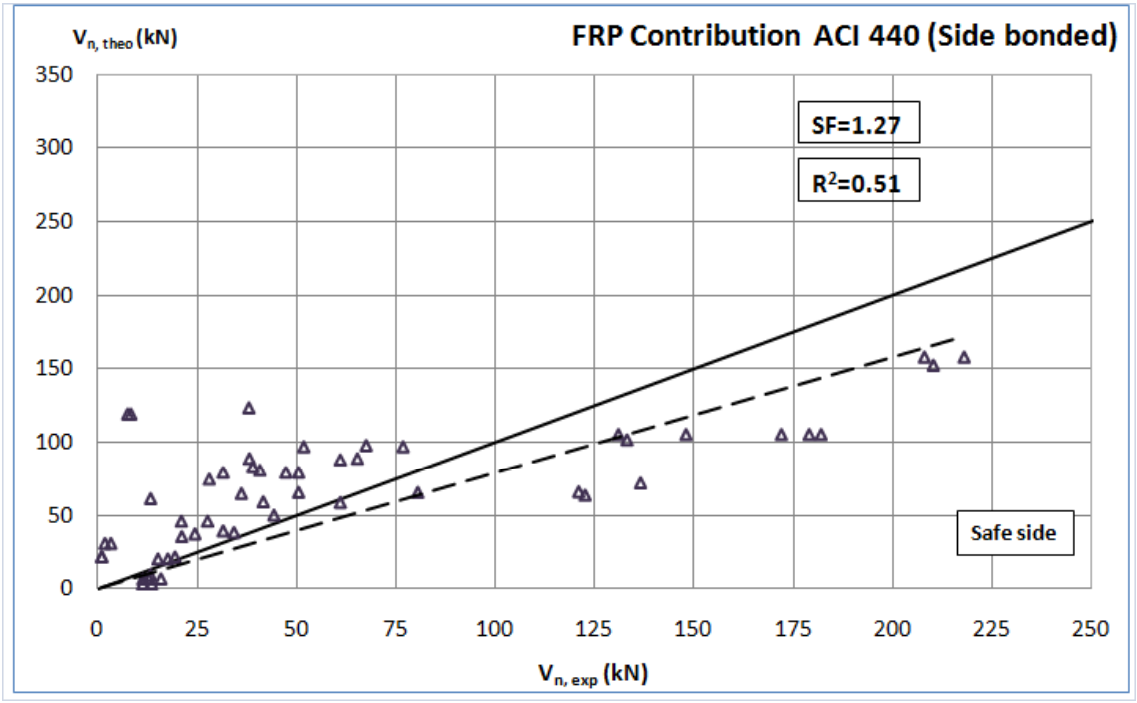

Figure No. 30. Comparison of experimental and theoretical values for ACI 440.

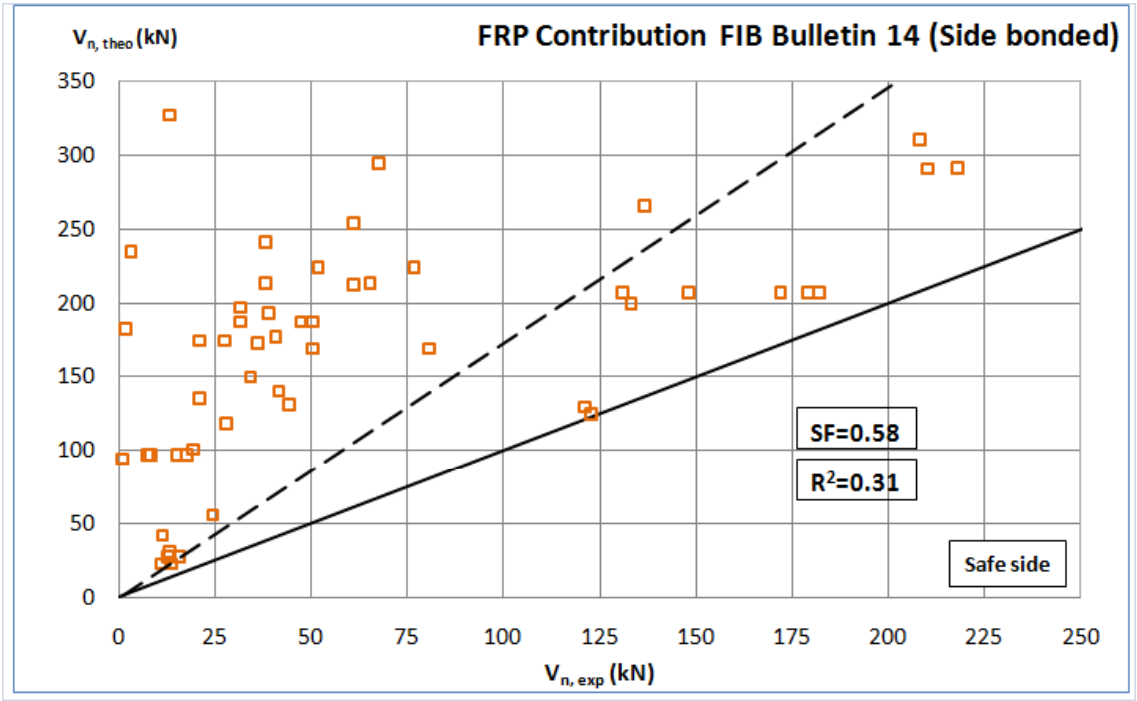

Figure No. 31. Comparison of experimental and theoretical values for *fib* BULLETIN 14.

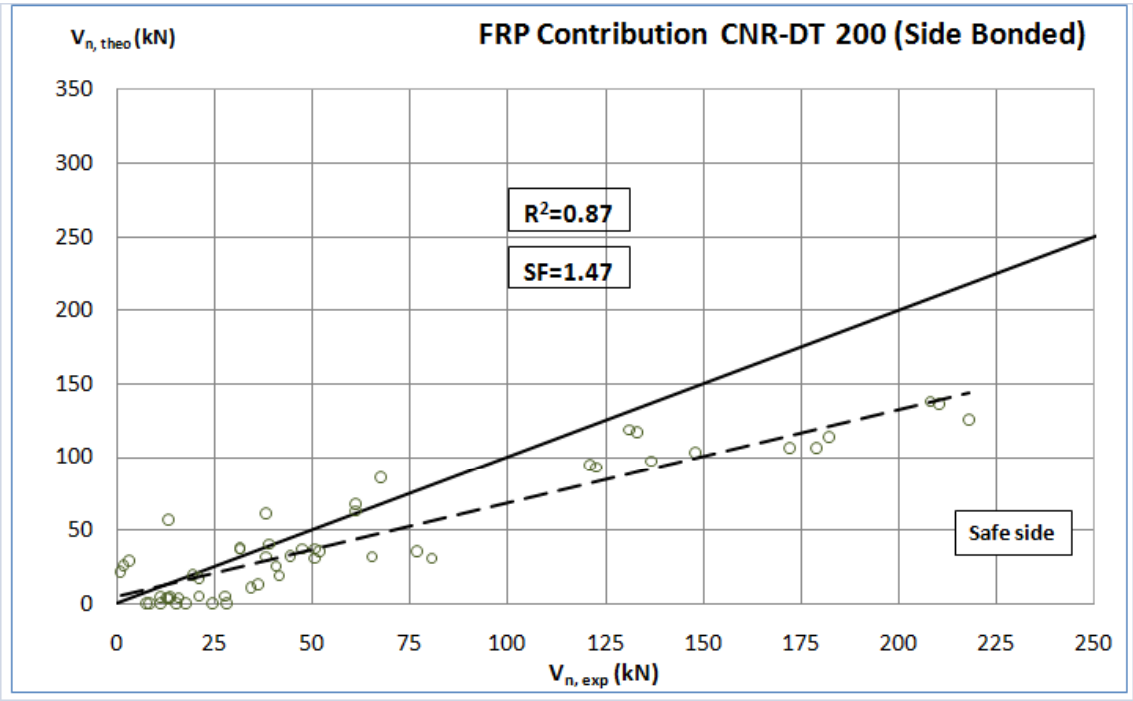

Figure No. 32. Comparison of experimental and theoretical values for CNR-DT 200.

As anticipated for the previous results, the total summation of penalties for the CNR-DT 200 has the lower value for the three compared codes (see Table No. 14). It is almost three times lower than the one obtained for the fib Bulletin and 40% lower than the one for the ACI 440. It has to be said that this value is significantly lower than the one found for the U-jacket configuration. For this case, the probability of having results below the range of reduced safety is 25%, which is still high but considerably lower than the one obtained for the U-jacket configuration (47%). However, the percentage in the extremely conservative for this case reaches a value of 18.8%. The *fib* BULLETIN is not able to predict results above the dangerous zone which, again, implies that a deep revision of their equations should be carried out. For the ACI 440, even though a global SF in the appropriate safety range is found, it is observed that almost the 50% of the data predicted by the code can be considered as dangerous or extremely dangerous.

Table No. 14. Comparison of codes for FRP shear contribution for Side bonded configuration.

SAFETY FACTOR	CLASIFICATION	PEN	ACI 440	FIB Bulletin 14	CNR-DT 200
<0.60	Extr. Dangerous	10	0.328	0.813	0.203
0.60-0.80	Dangerous	5	0.172	0.109	0.047
0.80-1.00	Reduced Safety	2	0.125	0.078	0.125
1.00-1.40	Appropriate Safety	0	0.141	0.000	0.188
1.40-2.40	Conservative	1	0.172	0.000	0.250
>2.40	Extr. Conservative	2	0.063	0.000	0.188
		Summation	4.688	8.828	3.141

6.5. Influence of steel shear reinforcement

As pointed out for some researches (Pellegrino and Modena, 2002), the influence of the amount of existing transverse steel reinforcement on the shear capacity a beam strengthened in shear with FRP is still not totally understood and its worth clarifying.

In order to study, the influence of the shear steel reinforcement, the database a reduced database was created, including the data for the samples made with and without shear steel reinforcement (SSR and NSSR). The comparison was made for the U-jacket and side bonding configuration separately because, as it was seen in 6.4, the performance of the test is highly influenced by the type of strengthening scheme.

6.5.1. U-Jackets configuration

In Figure No. 33, Figure No. 34 and Figure No. 35, it is possible to observe the evaluation of the three studied codes. For this case, it is seen that the ACI 440 presents the higher value of the safety factor (SF=1.47) which is in the conservative category. This value is 22.5% higher than the one presented in Figure No. 26. This code also presents the higher value of the correlation coefficient, which is again, significantly higher than the one computed when the data with and without shear steel reinforcement was studied. This behavior implies that for the case of the equations proposed by the ACI 440, the influence of the transverse reinforcement should be studied in order to improve the performance of the code. For the *fib* BULLETIN and the CNR-DT 200, the same behavior is observed, this is an improvement in the correlation and safety factors but It is worth notice that the three codes still have correlation factors behind the set limit.

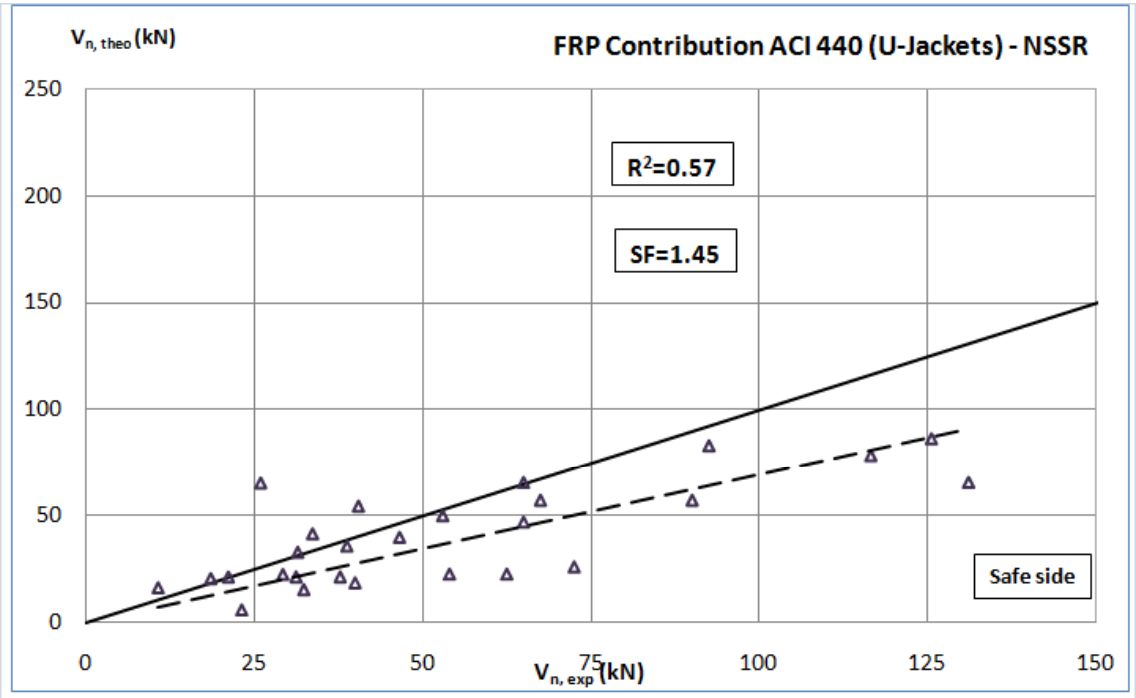

Figure No. 33. Comparison of experimental and theoretical values for ACI 440 without shear steel reinforcement.

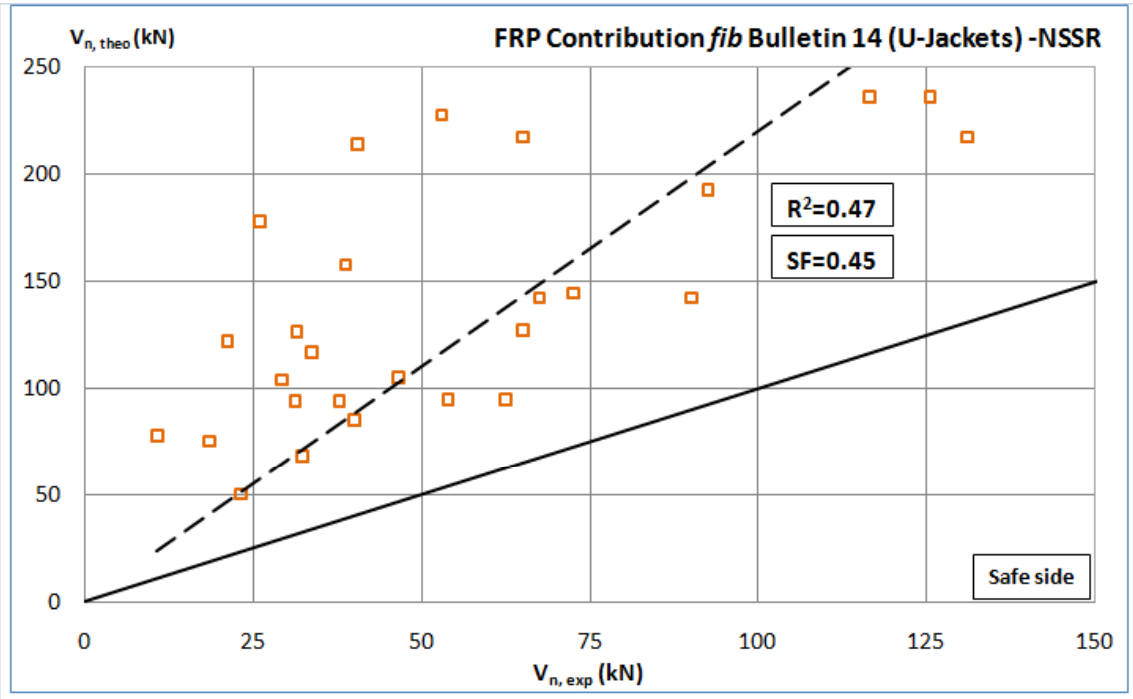

Figure No. 34. Comparison of experimental and theoretical values for *fib* bulletin 14 without shear steel reinforcement.

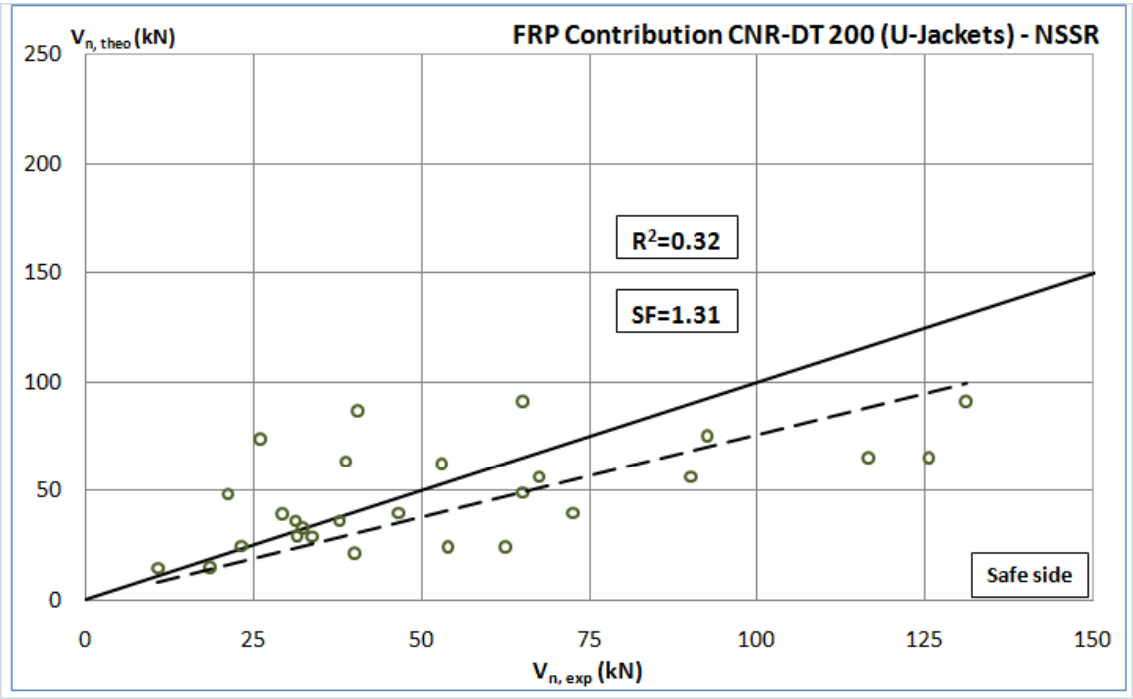

Figure No. 35. Comparison of experimental and theoretical values for CNR-DT 200 without shear steel reinforcement.

Figure No. 36, Figure No. 37 and Figure No. 38 present the SF and R^2 values found for the samples that include shear steel reinforcement. In order to compare the behavior of the samples with and without shear steel reinforcement, these graphs also include the NSSR points. In all these graphs it is easily seen the reduction of the safety achieved for the database that only included the SSR samples.

As matter of fact, for the SSR, all the codes produce SF lower than the reduced safety range. When the correlation factors are compared, also a significant reduction is observed.

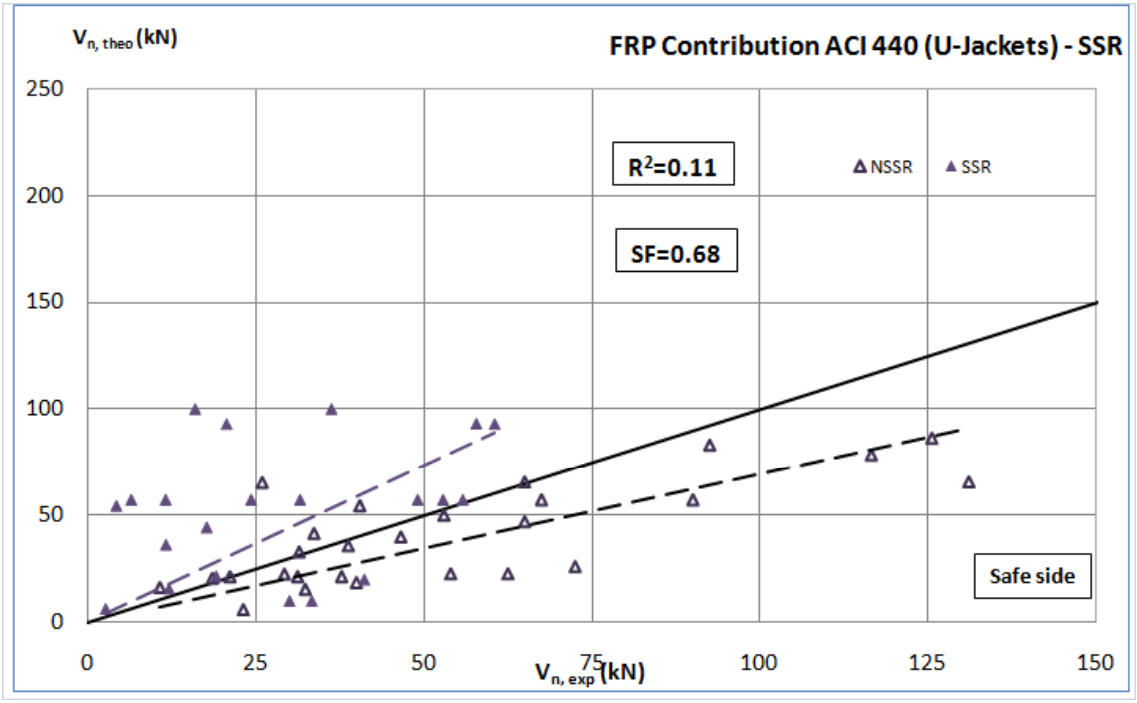

Figure No. 36. Comparison of experimental and theoretical values for ACI 440 with and without shear steel reinforcement.

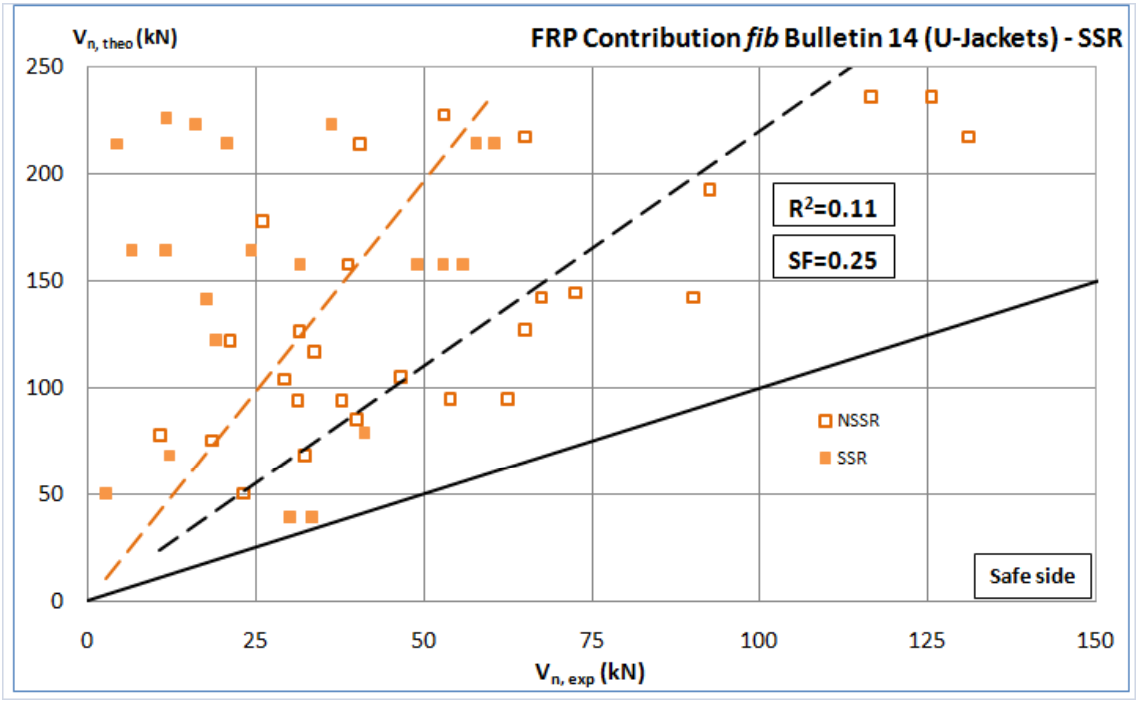

Figure No. 37. Comparison of experimental and theoretical values for *fib* bulletin 14 with and without shear steel reinforcement.

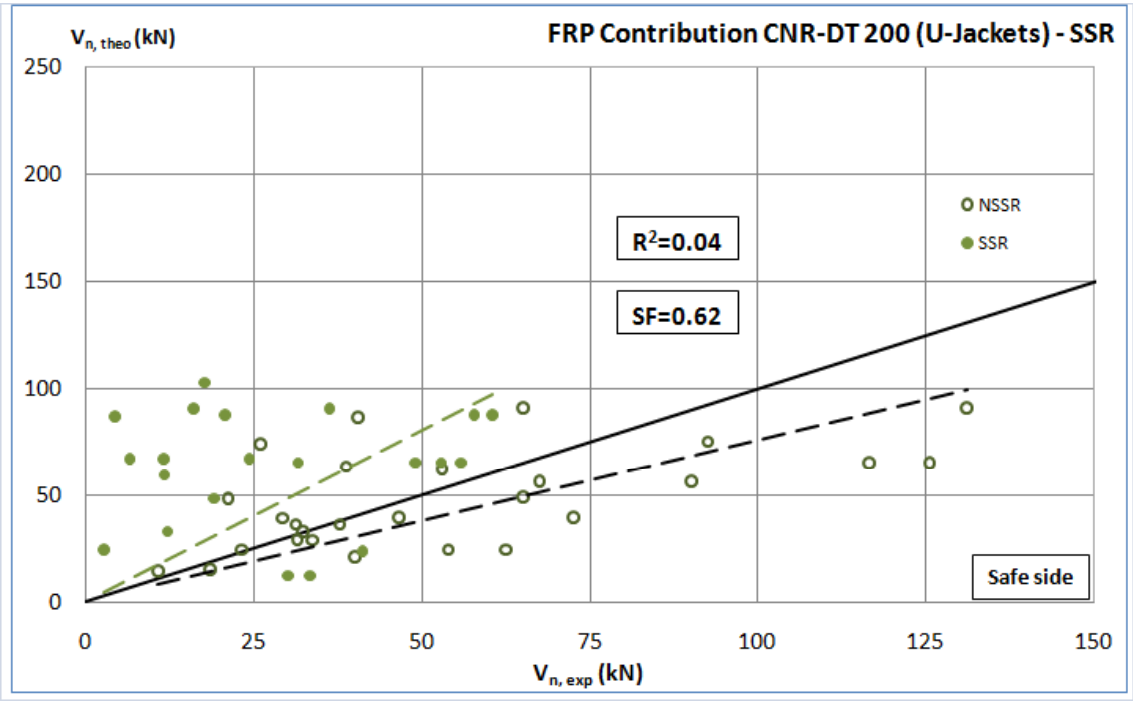

Figure No. 38. Comparison of experimental and theoretical values for CNR-DT 200 with and without shear steel reinforcement.

Table No. 15 presents a comparison of the results found using the demerit classification points for the database including shear steel reinforcement and for the one with only the samples with NSSR. It is seen that only the fib bulletin presents a worst performance for the NSSR condition, but it has to be noticed that for this particular case, the change in behavior is not significant due to the fact that the predictions of this code for both cases are mostly in the extremely dangerous zone. On the other hand, the ACI 440 and the CNR-DT 200 present a significant improvement in the total penalties summation, but this change is more important for the American code. For this case, only there is 11% probability of getting results under the reduced safety range. This allows concluding that the equations of this code are appropriate for concrete beams without shear reinforcement but should be improved for concrete elements that include transverse steel.

Table No. 15. Comparison of codes for FRP shear contribution with and without shear steel reinforcement (U-jacket configuration).

SAFETY FACTOR	ACI 440			FIB Bulletin 14			CNR-DT 200		
	TOTAL	NSSR	SSR	TOTAL	NSSR	SSR	TOTAL	NSSR	SSR
<0.60	0.229	0.037	0.524	0.896	0.889	0.905	0.333	0.111	0.619
0.60-0.80	0.125	0.074	0.143	0.083	0.111	0.048	0.146	0.148	0.143
0.80-1.00	0.104	0.185	0.190	0.021	0.000	0.048	0.125	0.148	0.095
1.00-1.40	0.229	0.259	0.000	0.000	0.000	0.000	0.167	0.296	0.000
1.40-2.40	0.125	0.333	0.048	0.000	0.000	0.000	0.167	0.259	0.048
>2.40	0.188	0.111	0.095	0.000	0.000	0.000	0.063	0.037	0.000
	3.625	1.667	6.571	9.417	9.444	9.381	4.604	2.481	7.143

6.5.2. Side bonded configuration

In Figure No. 39, Figure No. 40 and Figure No. 41, it is possible to observe the evaluation of the three studied codes for side bonded configuration without shear steel reinforcement.

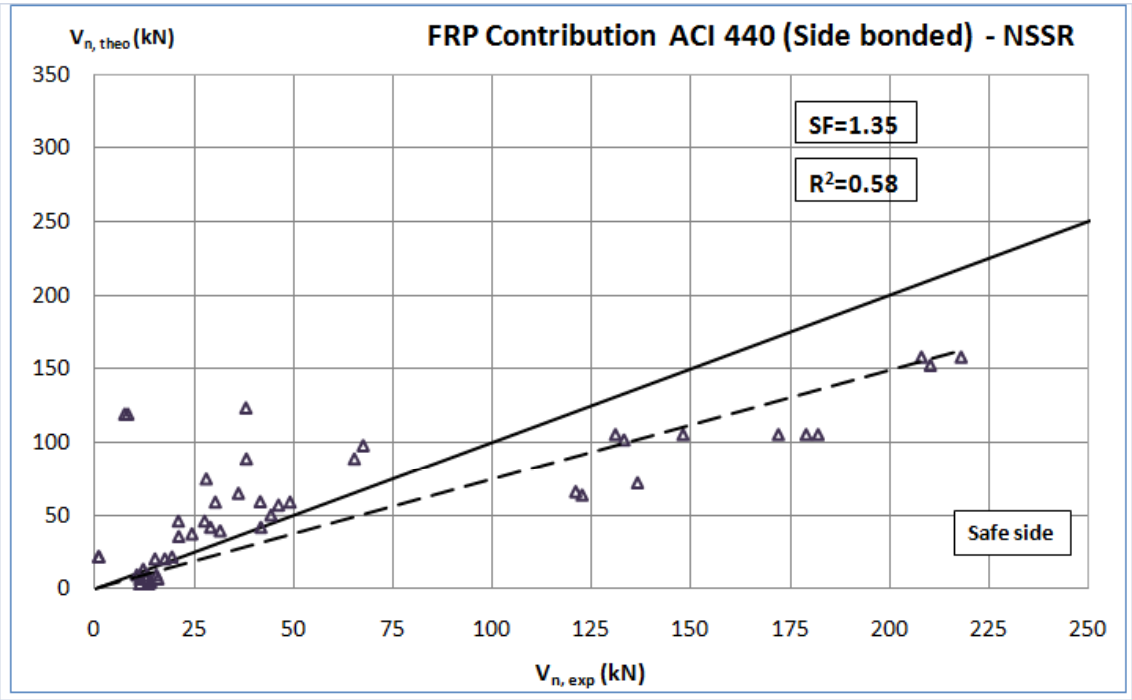

Figure No. 39. Comparison of experimental and theoretical values for ACI 440 without shear steel reinforcement.

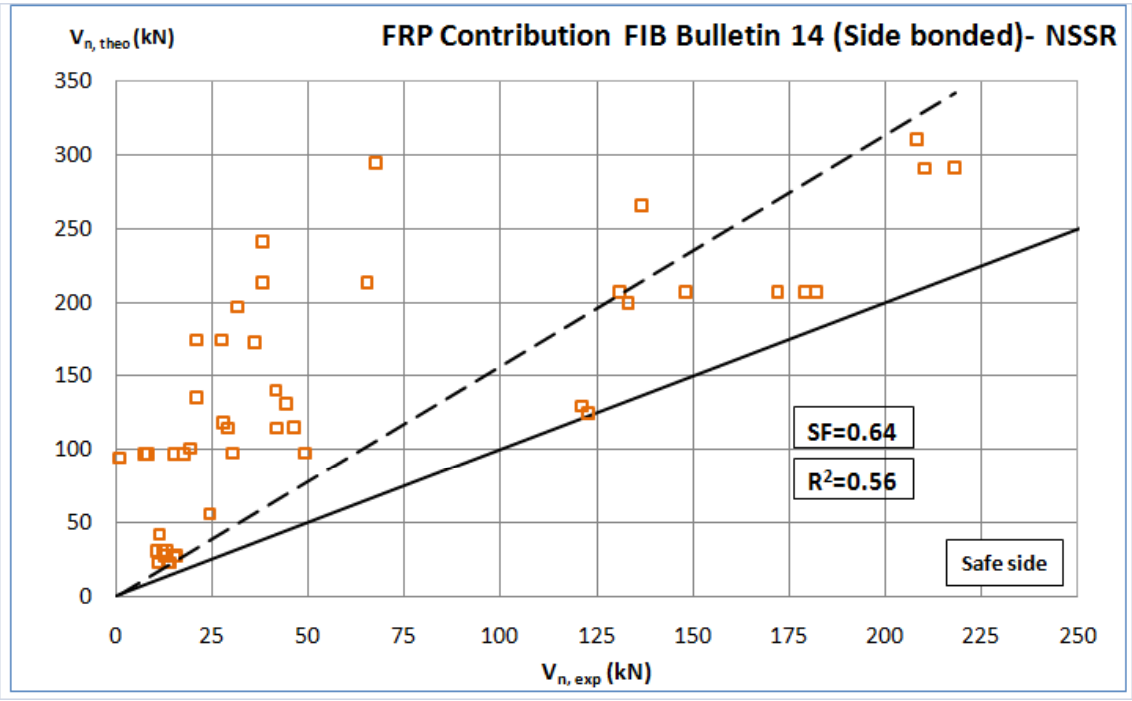

Figure No. 40. Comparison of experimental and theoretical values for *fib* bulletin 14 without shear steel reinforcement.

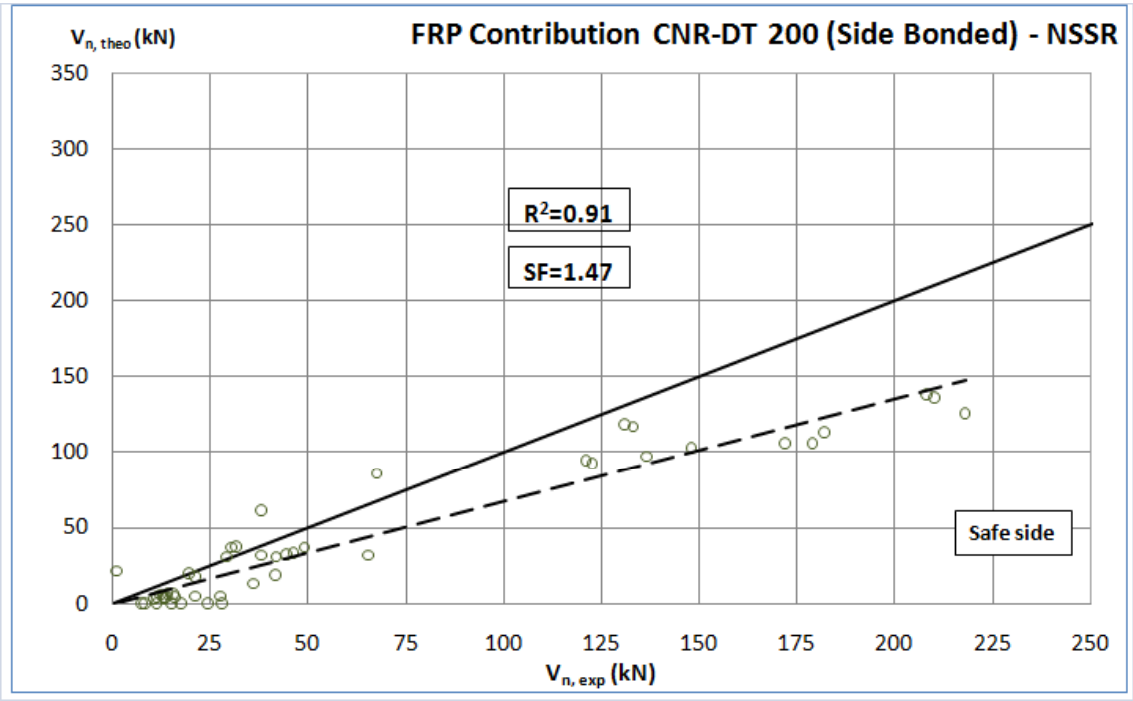

Figure No. 41. Comparison of experimental and theoretical values for CNR-DT 200 without shear steel reinforcement.

It is seen that for all the codes there is an improvement in the correlation factors and the safety factors with the only exception of the SF of the ACI 440 that remains the same. However, the increase in the safety factors of the other two codes is not important and it can be said that the performance of the code for beams with or without shear steel reinforcement is almost the same for side bonded configuration. For the correlation factor, the increase for the ACI 440 is less than the 5% but the obtained R^2 for this case is remarkably high (R^2=0.91) and can be understood as a almost perfect correlation between the experimental and the theoretical values. The behavior of the *fib* BULLETIN and the CNR-DT 200 as long as the values of R^2 implies that the equations given in these two codes are not able to give a good correlation for the data.

Figure No. 42,Figure No. 43 and Figure No. 44 present the SF and R^2 values found for the samples that include shear steel reinforcement and the comparison with the NSSR samples. As it was found for the U-jacket configuration, a significant reduction in the SF is found for ACI 440 and the *fib* BULLETIN, but for the CNR-DT 200 it almost remains the same. The R^2 reduces for the *fib* BULLETIN and the CNR-DT 200 but has an increase of 20% for the ACI 440.

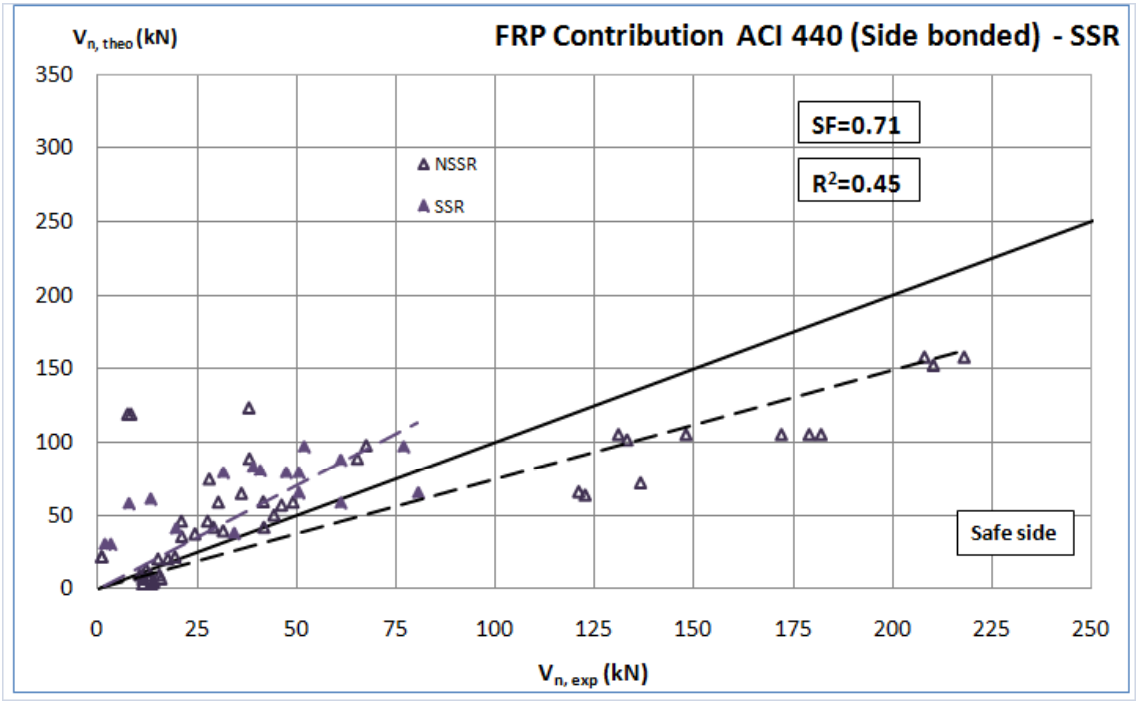

Figure No. 42. Comparison of experimental and theoretical values for ACI 440 with and without shear steel reinforcement.

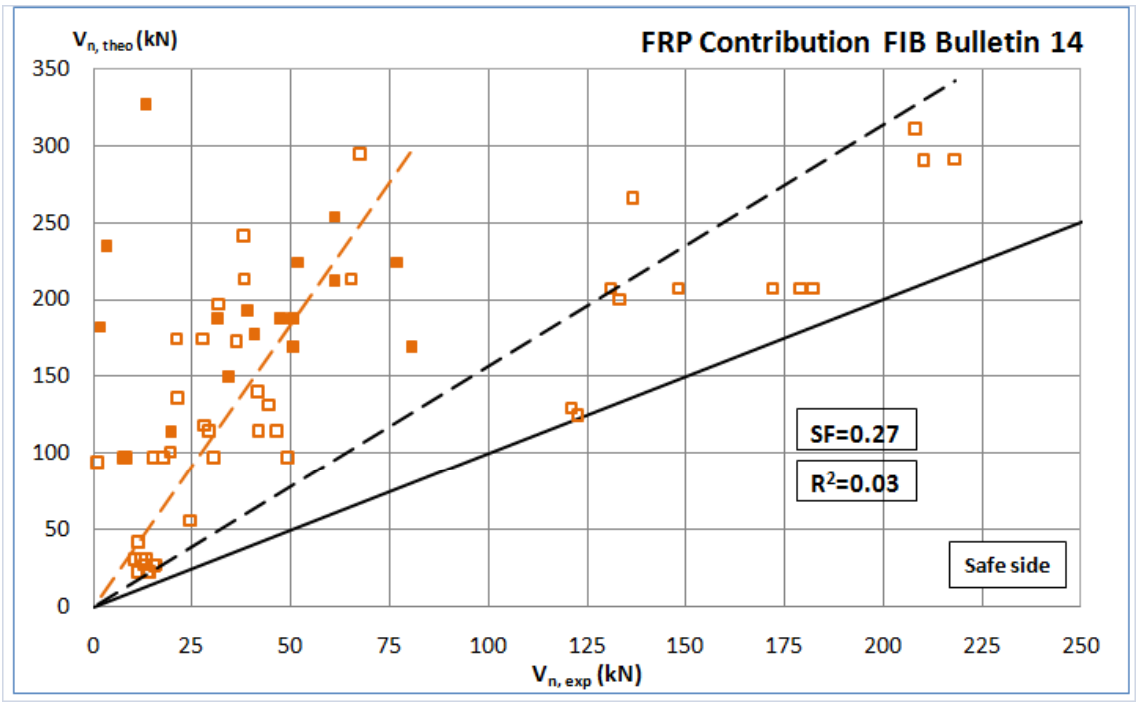

Figure No. 43. Comparison of experimental and theoretical values for *fib* bulletin 14 with and without shear steel reinforcement.

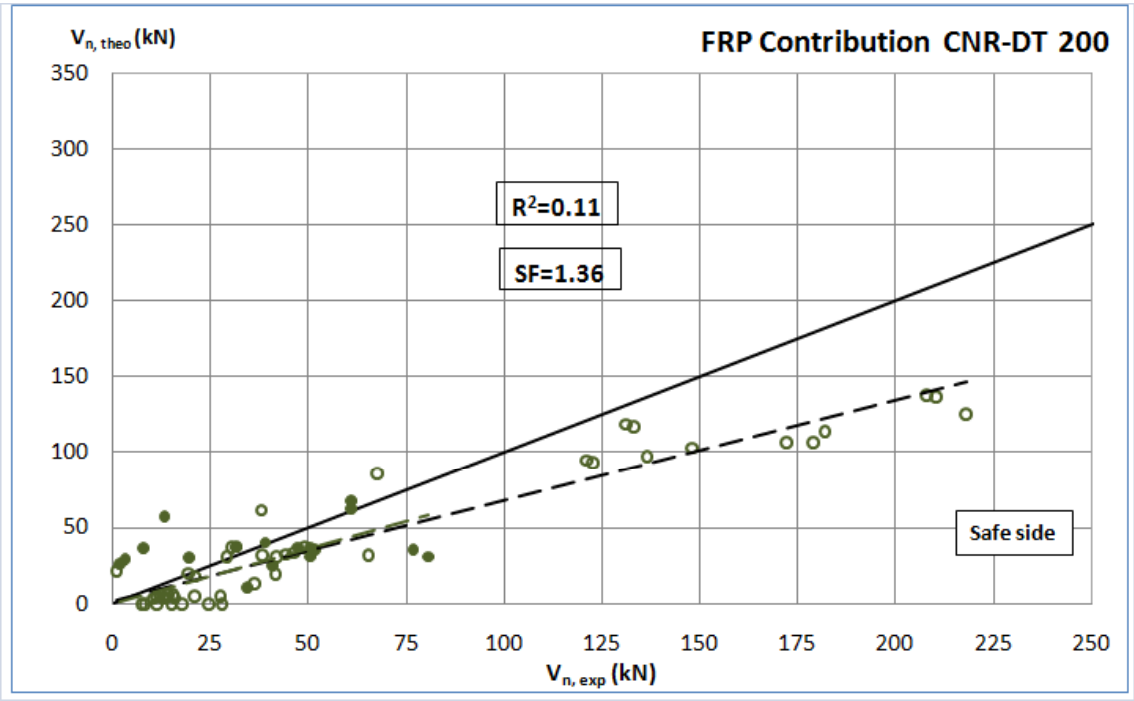

Figure No. 44. Comparison of experimental and theoretical values for CNR-DT 200 with and without shear steel reinforcement.

In Table No. 16, it is seen that there is an important reduction in the total summation for NSSR according to the *fib* BULLETIN which actually corresponds to best behavior obtained with this code. For the ACI 440, the improvement is more important, passing from 7.176 to 3.787. For the CNR-DT 200 the results remain almost the same. The change is principally due to the augment of the percentage under the reduced safety level. However, this code still remains the one with the lowest summation and when this is added to that fact that it also presents the higher R^2, it is clear that the Italian Guideline corresponds to the code with the best performance for the NSSR.

Table No. 16. Comparison of codes for FRP shear contribution with and without shear steel reinforcement (Side bonded configuration).

SAFETY FACTOR	ACI 440			FIB Bulletin 14			CNR-DT 200		
	TOTAL	NSSR	SSR	TOTAL	NSSR	SSR	TOTAL	NSSR	SSR
<0.60	0.328	0.234	0.588	0.813	0.745	1.000	0.203	0.191	0.235
0.60-0.80	0.172	0.149	0.235	0.109	0.149	0.000	0.047	0.106	0.059
0.80-1.00	0.125	0.149	0.059	0.078	0.106	0.000	0.125	0.085	0.235
1.00-1.40	0.141	0.149	0.118	0.000	0.000	0.000	0.188	0.191	0.118
1.40-2.40	0.172	0.234	0.000	0.000	0.000	0.000	0.250	0.234	0.235
>2.40	0.063	0.085	0.000	0.000	0.000	0.000	0.188	0.191	0.118
	4.688	3.787	7.176	8.828	8.404	10.000	3.141	3.234	3.588

6.6. Overall comparison

Table No. 17 shows a global comparison of the codes according to the parameters studied in this chapter. It presents the values of R^2, SF, the summation of penalties and the percentage of unsafe results. In this table it is possible to observe the codes that present the best and

the global behavior for the different set of databases studied. It is also highlighted the highest and lowest values for each one of the comparison studied which represents the best and worst global achieved behavior.

Table No. 17. Overall comparison of the codes.

CODE		R^2	SF	PEN	% NSR
$V_c + V_s + V_{frp}$ (W, U, S)	ACI 318 + ACI 440	0.76	1.34	1.115	8.0%
	EC2 + *fib* BULLETIN 14	0.63	0.70	6.389	77.9%
	IBC + CNR-DT 200	0.82	1.03	1.566	14.2%
	EC2 + CNR-DT 200	0.73	1.12	1.345	10.6%
	EC2 + *fib* BULLETIN 14 (θ)	0.66	0.74	6.115	75.2%
	EC2 + CNR-DT 200 (θ)	0.67	1.17	1.177	7.1%
V_{frp} (W, U, S)	ACI 440	0.49	1.26	3.832	38.9%
	fib BULLETIN 14	0.26	0.51	8.770	92.0%
	CNR-DT 200	0.51	1.33	3.124	27.4%
V_{frp} (U-Jackets)	ACI 440	0.15	1.20	3.625	35.4%
	fib BULLETIN 14	0.14	0.40	9.417	97.9%
	CNR-DT 200	0.05	1.09	4.604	47.9%
	ACI 440 (NSSR)	0.57	1.45	1.667	11.1%
	fib BULLETIN 14 (NSSR)	0.47	0.45	9.444	**100.0%**
	CNR-DT 200 (NSSR)	0.32	1.31	2.481	25.9%
	ACI 440 (SSR)	0.11	0.68	6.571	66.7%
	fib BULLETIN 14 (SSR)	0.11	**0.25**	9.381	95.2%
	CNR-DT 200 (SSR)	0.04	0.62	7.143	76.2%
V_{frp} (Side bonded)	ACI 440	0.51	1.27	4.688	50.0%
	fib BULLETIN 14	0.31	0.58	8.828	92.2%
	CNR-DT 200	0.87	**1.47**	3.141	25.0%
	ACI 440 (NSSR)	0.58	1.35	3.787	38.3%
	fib BULLETIN 14 (NSSR)	0.56	0.64	8.404	89.4%
	CNR-DT 200 (NSSR)	**0.91**	**1.47**	3.234	29.8%
	ACI 440 (SSR)	0.45	0.71	7.176	82.4%
	fib BULLETIN 14 (SSR)	**0.03**	0.27	**10.000**	**100.0%**
	CNR-DT 200 (SSR)	0.11	1.36	3.588	29.4%

R^2: Correlation coefficient. SF: Global safety factor. UJ+SB: Only U-Jacket + Side bonded strengthened elements
PEN: Summation of penalties. NSR: Not safe results (values with a partial safety factor below 0.80).

1	**Best particular behavior**
1	**Worst particular behavior**
1	**Best global behavior**
1	**Worst global behavior**

First of all, it is seen that the *fib* BULLETIN 14 has the worst behavior in all the parameters evaluated with the exception of the correlation coefficient achieved by the CNR-DT 200 in the V_{frp} contribution for the U-jacket configuration. It is remarkable how the BULLETIN is not able to predict an acceptable percentage of safe values. As a matter of fact, all the results found for the V_{frp} contribution for the U-jacket and side bonded configuration schemes are unsafe. However, it has to be said that at the moment the recommendations of the *fib* BULLETIN 14 are going under revision which is understood after analyzing the results found in this document.

As long as the ACI 440 and the CNR-DT 200, both show a similar behavior but still aren't able to predict an appropriate percentage of safer values, especially for the case of V_{frp} contribution for the U-jacket configuration. For this case, it is remarkable how the behavior of these codes is worst for the case of beams with SSR, which implies that the equations provided for these guidelines should be improved for the case of concrete beams with the presence of steel reinforcement for shear.

For the side bonded configuration, it is seen how the CNR-DT 200 has the best behavior and that the equations are good enough for SSR and NSSR beams. As a matter of fact, the behavior is almost the same but there is a remarkable reduction in the correlation coefficient for the SSR case. It is also seen that for the case of the NSSR CNR-DT 200 for side bonded scheme, a correlation factor of 0.91 is found which corresponds to an almost perfect match between the theoretical and experimental values.

7. PELLEGRINO AND MODENA MODEL (2008)

On the basis of the typical experimental failures modes of side-bonded and U-jacketed beams observed by Pellegrino and Modena (2008), shown here in Figure No. 45, the peeling-off failure of the FRP, involving the concrete cover in a lateral triangular portion above the principal diagonal crack from the bearing to the load point, was assumed for the U-jacket beams, and the similar failure in a lateral triangular portion under diagonal crack was assumed for the side-bonded beams in order to develop a new model for the FRP contribution of beams strengthened for shear in this fashion.

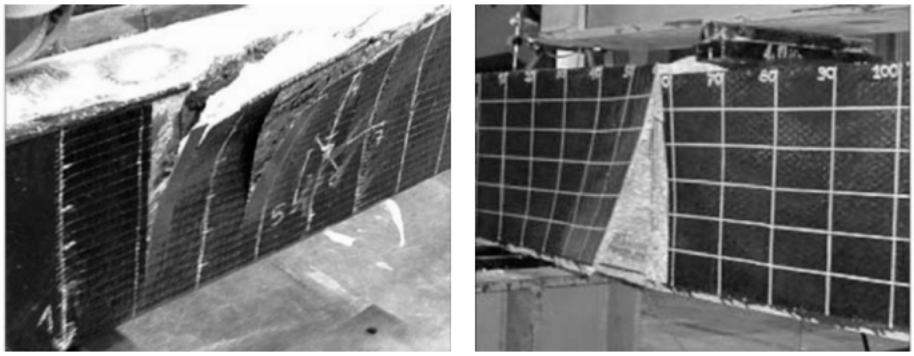

Figure No. 45. Typical failure of: Left: U-jacketed and Right: side-bonded beams (Pellegrino and Modena, 2008).

The authors assumed that if the external FRP strains are equal to those of internal stirrups, the effective FRP strain ε_{fe} and, consequently, the FRP shear contribution V_f can be obtained from the rotation equilibrium of the forces F_f and F_c operating in the FRP and concrete surface, respectively at failure (see Figure No. 46). The equilibrium equation is written with respect to the point around which the experimentally observed peeling-off rotation occurs. This point is in the lower part of cross section for U-jacket beams and in the upper lateral part for side-bonded ones. Thus, they had:

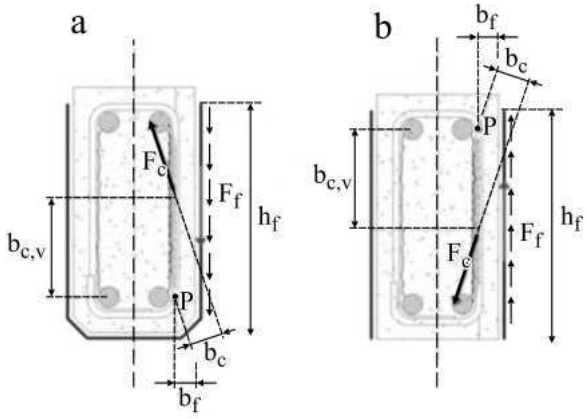

Figure No. 46. Forces acting in the cross section of Left: U-jacketed and Right: side-bonded beams (Pellegrino and Modena, 2008).

$$(2)\ F_f b_f = F_c b_c \rightarrow n_f t_f L_f \frac{d_f - l_e}{d_f} E_f \varepsilon_{fe} b_f = \left(f_{ct} A_c \cos\phi \cos\phi + \tau_c A_c \sin\phi \cos\phi\right) b_{c,v}$$

$$(3)\ \varepsilon_f = \frac{2 f_{ct} A_c \cos^2\phi b_{c,v}}{n_f t_f L_f E_f \frac{h_f - l_e}{h_f} b_f},\ V_f = \frac{2 n_f t_f L_f w_f \varepsilon_{fe} E_f h_f}{s_f}$$

In the previous equation f is the angle characterizing the conventional roughness of the interface, which is assumed equal to 79°, according to the cal ibration process based on the experimental ultimate shear capacities described by Pellegrino and Modena (2006).

The authors also proposed a new formulation for the contribution of the transverse steel, modified with respect to that proposed by the codes for non-strengthened RC structures, on the basis of the following concepts:

- Assuming a variable amplitude for the diagonal crack, a reduction coefficient a=0.75 for the transverse steel stress is introduced to take into account the fact that not all the stirrups intercepted in the tensile zone reach the yield limit.
- In the presence of an external FRP reinforcement, the maximum stress in the internal transverse steel is equal to its yield value only if the effective FRP strain is higher than the steel yield stress.

Therefore the formulation for the steel contribution in the presence of an external FRP reinforcement, according to Pellegrino and Modena (2008), can be computed as:

$$(4)\ V_s = \left[\alpha \rho_v \left(1 - \frac{c}{d}\right) \cot\theta \min(\varepsilon_{fe} E_s, f_y\right] b_w d$$

Where ρv is the transverse steel ratio, f_y is the yield stress of the transverse steel, c is the depth of the neutral axis and d is the effective depth. For this model, the nominal shear capacity can be calculated by summing the concrete contribution provided by the Eurocode 2.

In order to evaluate the performance of the Pellegrino and Modena model, the CNR-DT 200 and the ACI 440 codes were selected in order to make a comparison using the same parameters established before. These two codes were selecting taking into account that they had the best behavior in the previous comparison and that the *fib* BULLETIN is going under revision at the moment and further study of its behavior is not worth it. The comparison was made first for the total theoretical strength and then for the individual V_{frp} contribution. It is also important to say that in this comparison, new set of databases were evaluated but only the data of the comparison parameters for the CNR-DT 200 and the ACI 440 is included and only the graphs of the Pellegrino and Modena model are presented.

7.1. Total Shear Strength

Figure No. 47 show the data obtained for the Pellegrino and Modena model for the total shear strength (concrete, steel and FRP contribution) and it includes the values of SF and R^2. Table No. 18, in the other hand, shows the comparison with the selected codes. It is worth notice that in that table, it has been included the evaluation of the codes for NSSR and SSR elements.

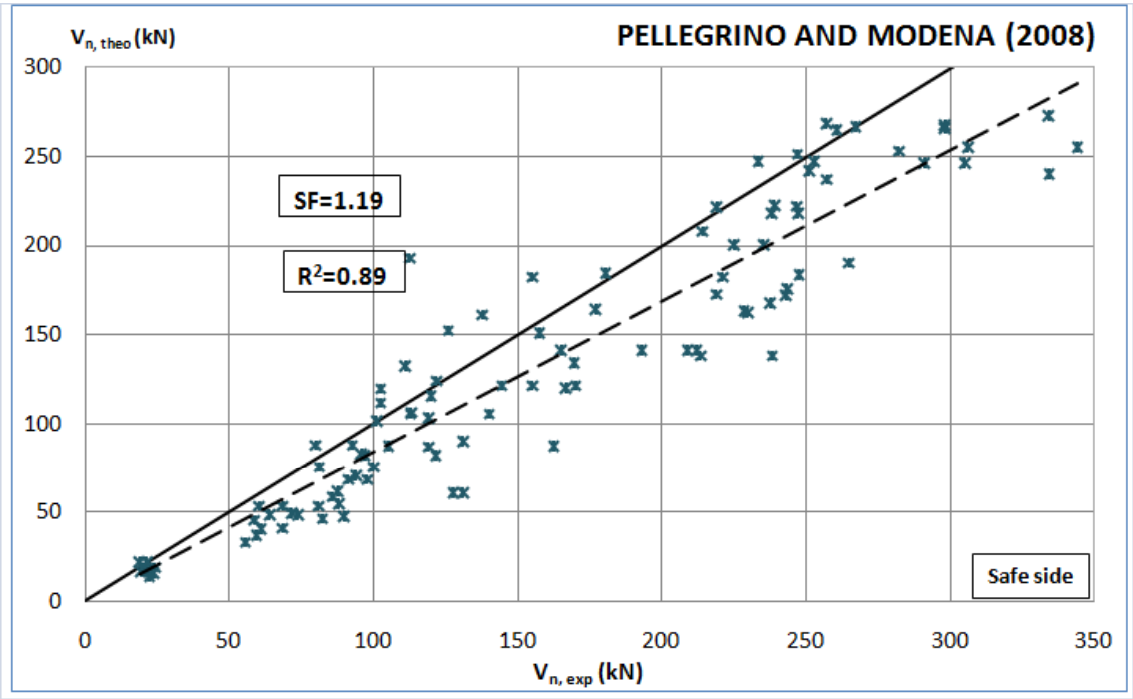

Figure No. 47. Comparison of experimental and theoretical values for Pellegrino and Modena Model – Total Shear Strength.

Table No. 18. Assessment of Pellegrino and Modena Model for Total Shear Strength.

	CODE	R^2	SF	PEN	% NSR
$V_c + V_s + V_{frp}$ (UJ + SB)	ACI 318 + ACI 440	0.79	1.34	0.913	4.9%
	EC2 + CNR-DT 200	0.80	1.14	0.999	7.8%
	PELLEGRINO AND MODENA	0.89	1.19	0.699	1.0%
	ACI 318 + ACI 440 (NSSR)	0.89	1.42	0.769	1.5%
	EC2 + CNR-DT 200 (NSSR)	0.94	1.26	0.538	0.0%
	PELLEGRINO AND MODENA (NSSR)	0.92	1.21	0.585	0.0%
	ACI 318 + ACI 440 (SSR)	0.43	1.26	1.158	10.5%
	EC2 + CNR-DT 200 (SSR)	0.49	1.05	1.766	21.1%
	PELLEGRINO AND MODENA (SSR)	0.67	1.18	0.895	2.6%

R^2: Correlation coefficient. SF: Global safety factor. UJ+SB: Only U-Jacket + Side bonded strengthened elements

PEN: Summation of penalties. NSR: Not safe results (values with a partial safety factor below 0.80).

1 Best particular behavior

1 Worst particular behavior

From the previous table, it is possible to see how the Pellegrino and Modena presents in general a better behavior than the selected codes, especially as the percentage of unsafe results is concerned. As a matter of fact, for NSSR concrete beams, the use of this model would imply obtaining results that are mostly safe. In addition to that, for SSR elements a value of unsafe results of 2.6% is found, which is considerably low than the one obtained for the ACI 440 and the CNR-DT 200. For that case, also the Pellegrino and Modena presents the higher value of correlation factor (R^2=0.67) that is a little bit lower than the accepted value but it is still much higher than the obtained with the other codes.

The previous table also allows concluding that the behavior of the concrete beams with shear steel reinforcement is different from the ones without this kind of reinforcement. This aspect should be studied more in detail in order to improve and update the equations given by the codes.

7.2. FRP Contribution

The comparison of the codes for the V_{frp} contribution is presented here. In Figure No. 48, the data for the U-jacket and side bonded configurations predicted by the Pellegrino and Modena model is included. For Figure No. 49 and Figure No. 50, the database was divided according to the configuration scheme. In these graphs, it is possible to see that there is reduction of the correlation factor when it is compared with the one presented in Figure No. 47. This difference is explained by the fact that the R^2 found for the U-jacket configuration is significantly lower than the one found for the side bonded scheme.

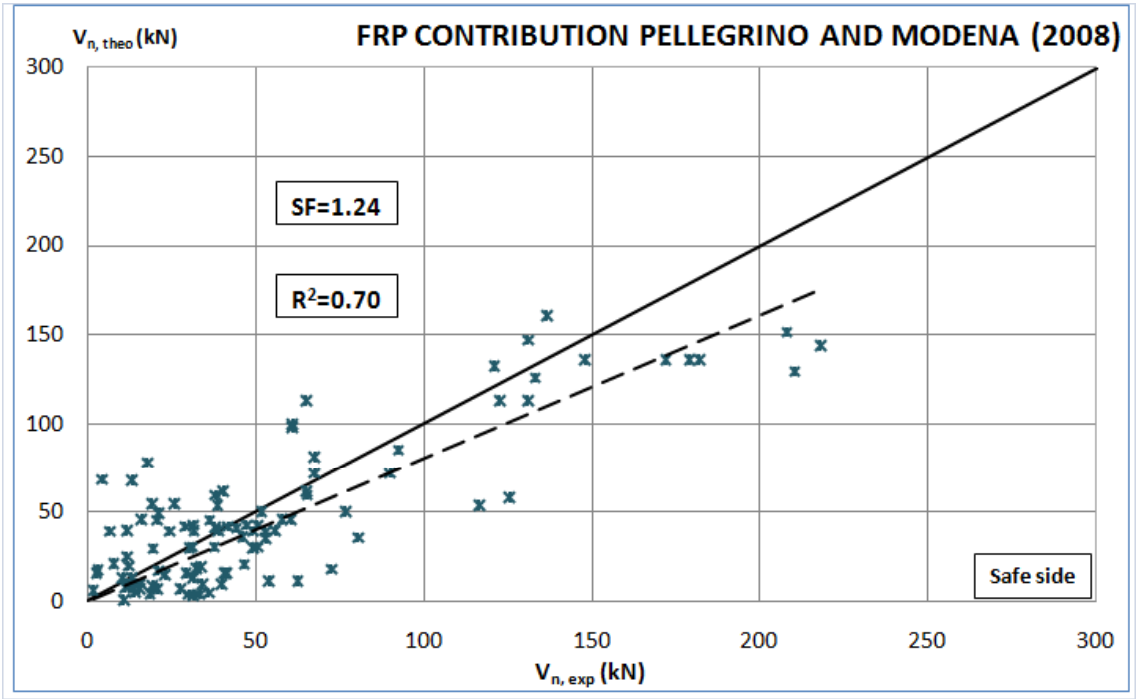

Figure No. 48. Comparison of experimental and theoretical values for Pellegrino and Modena Model – V_{frp} contribution.

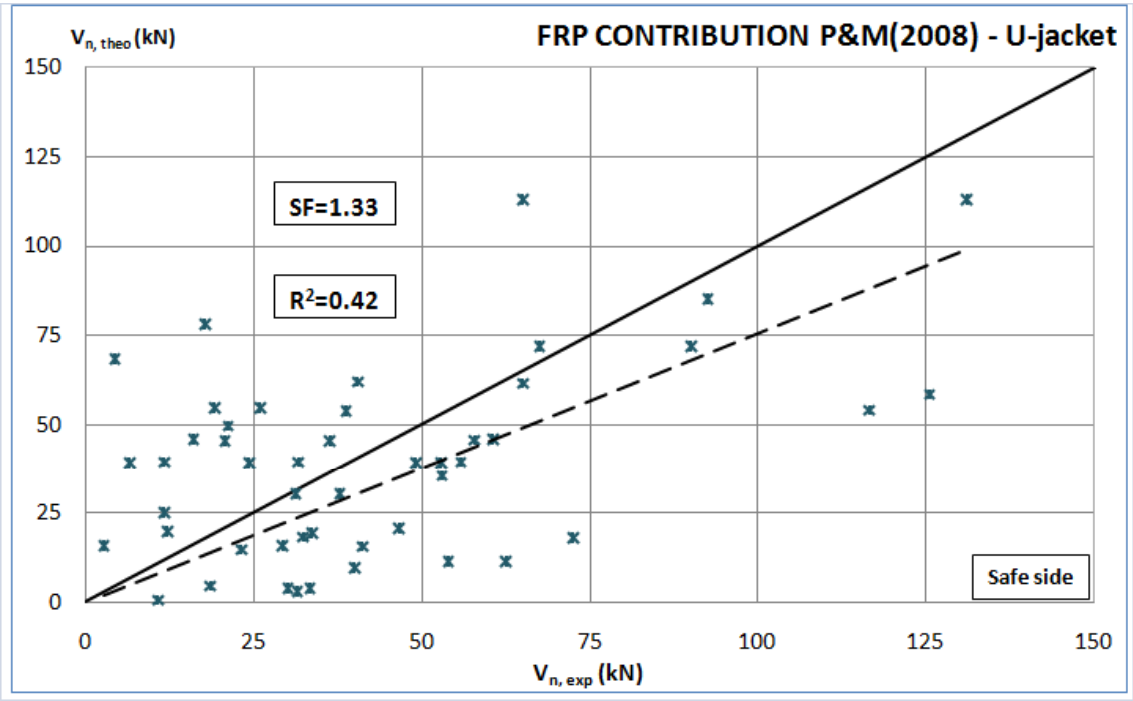

Figure No. 49. Comparison of experimental and theoretical values for Pellegrino and Modena Model for U-jacket scheme– V_{frp} contribution.

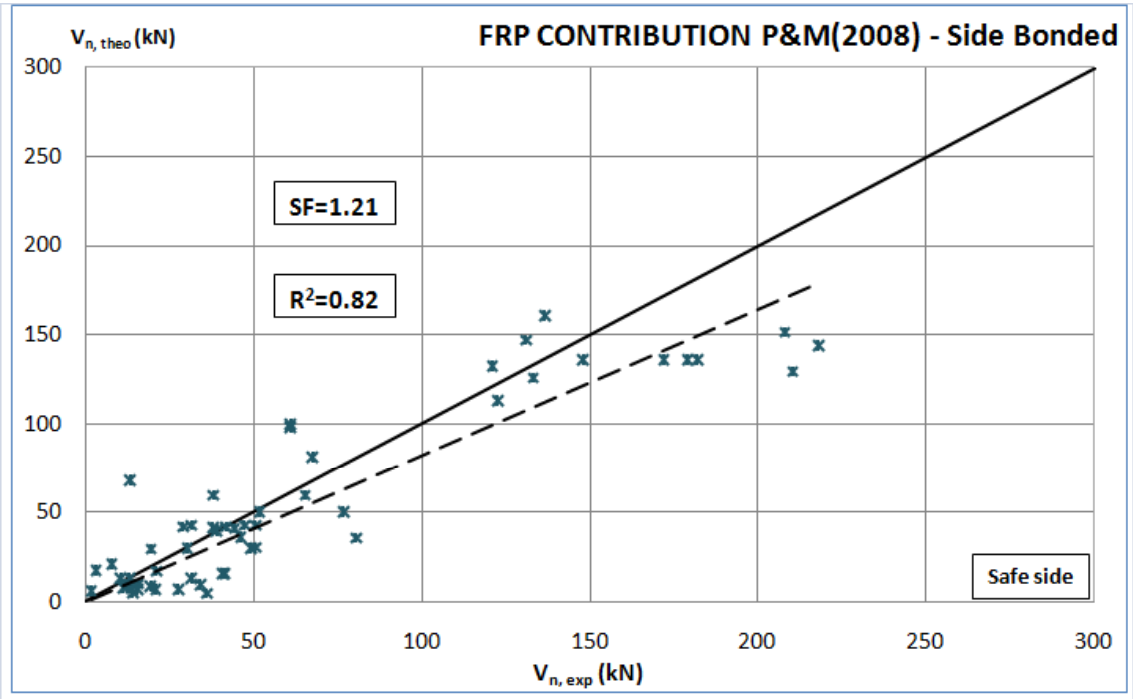

Figure No. 50. Comparison of experimental and theoretical values for Pellegrino and Modena Model for Side bonded scheme– V_{frp} contribution.

In Table No. 19, the comparison of the codes with the model of Pellegrino and Modena (2008) is presented.

Table No. 19. Assessment of Pellegrino and Modena Model for V_{frp} Contribution.

	CODE	R^2	SF	PEN	% NSR
V_{frp} (UJ + SB)	ACI 440	0.49	1.26	3.832	38.9%
	CNR-DT 200	0.51	1.33	4.078	40.8%
	PELLEGRINO AND MODENA	0.70	1.24	2.874	27.2%
	ACI 440 (NSSR)	0.70	1.39	2.462	21.5%
	CNR-DT 200 (NSSR)	0.80	1.43	1.800	13.8%
	PELLEGRINO AND MODENA (NSSR)	0.93	1.21	1.738	12.3%
	ACI 440 (SSR)	0.24	0.70	6.843	73.7%
	CNR-DT 200 (SSR)	0.07	0.93	5.658	53.3%
	PELLEGRINO AND MODENA (SSR)	0.67	1.18	4.816	52.6%
V_{frp} (U-Jackets)	ACI 440	0.15	1.2	3.625	35.4%
	CNR-DT 200	0.05	1.09	4.604	47.9%
	PELLEGRINO AND MODENA	0.42	1.33	3.708	35.4%
	ACI 440 (NSSR)	0.57	1.45	1.667	11.1%
	CNR-DT 200 (NSSR)	0.32	1.31	2.481	25.9%
	PELLEGRINO AND MODENA (NSSR)	0.60	1.39	2.370	18.5%
	ACI 440 (SSR)	0.11	0.68	6.571	66.7%
	CNR-DT 200 (SSR)	**0.04**	**0.62**	**7.143**	76.2%
	PELLEGRINO AND MODENA (SSR)	0.25	1.08	5.429	57.1%
V_{frp} (Side bonded)	ACI 440	0.51	1.27	4.688	50.0%
	CNR-DT 200	0.87	**1.47**	3.141	25.0%
	PELLEGRINO AND MODENA	0.82	1.21	2.145	20.2%
	ACI 440 (NSSR)	0.58	1.35	3.787	38.3%
	CNR-DT 200 (NSSR)	0.91	**1.47**	3.234	29.8%
	PELLEGRINO AND MODENA (NSSR)	0.89	1.23	**1.289**	**7.9%**
	ACI 440 (SSR)	0.45	0.71	**7.176**	**82.4%**
	CNR-DT 200 (SSR)	0.11	1.36	3.588	29.4%
	PELLEGRINO AND MODENA (SSR)	0.56	1.10	3.059	27.1%

R^2: Correlation coefficient. SF: Global safety factor. UJ+SB: Only U-Jacket + Side bonded strengthened elements

PEN: Summation of penalties. NSR: Not safe results (values with a partial safety factor below 0.80).

1	**Best particular behavior**
1	**Worst particular behavior**
1	**Best global behavior**
1	**Worst global behavior**

In the previous table, it is seen that the model of Pellegrino and Modena has in general the best behavior. However, it has to be said that all the codes and the model seem to have problems to predict the behavior of beams with shear steel reinforcement.

8. CONCLUSIONS

- The comparison procedure based on the parameters introduced in this document showed to be adequate for assessing the codes. With this procedure, it was possible to evaluate the correlation between the experimental and theoretical data as well as the level of safety achieved by the use of the given codes.

- The *fib* BULLETIN 14 presents, in general, the worst behavior of the studied codes for the comparison parameters included in this document. As a matter of fact, according to the evaluation carried out here, its use would lead to a high probability of getting an unsafe result. However, it has to be said that the provisions of this code are being evaluated and an update is supposed to be release soon.

- It was observed that the codes have a better behavior when the contribution of the concrete and of the steel is added to the FRP contribution. As example, the CNR-DT 200 and the ACI 440, when used in conjunction with their respective codes, show a performance with adequate levels of safety, including percentage of unsafe results of 14.2% and 8%. This values increase to 27.4% and 38.9% respectively when only the FRP contribution is analyzed.

- More than the 35% of the values predicted by the three codes for the U-jacket configuration are located under the reduced safety zone (SF lower than one) which implies that the probability of obtaining safe results is lower than the 35%. Taking this into account, it is highly recommended that a critical review of the equations given in the codes for the strengthening of concrete beams in this fashion is carried out. This is even clearer when the correlation factors are considered. All the three codes show a poor performance as long as the values of R^2 are concerned with a higher value of 0.15 when the target value in this document was set to 0.70. This disappointing behavior shows, again, that the proposed recommendations are not able to replicate the actual behavior of concrete beams strengthened by externally bonded FRP systems in a U-jacket configuration. For this case, it is seen that the equations are more reliable for the case of NSSR beams.

- The equations proposed by the CNR-DT 200 for the FRP contribution of concrete beams strengthened by a side bonding configuration, present a good agreement between the experimental data and the predicted values as can be concluded from the value of the correlation factor (R^2=0.87). For this configuration, the Italian Guideline also presents an adequate value of global safety factor (SF=1.47) but still there is a 25% probability of getting values under the reduced safety level. However, the performance of the CNR-DT 200 is by far the best of the studied codes and its use should be recommended to establish the FRP contribution for this type of strengthening configuration. For the side bonded configuration, it is seen how the CNR-DT 200 has the best behavior and that the equations are good enough for

SSR and NSSR beams. As a matter of fact, the behavior is almost the same but there is a remarkable reduction in the correlation coefficient for the SSR case.

- The influence of the shear steel reinforcement is notorious, especially for the case of U-jacket strength configuration. This allows concluding that this aspect should be studied more in detail in order to improve and update the equations given by the codes.
- The Pellegrino and Modena model showed to have a behavior that in some cases is better than the one presented by the standards. This is especially noticed for the case of concrete beams with side bonded configuration. However, it is also seen that some improvements are still needed in order to evaluate the influence of the presence of shear steel reinforcement.

9. REFERENCES

ACI “440.2R-02: Guide for the design and construction of externally bonded FRP systems for strengthening of concrete structures”, 2002, Reported by ACI Committee 440.

fib “Bulletin 14 – Externally Bonded FRP reinforcement for RC structures” Technical report, 2001, Task Group 9.3 FRP (fiber reinforced polymer) reinforcement for concrete structures.

CNR-DT200 “Guidelines for desing, execution and control of strengthening interventions by means of fiber reinforced composites”, 2004, National Research Council.

Adhikary, B.B., Mutsuyoshi, H., Behavior of concrete beams strengthened in shear with carbon-fiber sheets, Journal of Composites for Construction may-june 2004; pp. 258-264.

Adhikary, B.B., Mutsuyoshi, H., Ashraf, M., Effective shear strengthening of concrete beams using FRP sheets with bonded anchorage, FRPRCS.6: Externally bonded reinforcement for shear 2003: pp. 457-466.

Banerjee, S., Mosallan, A. S., Shear enhancement of reinforced concrete beams strengthened with FPR composite laminates, Composites Part B 38 2007; pp. 781 – 793.

Barros, J.A.O., Dias, S.J.E., Near surface mounted CFRP laminates for shear strengthening of concrete beams, Cement & Concrete Composites, Vol. 28 2006; pp. 276-292.

Bousselhan, A., Chaallal, O., Maximum shear strength of RC beams retrofitted in shear with FRP composites, Journal of Composites for Construction july – august 2009; pp. 302 – 314.

Chaallal, O., Bousselham, A., Behavior of reinforced concrete T-Beams strengthened in shear with carbon fiber-reinforced polymer. An experimental study, ACI Structural Journal 2006; pp. 339-347.

Chaallal, O., Bousselham, A., Effect of transverse steel and shear span on the performance of RC beams strengthened in shear with CFRP, Composites: part B (engineering) Vol. 37 2006; pp. 37-46.

Chaallal, O., Nollet, M. J., Perraton, D., Shear strengthening of RC beams by externally bonded side CFRP strips, Journal of Composites for Construction 1998; pp. 111-113.

Cao, S., Chen, J., Teng, J., Hao, Z., Debonding in RC beams shear strengthened with complete FRP wraps, Journal of composites construction sept.-oct. 2005; pp. 417-428.

Caicedo, N., Use of FRP and TRM jackets for ductility in reinforced concrete columns, Rose School Master’s thesis, 2007.

Deniaud, C., Cheng, J.J.R., Reinforced concrete T-beams strengthened in shear with fiber reinforced polymers sheets, Journal of Composites for Construction 2003; pp. 302-310.

Fico, R., Prota, A., Manfredi, G., Assesment of Eurocode-like design equations for the shear capacity of FRP RC members, Composites: Part B 39 2008; pp. 792-806.

Guadagnini, M., Pilakoutas, K., Waldron, P., Shear resistance of FRP RC beams: Experimental study, Journal of Composites for Construction nov. – dec. 2006; pp. 464 – 473.

Godat, A., Neale, K. W., Labossiere, P., Numerical modeling of FRP shear-strengthened reinforced concrete beams, Journal of Composites for Construction nov. – dec. 2007; pp. 640 – 649.

Ianniruberto, U., Imbimbo, M., Role of fiber reinforced concrete beams using carbón fiber reinforced polymers laminates, Journal of Composites for Construction sept.-oct. 2004; pp. 415-424.

Islam, R., Inventory of FRP strengthening methods in masonry structures, MSC-SAHC Master's thesis, 2008.

Khalifa, A, Nanni, A., Rehabilitation of rectangular simply supported RC beams with shear deficiencies using CFRP composites, Construction & Building vol. 16 2002; pp. 135-146.

Khalifa, A, Nanni, A., Improving shear capacity of existing RC T-section beams using CFRP composites, Cement & Concrete Composites vol. 22 2000; pp. 165-174.

Khalifa, A., Nanni, A., Belarbi, A., Tumialan, G., Shear strengthening of continuous reinforced concrete beams using externally bonded carbón fiber reinforced polymer sheets, FRPRCS-4:Externally bonded reinforcement for shear 1999; pp. 995-1008.

Leung, K. Y. L., Chen, Z., Lee, S., Ng, M., Xu, M., Tang, J., Effect of size on the failure of geometrically similar concrete beams strengthened in shear with FRP strips, Journal of Composites for Construction 2007; pp. 487-496.

Lima, J.L.T., Barros, J.A.O., Desing models for shear strengthening of reinforced concrete beams with externally bonded FRP composites: A statistical versus reliability approach, FRPRCS-8 2007.

Megalooikonomou, K., Modelling of FRP-confinement of rectangular RC sections, Rose School Master's thesis, 2007.

Monti, G., Liotta, M., Test and desing equations for FRP-strengthening in shear, Construction & Building Materials 21 2007; pp. 799-809.

Pellegrino, C., Modena, C., An experimentally based analytical model for the shear capacity of FRP-strengthened reinforced concrete beams, Mechanics of Composite Materials Vol. 44 No. 3 2008; pp. 231-244.

Pellegrino, C., Modena, C., Fiber reinforced polymer shear strengthening of reinforced concrete beams with transverse steel reinforcement, Journal of Composites for Construction 2002; pp. 104-111.

Peloso, S., FRP seismic retrofit of square hollow section bridge piers, Rose School Maters's thesis, 2003.

Sas, G., Taljsten, B., Barros, J., Lima, J., Carolin, A., Are available models reliable for predicting the FRP contribution to shear resistance of RC beams?, Journal of Composites for Construction nov.-dec. 2009; pp. 514-534.

Sas, G., Carolin, A., Taljsten, B., A model for predicting the shear bearing capacity of FRP-strengthened beams, Mechanics of Composite Materials, Vol. 44 No. 3 2008; pp. 245 – 256.

Taljsten, B., Carolin, A., Experimental study of strengthening for increased shear bearing capacity, Journal of composites construction nov.- dec. 2005; pp. 488-496.

Taerwe, L, Khalil, H., Matthys, S., Behaviour or RC beams strengthening in shear by external CFRP sheets, FRPRCS-3: Non metallic (FRP) reinforcement for concrete structures 1997.

Taljsten, B., Strengthening concrete beams for shear with CFRP sheets, Construction & Building Materials vol. 17 2003, pp. 15-23.

Teng, J. G., Chen, G. M., Chen, J. F., Rosenboom, O. A., Lam, L. Behavior of RC beams shear strengthened with bonded or unbounded FRP wraps, Journal of Composites for Construction Sept.-Oct. 2009; pp. 394-404.

Triantafillou, T., Shear strengthening or reinforced concrete beams using epoxy-bonded FRP composites, ACI Structural Journal march-april 1998; pp. 107-115.

Triantafillou, T., Antonopoulos, C., Desing of concrete flexural members strengthened in shear with FRP, Journal of Composites for Construction Nov. 2000; pp. 198-205.

Yalim, B., Kalayci, A. S., Mirmiran, A., Performance of FRP-Strengthened RC beams with different concrete surface profiles, Journal of Composites for Construction nov.- dec. 2008; pp. 626-638.

Zhang, Z., Hsu, C., Shear strengthening of reinforced concrete beams using carbon fiber reinforced polymer laminates", Journal of composites for construction march-april 2005; pp. 158-169.